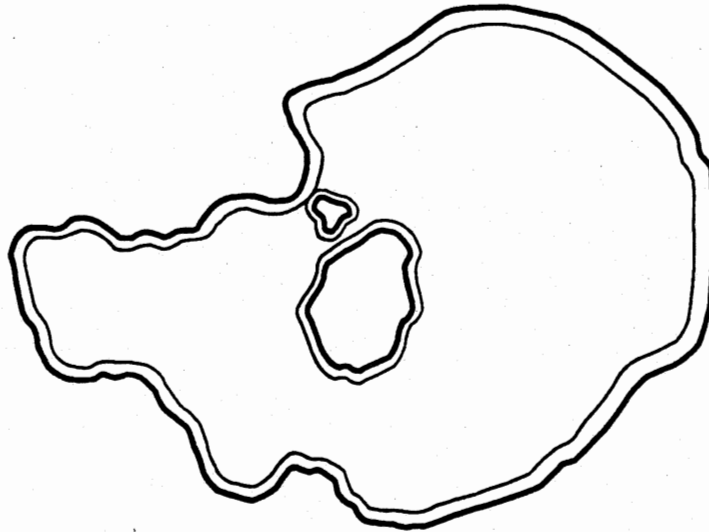


An Auxiliary Report
Prepared for the

MONO BASIN WATER RIGHTS EIR

50-Year DYRESM Simulations of Mono Lake with
Different Water Management Scenarios



Prepared under the Direction of:

California State Water
Resources Control Board
Division of Water Rights
P.O. Box 2000
Sacramento, CA 95810

Prepared With Funding from:

Los Angeles Department of
Water and Power
Aqueduct Division
P.O. Box 111
Los Angeles, CA 90051

**An Auxiliary Report
Prepared for the
Mono Basin Water Rights EIR Project**

This auxiliary report was prepared to support the environmental impact report (EIR) on the amendment of appropriative water rights for water diversions by the City of Los Angeles Department of Water and Power (LADWP) in the Mono Lake Basin. Jones & Stokes Associates is preparing the EIR under the technical direction of the California State Water Resources Control Board (SWRCB). EIR preparation is funded by LADWP.

SWRCB is considering revisions to LADWP's appropriative water rights on four streams tributary to Mono Lake, Lee Vining Creek, Rush Creek, Parker Creek, and Walker Creek. LADWP has diverted water from these creeks since 1941 for power generation and municipal water supply. Since the diversions began, the water level in Mono Lake has fallen by 40 feet.

The Mono Basin water rights EIR examines the environmental effects of maintaining Mono Lake at various elevations and the effects of possible reduced diversions of water from Mono Basin to Owens Valley and the City of Los Angeles. Flows in the four tributary creeks to Mono Lake and water levels in Mono Lake are interrelated. SWRCB's decision on amendments to LADWP's water rights will consider both minimum streamflows to maintain fish populations in good condition and minimum lake levels to protect public trust values.

This report is one of a series of auxiliary reports for the EIR prepared by subcontractors to Jones & Stokes Associates, the EIR consultant, and contractors to LADWP. Information and data presented in these auxiliary reports are used by Jones & Stokes Associates and SWRCB, the EIR lead agency, in describing environmental conditions and conducting the impact analyses for the EIR. Information from these reports used in the EIR is subject to interpretation and integration with other information by Jones & Stokes Associates and SWRCB in preparing the EIR.

The information and conclusions presented in this auxiliary report are solely the responsibility of the author.

Copies of this auxiliary report may be obtained at the cost of reproduction by writing to Jim Canaday, Environmental Specialist, State Water Resources Control Board, Division of Water Rights, P.O. Box 2000, Sacramento, CA 95810.

**50-Year DYRESM Simulations of Mono Lake
with Different Water Management Scenarios**

Written by:

**Jose Romero
Research Assistant
Marine Science Institute
University of California,
Santa Barbara**

May 10, 1992

50-Year DYRESM Simulations of Mono Lake with Different Water
Management Scenarios

INTRODUCTION

DYRESM, a one-dimensional (1-D) vertical mixing model, was used to simulate the effect of various water management policies on Mono Lake. The Los Angeles Aqueduct Model (LAAMP) determined fifty years sequences of monthly discharges into Mono Lake and monthly lake elevations under different management scenarios. These data and an annual meteorologic data set were used to determine the effect of different management scenarios on the seasonal stratification of Mono Lake. End of month temperature, conductivity, and density profiles and daily and monthly mixed layer and 35 m depth water properties were prepared for purposes of the Mono Lake EIR analysis (Figure 1).

MODEL

DYRESM is a 1-D vertical mixing model which has been used in a variety of applications, i.e. reservoirs (Imberger and Patterson, 1981), freshwater lakes (Patterson et al, 1984), lakes with winter ice cover (Patterson et al, 1988), and salt ponds (Schladow, 1983). We applied DYRESM to Mono Lake during a monomictic year (Jellison et al, 1991) and made several changes to the model for this application.

Conservation of the mass of water and salt were explicitly added. For freshwater applications, conservation of volume is nearly equivalent to conservation of mass because 1 liter of water is nearly equal to 1 kg of water. For saline waters this approximation is inappropriate (Steinhorn, 1991). For example, 1 liter of Mono Lake water is approximately 1.08 kg. Mass conservation of salt is generally not important in freshwater systems as salt concentrations are very low. For saline waters it is necessary to have a fixed salt budget. For 50 year simulations this improvement is necessary so the initial and final total lake salinity are equivalent. In this analysis conductivity at 25°C is used as a measure of salinity.

Stream discharge is an input to DYRESM, and the lake elevation is calculated. If the calculated lake elevation is lower than the elevation provided by LAAMP, the amount of water required to raise the lake level to the LAAMP value is added to the top layer. This amount of water is termed 'ungauged stream discharge and groundwater' in this analysis. Since Mono Lake is hypersaline, inputs of groundwater and ungauged surface flow are dilute relative to the lake water, and the assumption that all this water enters the top layer is justified.

MODEL INPUTS

Bathymetry

The depth-volume and depth-area data used are from the Pelagos (1987) survey.

Mono Lake Specific Properties

The latent heat of evaporation, the specific heat, and density equation for Mono Lake are discussed in Jellison et al (1991). Table 1 is a summary of these properties.

Meteorology

Daily average values of vapor pressure (mbar), wind speed (m s^{-1}) and temperature ($^{\circ}\text{C}$), and daily totals of shortwave radiation (KJ) and cloud cover (%) are inputs to the model. A consistent data set from Oct. 1, 1989 to Sept. 30, 1990 has been compiled from Paoha Island, Cain Ranch, and SNARL meteorology stations. The same year of meteorology was used for each year in the simulations. Each 50 year simulation uses the annual meteorological data set 50 times. Figure 2 shows the meteorological inputs.

These meteorological data are the best data available to date. Analysis of different stream release management scenarios and year to year differences within a simulation are more readily identified since every year has the same meteorological conditions. Differences among years from a simulation and among management scenarios will be the result of different hydrologic conditions.

Hydrology

Daily averages of stream temperature and stream salinity are inputs. Daily average stream temperature was measured for Convict Creek at SNARL and used in this simulation. Stream salinity was set to zero as Sierra runoff contributes a negligible amount of salinity to Mono Lake on a time scale of decades.

Monthly values of lake elevation and stream discharge from LAAMP were interpolated to daily values. Precipitation onto the surface of the lake was divided into an average for the month. Daily gauged stream discharges (Figures 3 to 5) and observed lake elevations (Figures 6 to 8) from 1983 to 1990 were hydrological inputs to the validation simulations.

MODEL VALIDATION

The simulations performed below used the observed lake elevations to determine the amount of additional ungauged surface runoff or groundwater to add to match the simulated elevation with the observed elevation. Calibration of a Mono Lake specific evaporation coefficient was done with the 1990 simulation.

1990 Simulation

A simulation with the above meteorological data yields excellent agreement in thermal structure (Figure 9) and conductivity (Figure 10) with measured profiles. Jellison et al (1991) comments on the discrepancy between simulated and observed hypolimnetic temperatures. This difference is acceptable for the seasonal time scale to be performed here.

An estimate of the bulk evaporation coefficient used to calculate the evaporative heat flux was done for Mono Lake. Energy budget studies are useful in estimating evaporation rates from inland water bodies (Stauffer, 1991). The energy budget method is normally the standard against which other evaporation estimates are compared, because the local water budget is usually too uncertain to provide an absolute standard (Winter, 1981). Since data for a complete energy budget study is lacking at Mono Lake, we arrived at an estimate by varying the bulk evaporation coefficient. The best match between the modeled and measured surface temperatures was the criteria for choosing the coefficient.

Simulations with 20% and 40% increases and decreases in the original DYRESM value of the bulk coefficient were performed. A value of 3.12 (20% decrease) matches best with the observed surface temperature values (Figures 12 and 13) which is equivalent to an annual evaporation of 48 to 50 inches (Table 2) for the simulation of 1983 to 1989. This value lies between the low estimate of 39 inches (no groundwater) and a high estimate of 57 inches (bulk

evaporation coefficient equal to 3.9). The total monthly percentage of the yearly evaporation total matches well between LAAMP and DYRESM (Table 3).

Evaporation is a function of the vapor pressure gradient between the vapor pressure in the atmosphere and the saturation vapor pressure at the air-water interface and the wind speed. The saturation vapor pressure at the surface of the lake is a function of the surface water temperature.

The relative change in the average monthly surface temperature during the 1990 simulation is greater during the cooler months (Figure 14). The changes in the saturation vapor pressure are greater during the warmer months (Figure 15) than the cooler months. Since vapor pressure is a nonlinear function of temperature, an incremental increase in surface temperature at low temperatures is small whereas at high temperatures it is much larger. Small changes in the surface temperature during the summer months can have a large effect on the saturation vapor pressure and thus the amount of evaporation.

Greater relative increases in evaporative mass flux results from increasing the bulk coefficient during cooler months than in warmer months (Figure 16). Approximately 20% less water is evaporated with a 20% decrease in the suggested DYRESM evaporation bulk coefficient. Figures 9 to 11 used the Mono Lake specific evaporation bulk coefficient.

An improved estimate of the annual evaporation would result with daily average surface temperatures from a surface probe rather than the few values from sampling days used in the present estimate. An even more reliable estimate of evaporation would result from a complete energy budget.

1983-90 Simulation

Simulation of the meromictic episode of the 1980's was performed to determine if DYRESM captured the essential features. A repeating annual meteorology with the same data set described above was used in these simulations. Exact agreement between observed and simulated profiles is not to be expected since the meteorological inputs for the simulation differed from the actual meteorological forcing on the lake.

During 1983 the lake developed a chemocline as a result of runoff from a deep Sierran snow pack. The simulated temperature profiles matched well with observed profiles (Figure 17).

In 1984 there were large deviations in the upper 15 m between the observed and simulated profiles (Figure 18). On day 84066 (the 66th day 1984) the simulation of the large temperature inversion was caused by a secondary chemocline at 5 m above the main chemocline at 15 m. During the winter the water column above the main chemocline cooled below the temperature of the hypolimnion. The chemical stratification

at 15 m prevented mixing of water above 15 m with the hypolimnetic water. The hypolimnion was effectively insulated from the surface energy inputs. As a result, during the winter cooling period the water cooled to a lower temperature than the hypolimnion.

During late winter to early spring a secondary chemocline developed at 5 m. A net flux of heat into the lake at this time caused warming of the upper 5 m, but there was insufficient energy to mix through the secondary chemocline until 84171. This resulted in a cold stratum of water between two warmer stratums (the hypolimnion and the mixed layer). As the simulation progresses through 1984, the simulated secondary chemocline is mixed. By the end of 1984, the simulation once again matches well with the observed profiles.

The same mechanism described above occurs for the years 1985 to 1989 (Figures 19 to 23). For the simulated years 1985 to 1989, the simulated mixed layer was shallower by several meters on average than observed mixed layer depths.

By 1990, a monomictic year (Figure 24), the simulation matched satisfactorily with observed profiles. Since 1990 meteorology data is used for the entire simulation a good match was anticipated for this year.

The observed breakdown in meromixis occurred in November, 1988, whereas the simulated breakdown in meromixis occurred February, 1990. The 15 month discrepancy in prediction of the termination of meromixis may be due to the

assumption that all groundwater goes into the upper 1 m of the lake. This may be erroneous especially during years with high Sierran runoff. The stability of the top layer in the simulation may be artificially high as a result. During periods with a significant amount of inflow, the duration of meromictic periods is likely to be overpredicted.

The simulation of meromixis shows that the DYRESM predicts long-term chemical stratification adequately. However, interpretation of simulated meromictic episodes must be performed with care. The hydrology appears to drive meromixis and seems to be more important than meteorology when modeling meromictic events.

Model Output for EIR Assessment

Daily average mixed layer depth, temperature, conductivity and density, and daily temperature, conductivity and density at 35 m, and end of month profiles were obtained as output.

The algorithm to determine the mixed layer depth estimated the depth adequately for the meromictic validation simulation (Figures 25 to 28). The observed mixed layer depths were estimated from observed profiles. The mixed layer depth estimates for 1983, 1984, 1987 and 1988 are several meters too low; 1985, 1986 and 1990 are estimated accurately. Since 1989 was incorrectly simulated as a meromictic year it is not considered.

Daily average mixed layer properties were converted to monthly averages for use in the EIR assessment. The monthly averages of the mixed layer and 35 m properties were calculated from the daily averages.

The conversion of the daily values to monthly values smooths plots of mixed layer properties. The monthly averaged mixed layer properties (Figures 29 to 30) match well with the daily values. The 1984 monthly averaged mixed layer depth of 13 m agrees well with the daily estimate (Figure 25). A gradual increase in the monthly averaged mixed layer depth through the meromictic period to 1988 is accurate. The 1990 turnover is readily identifiable in the monthly average mixed layer plot.

The monthly plots are used to determine if the lake was meromictic in the 50 year simulations. The monthly temperature plot (Figure 29) of the mixed layer and at 35 m clearly shows that the lake was meromictic since the temperature was 3°C throughout the simulation until the simulated turnover during February of 1990 in which the temperature noticeably changed indicating the water column mixed to 35 m. The conductivity and density plot also indicate the same conclusion in the same manner.

50-YEAR SIMULATIONS OF DIFFERENT MANAGEMENT ALTERNATIVES

Constant Hydrologic Inputs

Mill Creek and DeChambeau Creek are gauged creeks which are not part of the Los Angeles Aqueduct system (Figure 31). The discharges from these creeks were added to LAAMP stream scenario discharges from Walker, Parker, Lee Vining, and Rush creeks.

The 50-year record of Cain Ranch precipitation used in the simulations is shown in figure 32.

Form of Analysis

The 6372 ft, 6377 ft, 6383 ft, 6390 ft, and Point of Reference (POR) alternatives were simulated and evaluated. Emphasis is placed on timing and duration of meromictic events; comments about the mixing dynamics are added when important. Figures of yearly totals of groundwater estimates from LAAMP and DYRESM are provided and the models agree well.

The mixed layer plots are sometimes in error. The mixed layer determination algorithm did not record weakly stratified meromictic events during the winter (a density stratification less than 1 kg m^{-3}). In such cases, a year was classified as meromictic if the conductivity, temperature, and density at 35 m did not change during the year. This indicates that no vertical mixing reached 35 m and therefore the year was meromictic. If still unsure of

the meromictic status of a year, daily information was consulted.

Only meromictic events with at least a 3 year duration or a large density stratification (ca. $> 5 \text{ kg m}^{-3}$) are reported here.

6372 Ft Alternative

This is the lowest management target elevation evaluated and the most susceptible to meromictic events. The greater likelihood of meromixis occurring at this elevation is due to highest salinity relative to the other alternatives and smallest surface area. Hence a given amount of discharge will result in a thicker freshwater layer. Based on the LAAMP lake elevation inputs (Figure 33) meromictic events are likely to occur during 1952 (1.75 ft rise), 1956 (2.25 ft rise), 1967 (1 ft rise), 1969 (1.5 ft rise), and 1983 (1.5 ft rise). Stream discharges from LAAMP are given in Figure 34.

A 4 year meromictic period was simulated during 1956 to 1959 (Figures 35 and 36). A 14 year meromictic period was simulated during 1962 to 1975, though the simulation predicted weak stratification during the winters of 1963, 1965 and 1976. This suggests that the 14 year meromictic episode would likely be discontinuous. At least a 12 year meromictic period was simulated during 1978 to 1990.

As the lake level dropped near the target elevation (1956 - 6372.5 ft, 1962 - 6372.2 ft, 1978 - 6372.5 ft) long-

term meromixis occurred. Small stream discharges in conjunction with ungauged surface discharges and groundwater (Figure 40) were sufficient to cause meromictic episodes of long duration.

6377 Ft Alternative

Based on the LAAMP lake elevation inputs (Figure 41) meromictic events are likely to occur during 1941 (2.25 ft rise), 1956 (2.25 ft rise), 1962 (2 ft rise), 1967 (2.25 ft rise) 1969 (2.5 ft rise), 1978 (2.5 ft rise) and 1983 (2.25 ft rise). Stream discharges from LAAMP are given in Figure 42.

Figure 47 from the temperature, conductivity and density plots at 35 m depth shows a 5 year meromictic episode from 1983 to 1986. The lake elevation rose steadily from 1982 to 1984 and again in 1986 so it seems the meromixis was induced and persisted from hydrological forcing. The density gradient between the mixed layer and the 35 m was significantly less than those identified in the 6372 ft alternative.

A 4 ft difference between 6377 ft and 6372 ft target elevations had pronounced effects on the occurrence of meromixis. The 6377 ft target elevation simulation resulted in a lower frequency and duration of meromictic events than the 6372 ft alternative. The increased surface area and reduced salinity are hypothesized to be the major influences in the diminished meromictic behavior of the 6377 ft

alternative. Analysis of target elevations between 6372 and 6377 ft is recommended.

6383 Ft Alternative

Based on the LAAMP lake elevation inputs (Figure 49) meromictic events are likely to occur during 1941 to 1944 (5.5 ft rise in 3 years), 1952 (2.75 ft rise), 1956 (2.75 ft rise), 1962 (2 ft rise), 1963 (2 ft rise), 1967 (2.75 ft rise), 1969 (2.75 ft rise), 1978 (2.75 ft rise), and 1982 to 1983 (3.5 ft rise in two years). Stream discharges from LAAMP are given in Figure 50.

Figure 51 indicates that meromixis occurs during the entire decade of the 1940s. The mixed layer algorithm is accurate from the net heating period in 1942 to the end of the decade. Approximately a 20 m mixed layer occurs during the bulk of this meromictic period. The long duration of the simulated meromictic period is a result of increasing the lake elevation too quickly. Simulations with a management scenario where the target elevation is reached during a longer transition is recommended.

Figure 52 shows that this meromictic episode continues through the 1950s. The average mixed layer depth is approximately 30 m through this period. Mixing to 35 m occurred during late 1954 and early 1956 suggesting that the predicted duration of meromixis would be discontinuous. Once again a different management scenario with reduced stream inputs in 1952 and 1956 and slight increases in the

stream releases during other years probably will reduce the meromictic behavior of the lake.

Figures 54 and 55 show one long meromictic event occurring during 1978 to 1985. The density gradient during the winter periods of each year (2 kg m^{-3}) is not large and in early 1983 a mixing event to 35 m occurred which suggests that the duration of an actual meromictic event would be of shorter duration than simulated.

6390 Ft Alternative

Based on the LAAMP lake elevation inputs (Figure 57) meromictic events are likely to occur during 1941 to 1946 (8.5 ft rise in 5 years), 1952 (2.75 ft rise), 1956 (2.5 ft rise), 1958 (2 ft rise), 1962 to 1963 (4 ft rise in 2 years), 1965 (2 ft rise), 1967 (2.75 ft rise), 1969 (3.25 ft rise), 1969 (3.25 ft rise), 1978 (2.75 ft rise) and 1982 to 1983 (3.5 ft rise in 2 years). Stream discharges from LAAMP are given in Figure 58.

Figure 59 indicates that meromixis occurs during the entire decade of the 1940s. The density between the mixed layer and 35 m depth is strong (ca. $> 5 \text{ kg m}^{-3}$). The mixed layer algorithm is accurate from the net heating period in 1942 to the end of the decade. Approximately a 15 to 25m mixed layer occurs during the majority of this meromictic period. The long duration of the simulated meromictic period is a result of increasing the lake elevation too quickly as with the 6377 ft alternative. Simulations with a

management scenario where the target elevation is reached during a longer transition is recommended.

Figure 60 shows that this meromictic episode continues until 1954. Early 1952 saw substantial deepening which affected the 35 m depth water properties significantly. The average mixed layer depth is approximately 35 m through this period. Once again a different management scenario with reduced stream inputs in 1952 and slight increases in the stream releases during other years probably will reduce the meromictic behavior during this period.

Figure 61 shows a weak one year meromictic event during 1967-68. Even with a 3 ft increase in lake elevation, the mixed layer conductivity (73 to 78 mS cm^{-1}) is sufficiently low to reduce the meromictic influence of the freshwater inflows relative to the other target elevation alternatives. Figures 62 and 63 show that negligible meromictic behavior occurs once the target elevation has been reached.

Point of Reference (POR) Alternative

This simulation is not a target elevation alternative. This is the 50-year historical record of stream release. The highest salinities (i.e. lowest lake elevations) considered in this analysis are in this simulation. Based on the LAAMP lake elevation inputs (Figure 65) meromictic events are likely to occur during 1952 (2.5 ft rise), 1956 (2 ft rise), 1967 (3 ft rise), 1969 (4.25 ft rise), 1978 (4

ft), 1982 to 1984 (12 ft rise in 3 years), and 1986 (2.75 ft rise). Stream discharges from LAAMP are given in Figure 67.

Figure 68 shows a weak (ca. $< 3 \text{ kg m}^{-3}$) 3 year meromictic period from 1941 to 1943. Figure 69 shows a strong 1 year meromictic episode in 1952 and strong 2 year meromictic period from 1957 to 1958. Meromixis occurs from 1967 to 1990 (Figures 70 and 71) with one monomictic year in 1977. The stability of the final meromictic event is extremely high with a density gradient equal to 70 kg m^{-3} between the mixed layer and the 35 m depth for 1984 to 1987. This suggests that this may continue to be a very prolonged event.

The confidence associated with this simulation is lower than the others in this simulation. The high conductivities in the hypolimnion at the lower elevations (ca. 114 mS cm^{-1}) is well outside of the range which the density equation was determined.

Conclusion and Final Remarks

Figure 73 is a synopsis of the major simulated meromictic events of the five alternatives considered here. The 6372 ft target elevation appears to be one which is susceptible to meromictic behavior. The 6377 ft target elevation has only one significant meromictic event which occurs during the early 1980s. Simulations of the 6383 ft and 6390 ft alternatives both predicted long term meromixis during the 1940s into the 1950s, but longer transition

periods to reach target elevations was identified as the cause. The 6383 ft elevation simulation resulted in only one additional significant meromictic period from 1978 to 1986, but the density between the mixed layer and the 35 m depth was not strong. Once the target elevation was attained in the 6390 ft elevation simulation, no significant meromictic events occurred.

BIBLIOGRAPHY

Imberger, J. and Patterson, J.C. (1981) A dynamic reservoir simulation model - DYRESM. In Transport Models for Inland and Coastal Waters (H.B. Fischer ed.), pp. 310-361. Academic Press, New York.

Patterson, J.C. and Hamblin, P.F. (1988) Thermal simulation of a lake with winter ice cover. *Limnol. Oceanogr.* 33:323-338.

Patterson, J.C., Hamblin, P.F., and Imberger, J. (1984) Classification and dynamic simulation of the vertical density structure of lakes. *Limnol. Oceanogr.* 29:845-861.

Jellison, R., Dana, G.L., Romero, J.R., and Melack, J.M. (1991) Phytoplankton and brine shrimp dynamics in Mono Lake, California. 1990 Draft Report to LADWP.

Pelagos Corporation (1987) A bathymetric and geologic survey at Mono Lake, California. Unpublished report to the Los Angeles Department of Water and Power. San Diego.

Schladow, S.G. (1983) Stability of salt gradient solar ponds. Centre for Water Research. University of Western Australia. Rept. No. ED-83-061.

Stauffer, R.E. (1991). Testing lake energy budget models under varying atmospheric stability conditions. *J. Hydrology.*, 128:115-135.

Steinhorn, I. (1991) On the concept of evaporation from fresh and saline water bodies. *Water Resour. Res.* 27:645-48.

Winter, T.C. (1981) Uncertainties in estimating the water balance of lakes. *Water Resour. Bull.*, 17:82-115.

FIGURES

Figure 1. Schematic of Mono Lake hydrology and lake mixing model linkages and output.

Figure 2 . Short wave radiation, air temperature , wind speed, vapor pressure, and precipitation from October 1, 1989 (JDAY = 89274) to September 30, 1990 (JDAY = 90273) used in validation and EIR simulations.

Figures 3-5. Total daily gauged stream inputs into Mono Lake used in validation simulations.

Figures 6-8. Measured lake elevations used in validation simulations.

Figures 9-11. Simulated and observed temperature, simulated and observed corrected conductivity, and simulated density profiles of 1990 validation simulation.

Figures 12-13. Sensitivity analysis of simulated surface temperatures with 20% and 40% plus and minus changes in the bulk evaporation coefficient compared with observed surface temperatures.

Figures 14-16. Relative change in average monthly surface temperature, saturation vapor pressure, and mass of evaporative water loss from the evaporation bulk coefficient sensitivity analysis simulation performed from 1983 to 1990.

Figures 17-24. Observed and simulated temperature plots of validation simulation of 1983 to 1990.

Figures 25-28. Observed and simulated mixed layer depth for the 1983 to 1990 simulation.

Figures 29-30. Monthly averages of simulated mixed layer depth and temperature, corrected conductivity, and density for the mixed layer and at 35m depth for the 1983 to 1990 simulation.

Figure 31. Mill Creek and Dechambeau Creek discharges and precipitation used in 50-year simulations.

Figure 32. Monthly precipitation totals from Cain Ranch used in 50-year simulations.

Figure 33-40. 6372 ft alternative summary. Monthly elevation and gauged stream inputs from LAAMP are shown. Monthly averaged output of mixed layer depth, mixed layer temperature, mixed layer corrected conductivity, mixed layer density, temperature at 35m, corrected conductivity at 35m, and density at 35m are shown. Estimates of the yearly average of ungauged surface discharges and groundwater are shown.

Figure 41-48. 6377 ft alternative summary. Monthly elevation and gauged stream inputs from LAAMP are shown. Monthly averaged output of mixed layer depth, mixed layer temperature, mixed layer corrected conductivity, mixed layer density, temperature at 35m, corrected conductivity at 35m, and density at 35m are shown. Estimates of the yearly average of ungauged surface discharges and groundwater are shown.

Figure 49-56. 6383 ft alternative summary. Monthly elevation and gauged stream inputs from LAAMP are shown. Monthly averaged output of mixed layer depth, mixed layer temperature, mixed layer corrected conductivity, mixed layer density, temperature at 35m, corrected conductivity at 35m, and density at 35m are shown. Estimates of the yearly total of ungauged surface discharges and groundwater are shown.

Figure 57-64. 6390 ft alternative summary. Monthly elevation and gauged stream inputs from LAAMP are shown. Monthly averaged output of mixed layer depth, mixed layer temperature, mixed layer corrected conductivity, mixed layer density, temperature at 35m, corrected conductivity at 35m, and density at 35m are shown. Estimates of the yearly average of ungauged surface discharges and groundwater are shown.

Figure 65-72. Point of reference (POR) alternative summary. Monthly elevation and gauged stream inputs from LAAMP are shown. Monthly averaged output of mixed layer depth, mixed layer temperature, mixed layer corrected conductivity, mixed layer density, temperature at 35m, corrected conductivity at 35m, and density at 35m are shown. Estimates of the yearly average of ungauged surface discharges and groundwater are shown.

Figure 73. Frequency and duration of meromixis for simulations performed.

Table 1. Table of properties of Mono Lake Water. All values are for a temperature of 15°C.

Viscosity (Pa)	1.137 X 10 ⁻³
Kinematic Viscosity (m ² s ⁻¹)	1.27 X 10 ⁻⁶
Specific Heat (J g ⁻¹ °C ⁻¹)	3.867
Latent Heat of Evaporation (J kg ⁻¹)	2.477 X 10 ⁶

Table 2. Monthly evaporation totals for 1983 to 1990 simulation of Mono Lake.

	1983 (cm)	1984 (cm)	1985 (cm)	1986 (cm)	1987 (cm)	1988 (cm)	1989 (cm)
1		3.45	3.52	3.59	3.55	3.67	3.91
2		3.44	3.44	3.43	3.49	3.57	3.67
3		6.00	6.20	6.03	6.02	5.95	5.80
4	9.65	10.06	9.99	9.74	9.88	9.92	9.91
5	15.18	15.22	15.10	15.17	15.02	15.07	14.64
6	15.37	16.05	15.89	15.92	15.97	15.71	15.20
7	18.33	18.01	17.85	18.15	17.77	17.42	17.55
8	19.60	19.17	18.93	19.18	19.07	18.71	17.93
9	15.23	14.84	14.69	14.86	14.57	14.25	13.52
10	9.87	10.15	10.09	10.19	10.02	9.50	9.60
11	8.41	7.89	7.84	7.89	7.84	7.89	8.47
12	3.60	3.63	3.66	3.61	3.69	3.85	4.19
Total		127.90	127.19	127.75	126.88	125.50	124.38

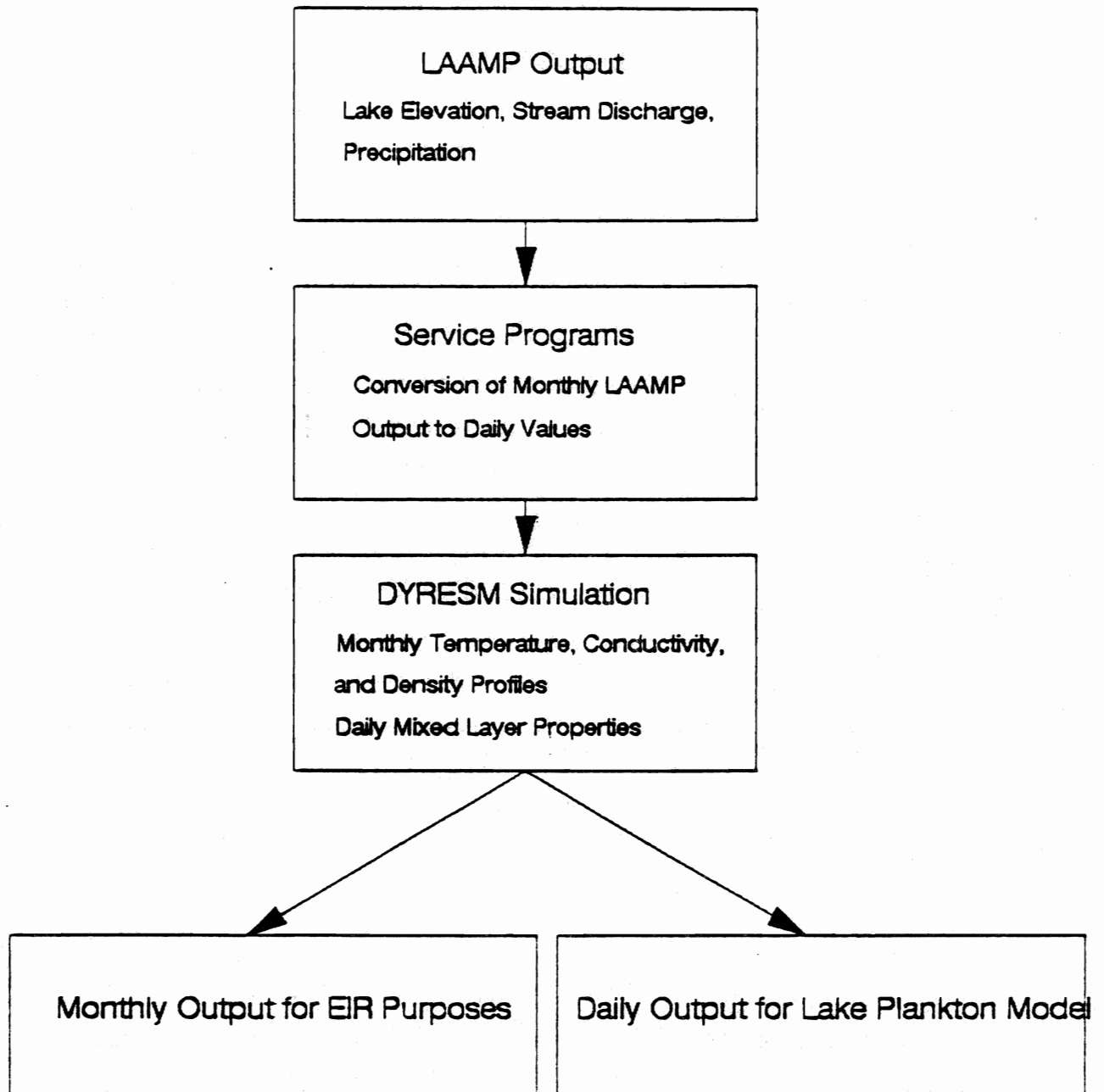
Table 2. Monthly evaporation totals for 1983 to 1990 simulation of Mono Lake.

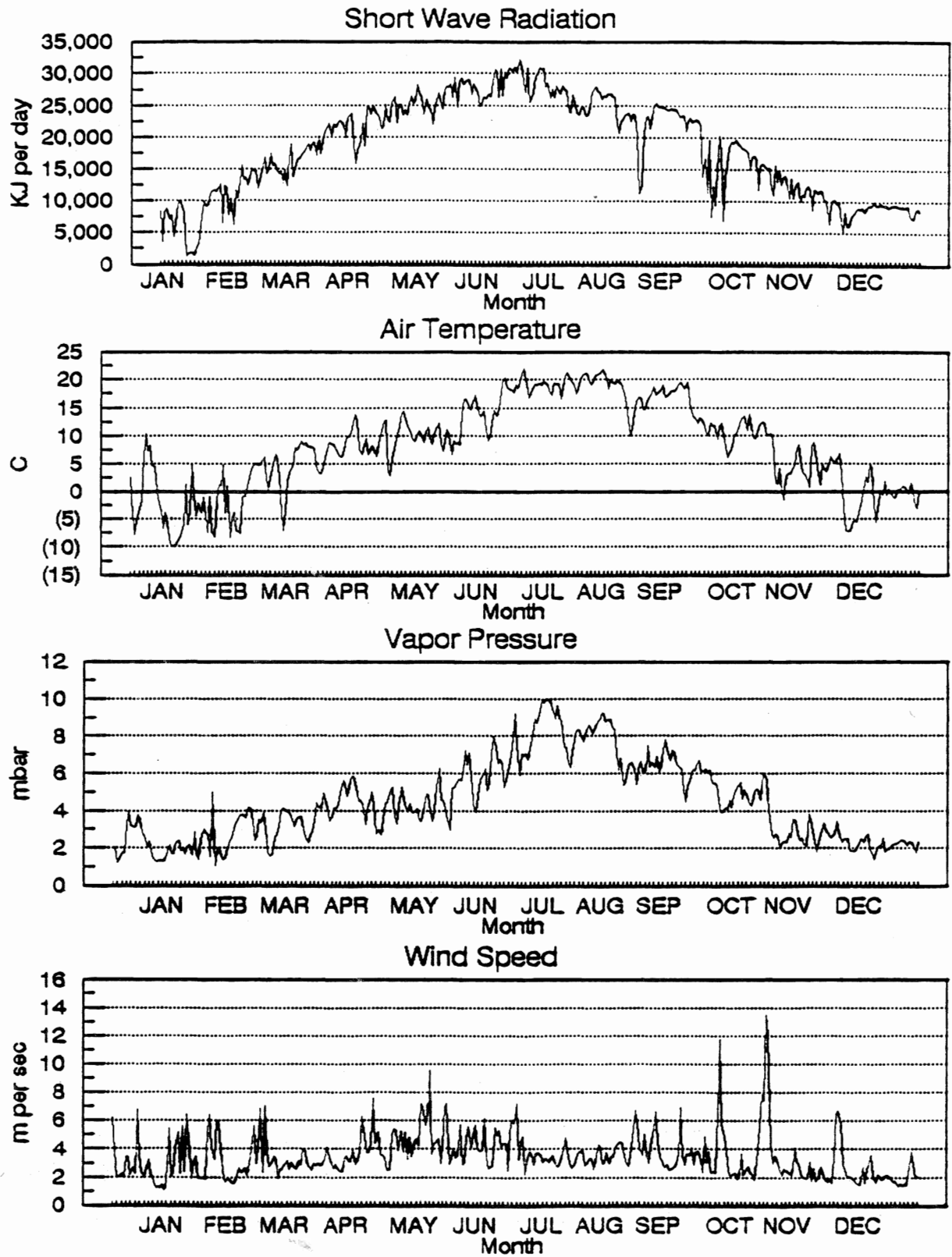
Month	1983 (in)	1984 (in)	1985 (in)	1986 (in)	1987 (in)	1988 (in)	1989 (in)
1		1.36	1.38	1.41	1.40	1.44	1.54
2		1.35	1.35	1.35	1.37	1.40	1.45
3		2.36	2.44	2.37	2.37	2.34	2.28
4	3.80	3.96	3.93	3.83	3.89	3.91	3.90
5	5.98	5.99	5.95	5.97	5.91	5.93	5.76
6	6.05	6.32	6.26	6.27	6.29	6.18	5.98
7	7.22	7.09	7.03	7.15	6.99	6.86	6.91
8	7.72	7.55	7.45	7.55	7.51	7.37	7.06
9	6.00	5.84	5.78	5.85	5.74	5.61	5.32
10	3.89	4.00	3.97	4.01	3.94	3.74	3.78
11	3.31	3.10	3.09	3.11	3.09	3.11	3.34
12	1.42	1.43	1.44	1.42	1.45	1.52	1.65
Total		50.35	50.07	50.29	49.95	49.41	48.97

Table 3. Monthly evaporation averages for the 1983 to 1990 simulation of Mono Lake.

Month	Simulation			LAAMP		
	Average (in)	Average (cm)	% of Simulated Yearly Total	Average (in)	Average (cm)	% of LAAMP Yearly Total
1	1.42	3.61	2.85	1.80	4.57	3.75
2	1.38	3.50	2.77	1.28	3.24	2.66
3	2.36	6.00	4.74	1.05	2.67	2.19
4	3.89	9.88	7.80	2.06	5.24	4.30
5	5.93	15.06	11.89	4.20	10.67	8.75
6	6.19	15.73	12.42	5.69	14.46	11.86
7	7.03	17.87	14.11	6.36	16.14	13.24
8	7.46	18.94	14.96	7.88	20.01	16.41
9	5.73	14.57	11.51	6.31	16.03	13.15
10	3.90	9.92	7.83	5.45	13.85	11.36
11	3.16	8.03	6.35	3.82	9.69	7.95
12	1.47	3.75	2.96	2.10	5.34	4.38
Total	49.84	126.60	100.00	48.00	121.92	100.00

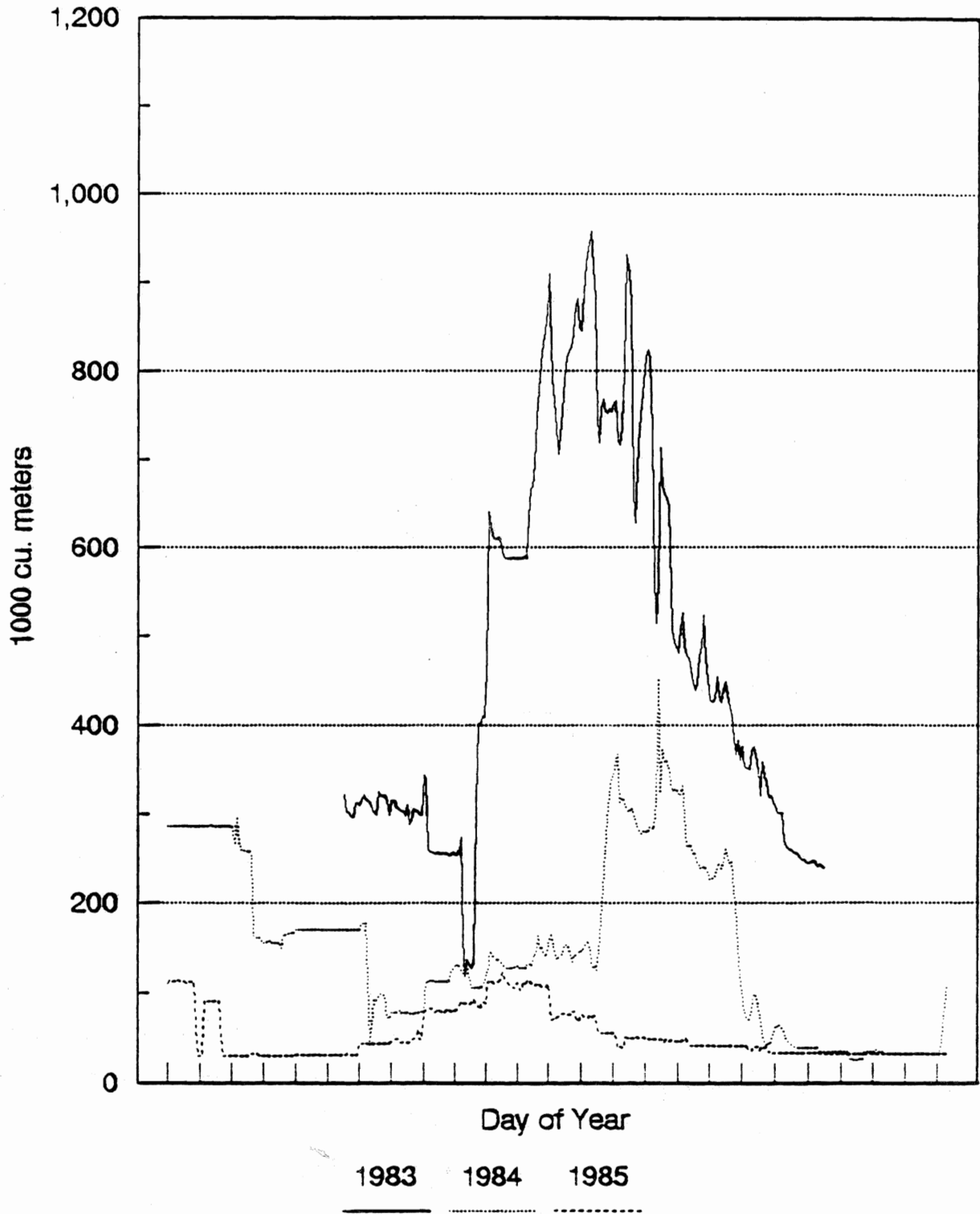
Schematic of Mono Lake Vertical Mixing Model





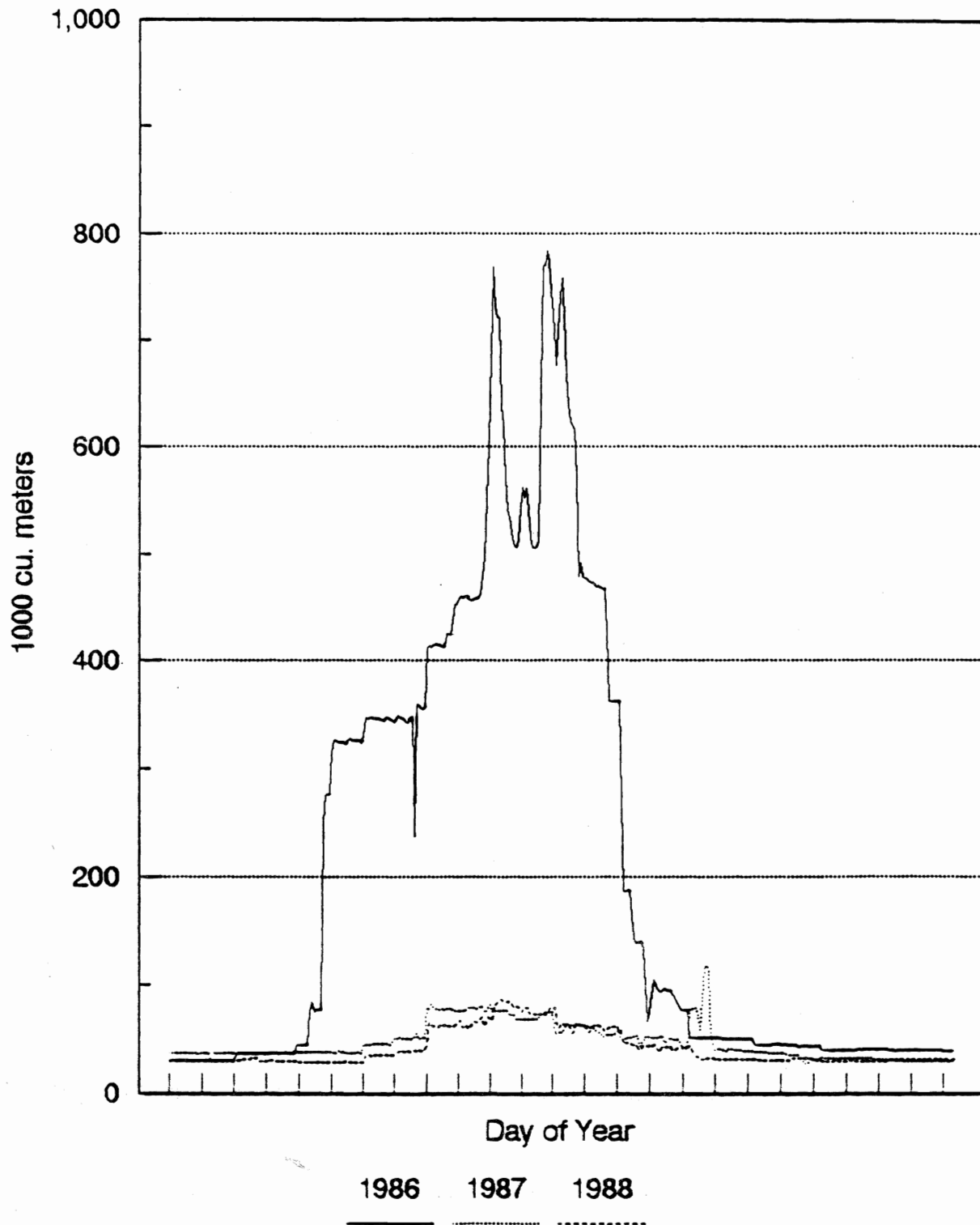
Gauged Stream Discharges

Rush, Parker, Walker, Lee Vining and Mill Creeks



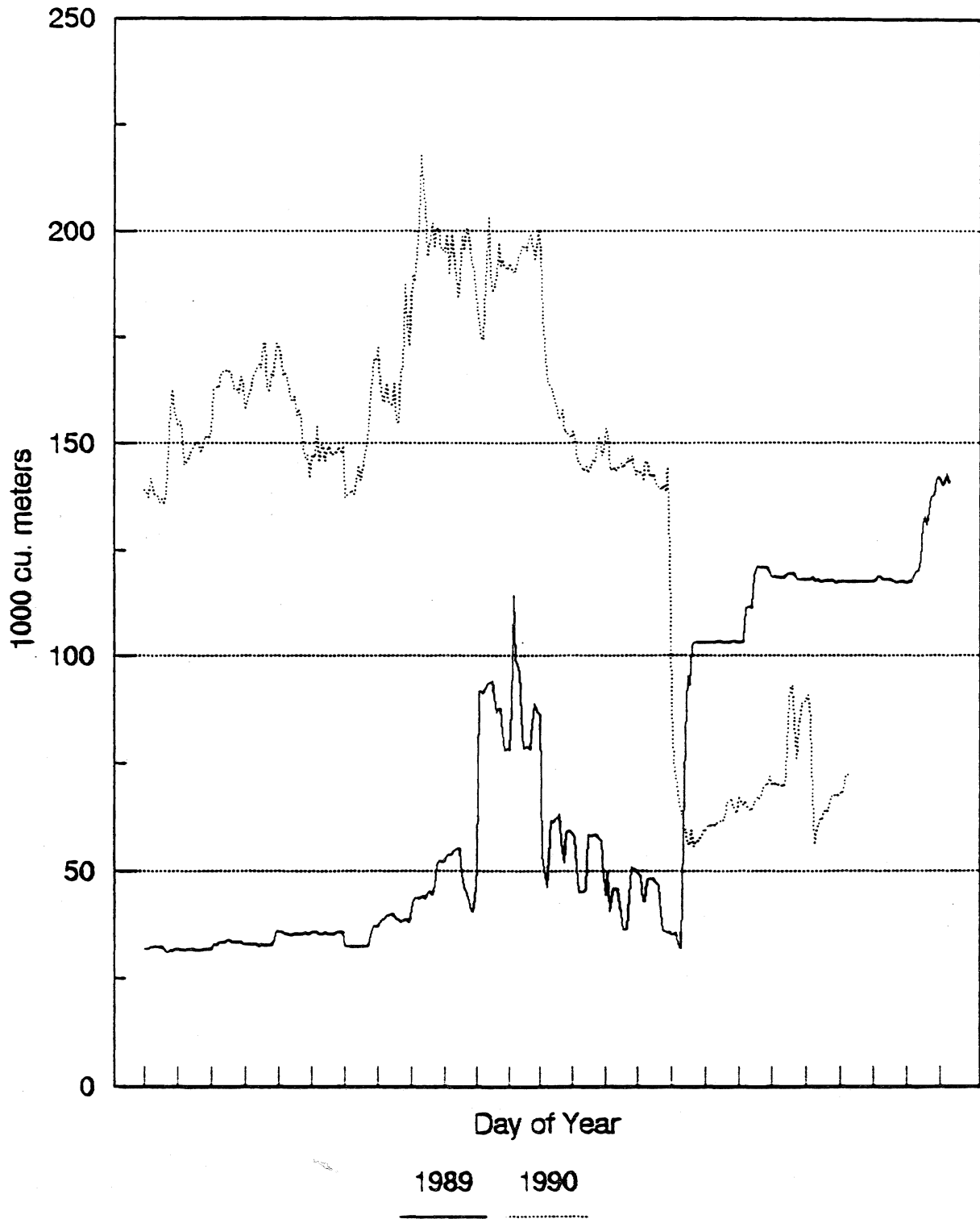
Gauged Stream Discharges

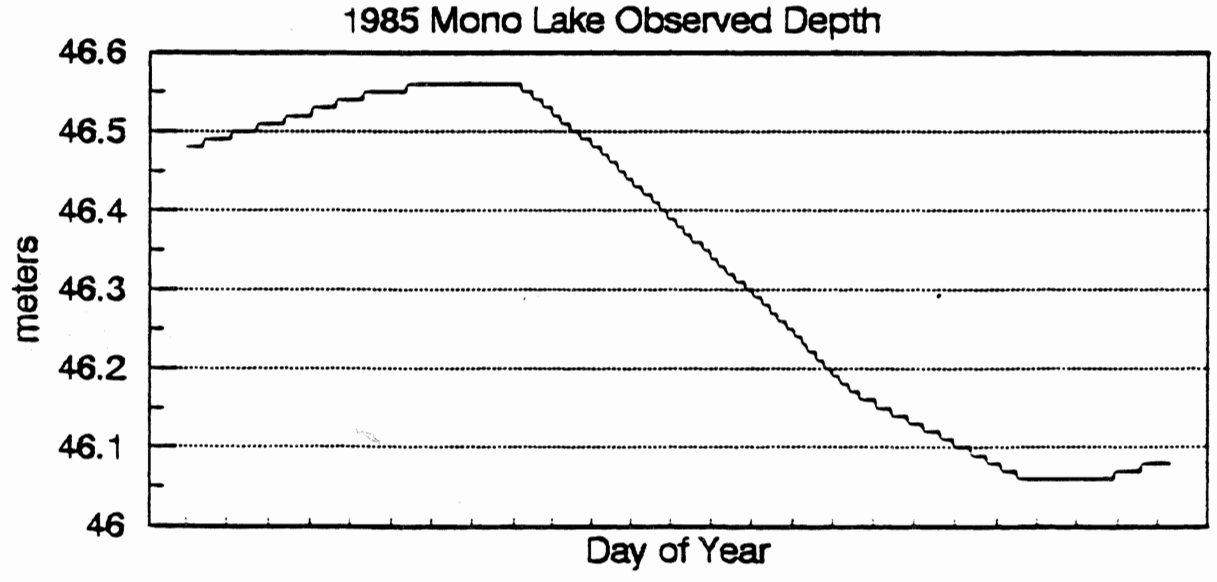
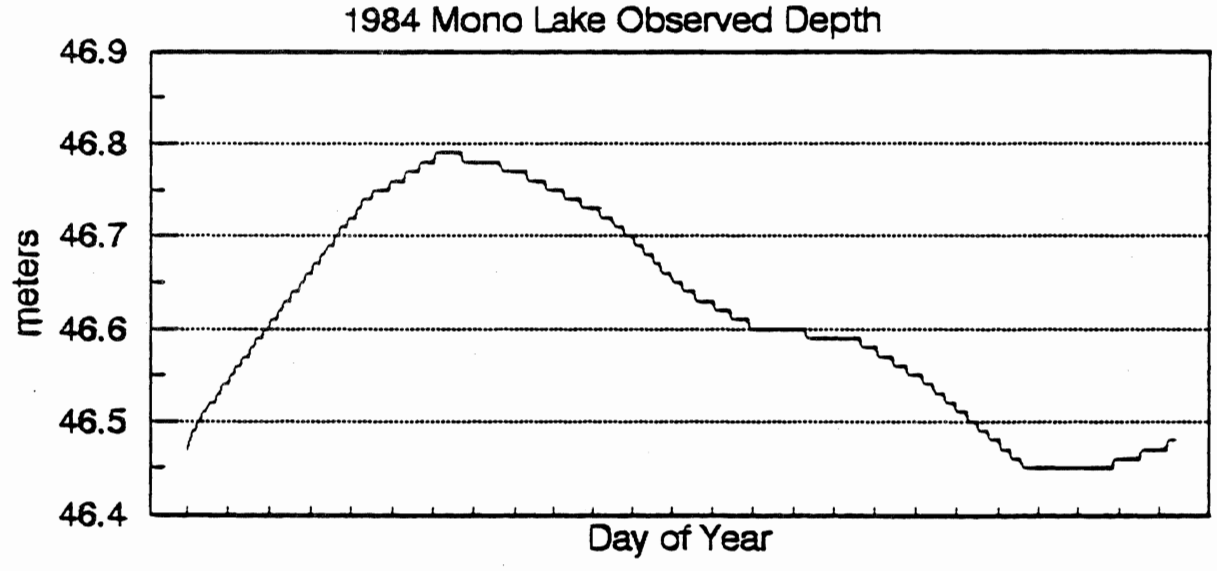
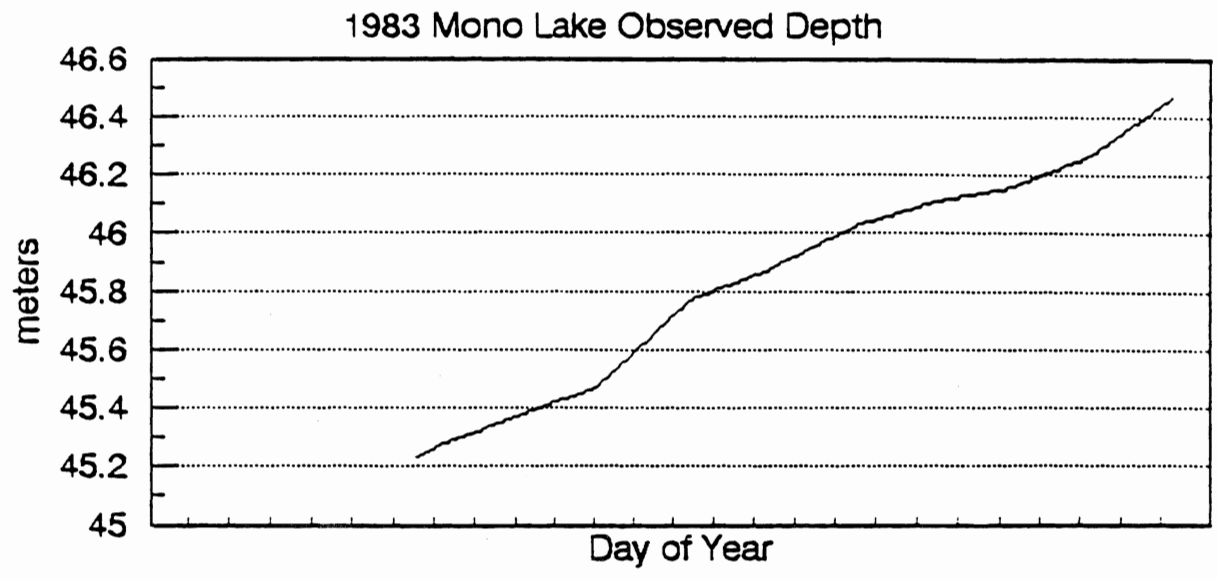
Rush, Parker, Walker, Lee Vining and Mill Creeks

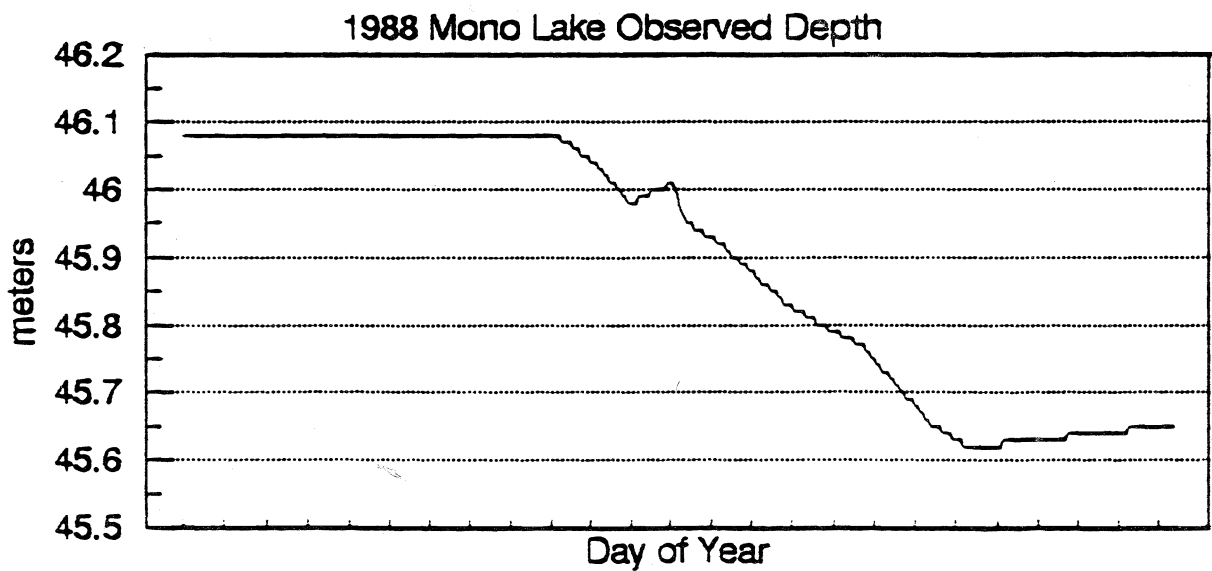
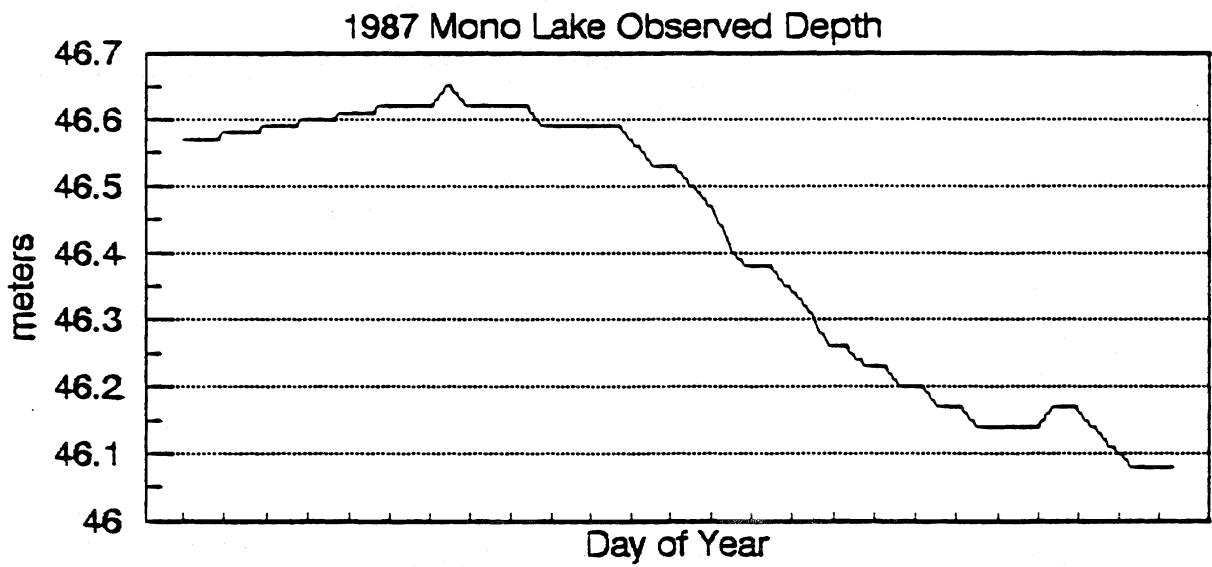
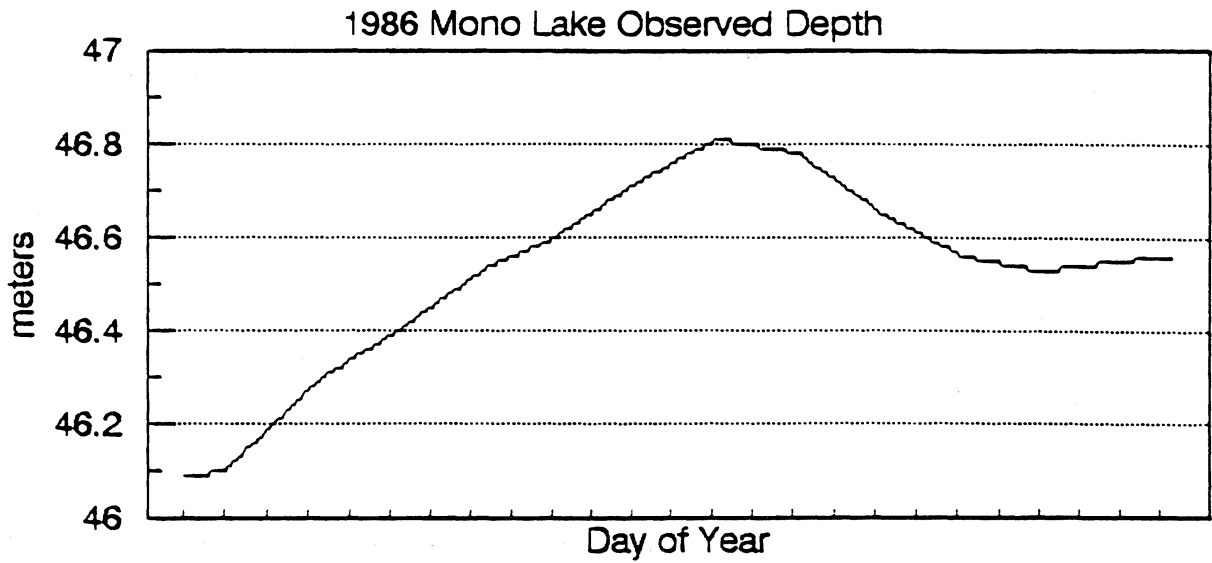


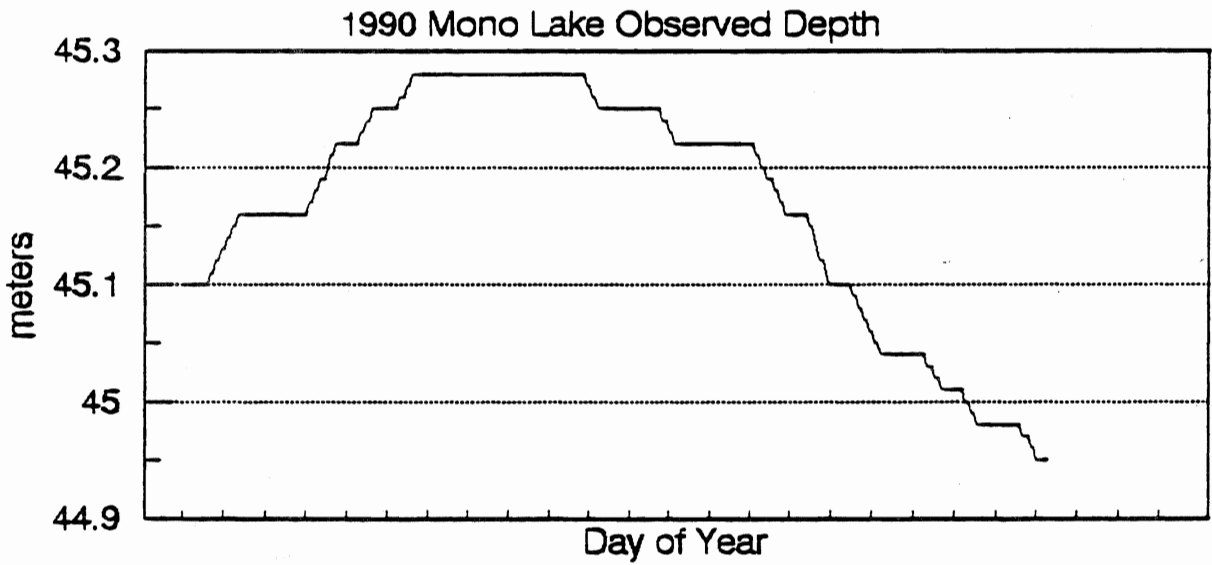
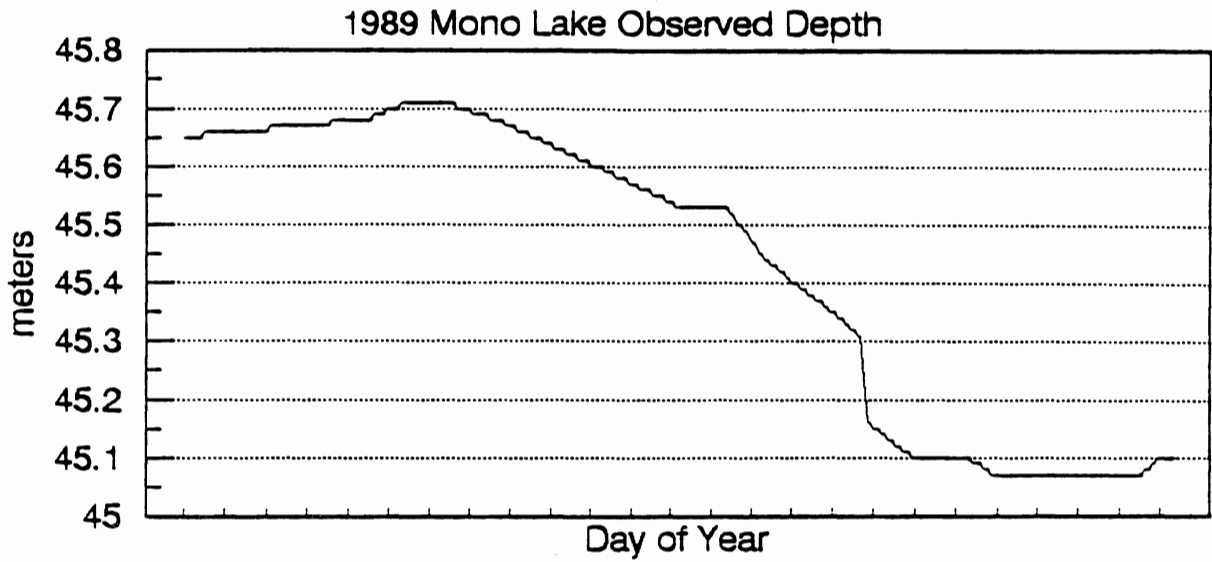
Gauged Stream Discharges

Rush, Parker, Walker, Lee Vining and Mill Creeks









Temperature Plot of Mono Lake

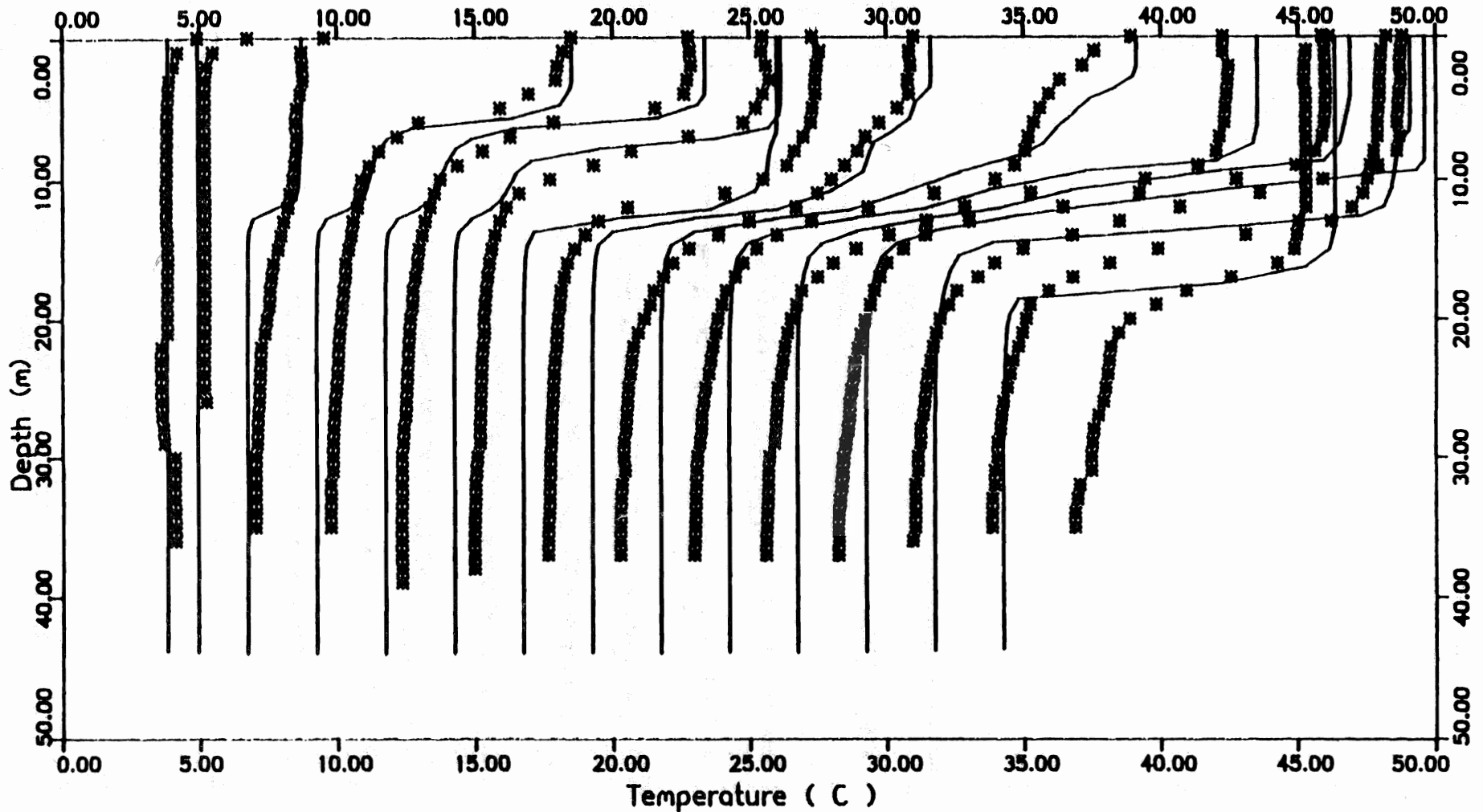


Figure 9

Julian dates of profiles in order:

90027 90073 90112 90145 90172 90208 90250
 90046 90099 90129 90155 90193 90223 90295

Offset between each Temperature plot is : 2.50 degrees C

Conductivity Plot of Mono Lake

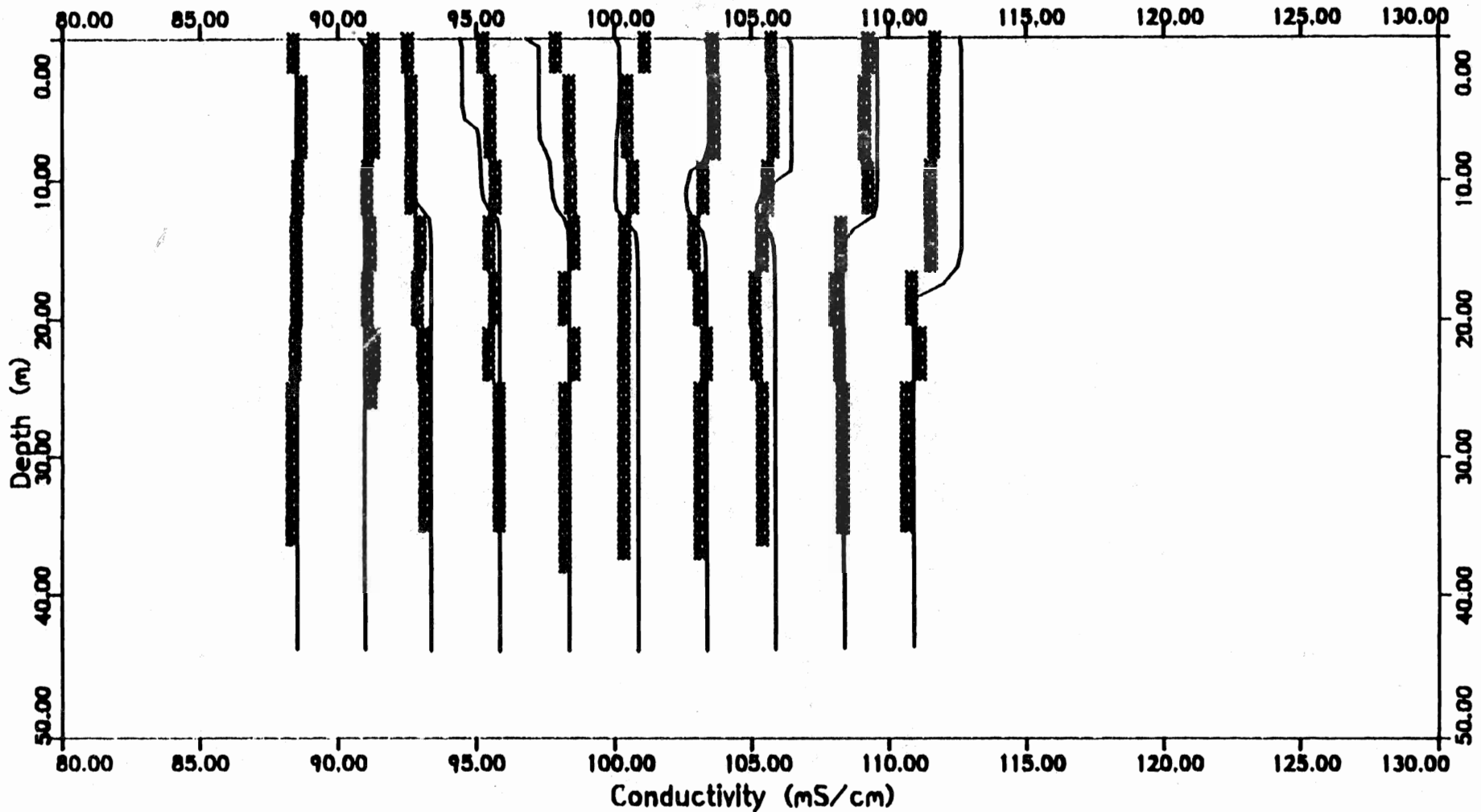


Figure 10

Julian dates of profiles in order:

90027 90073 90129 90193 90250
 90046 90099 90155 90223 90295

Offset between each Conductivity plot is : 2.50 mS/cm

Density Plot of Mono Lake

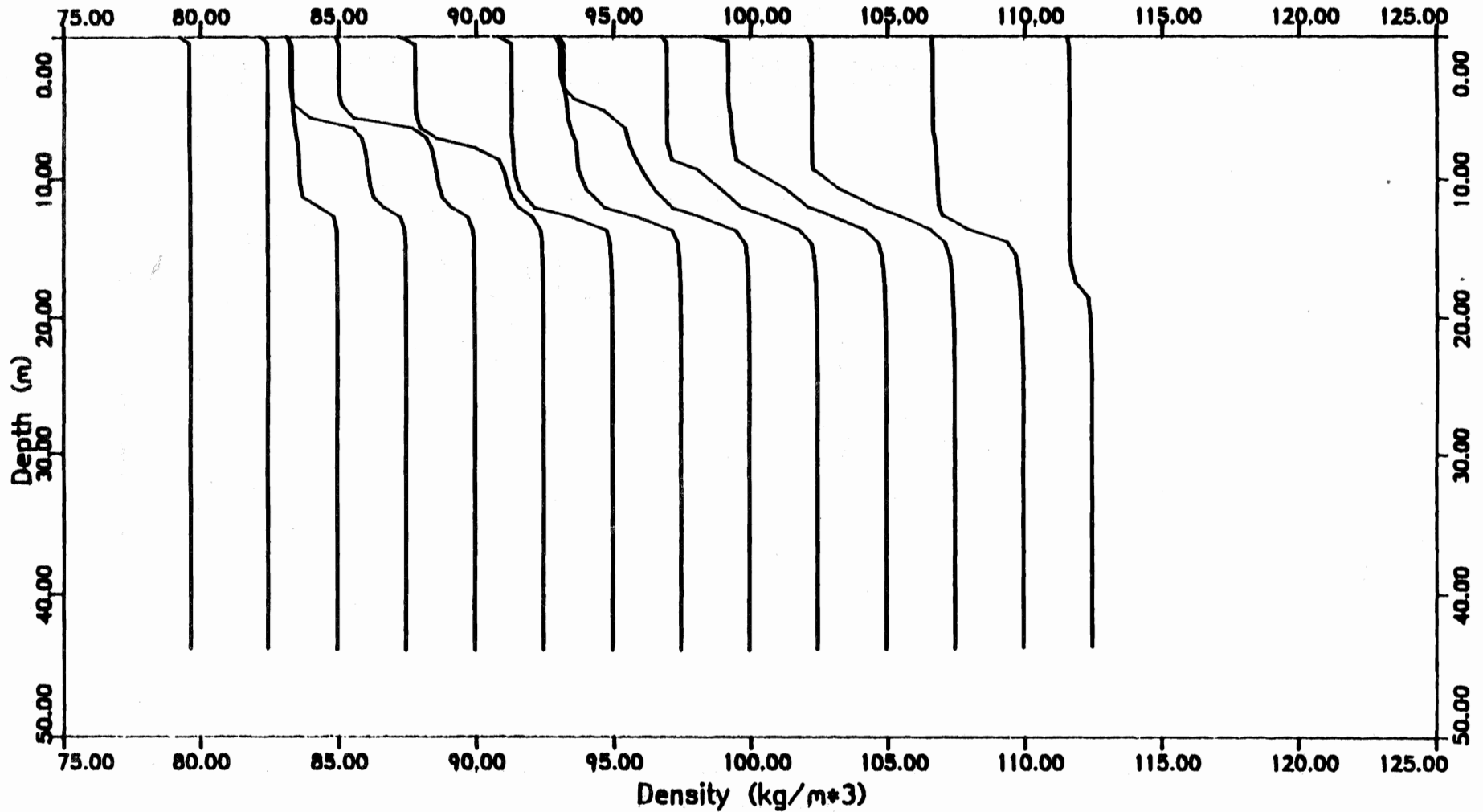


Figure 11

Julian dates of profiles in order:

90027 90073 90112 90145 90172 90208 90250
 90046 90099 90129 90155 90193 90223 90295

Offset between each Density plot is : 2.50 kg/m³

**Simulated and Observed Surface Temperatures
Evaporation Sensitivity Analysis
Days 90027 to 90175**

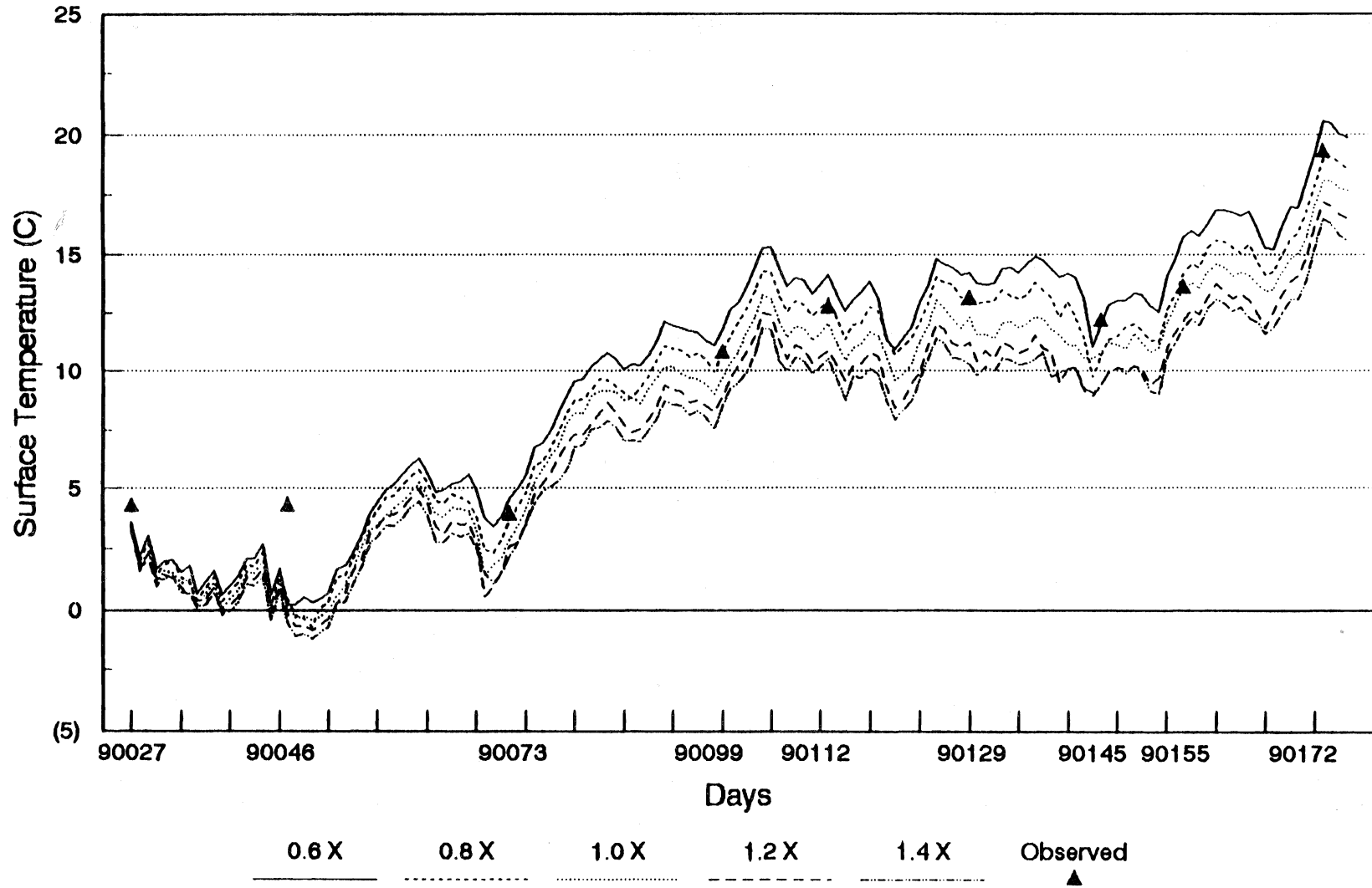


Figure 12

**Simulated and Observed Surface Temperatures
Evaporation Sensitivity Analysis
Days 90176 to 90320**

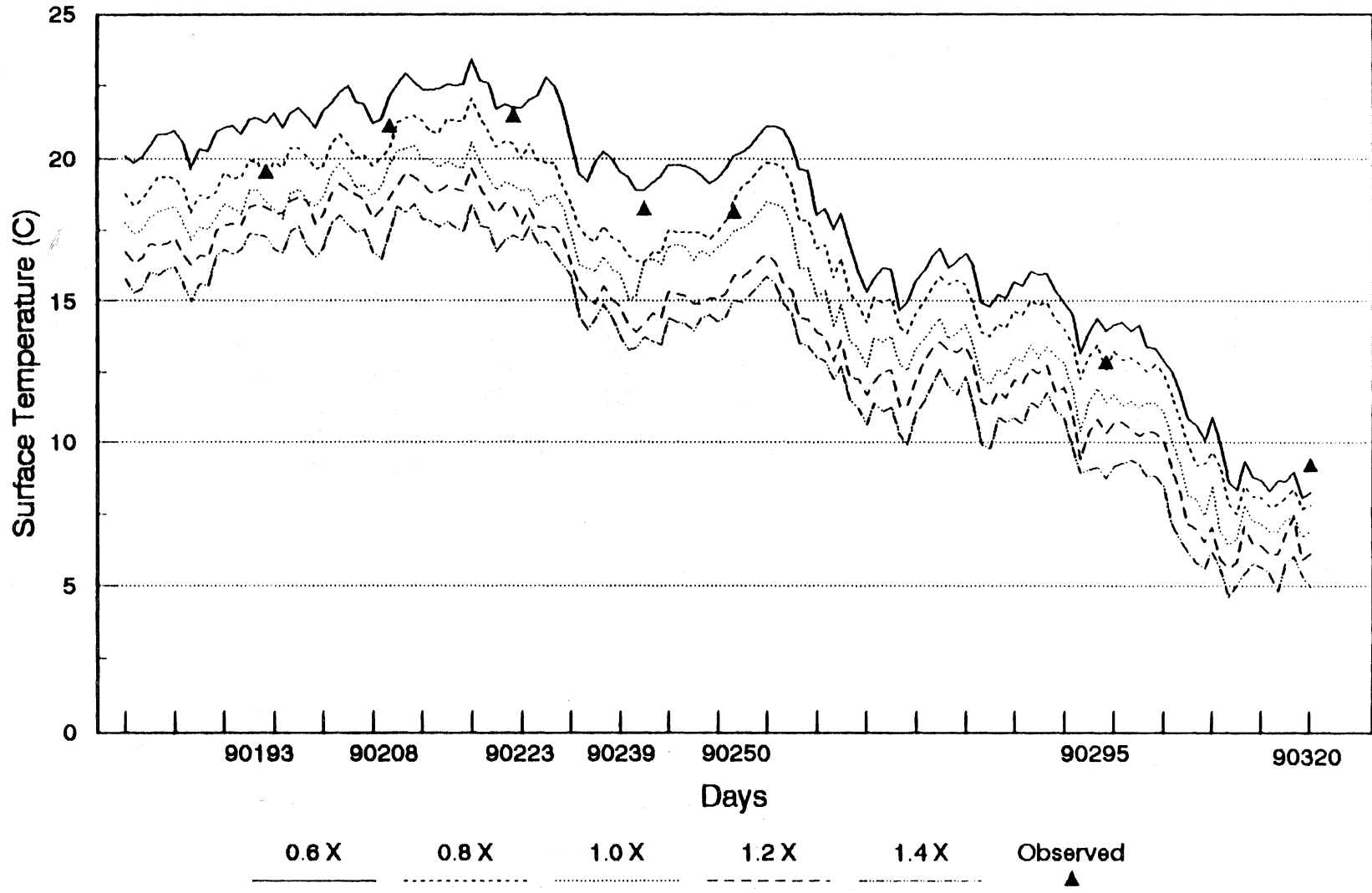


Figure 13

**Relative Change in Average Monthly
Surface Temperature
Evaporation Sensitivity Analysis**

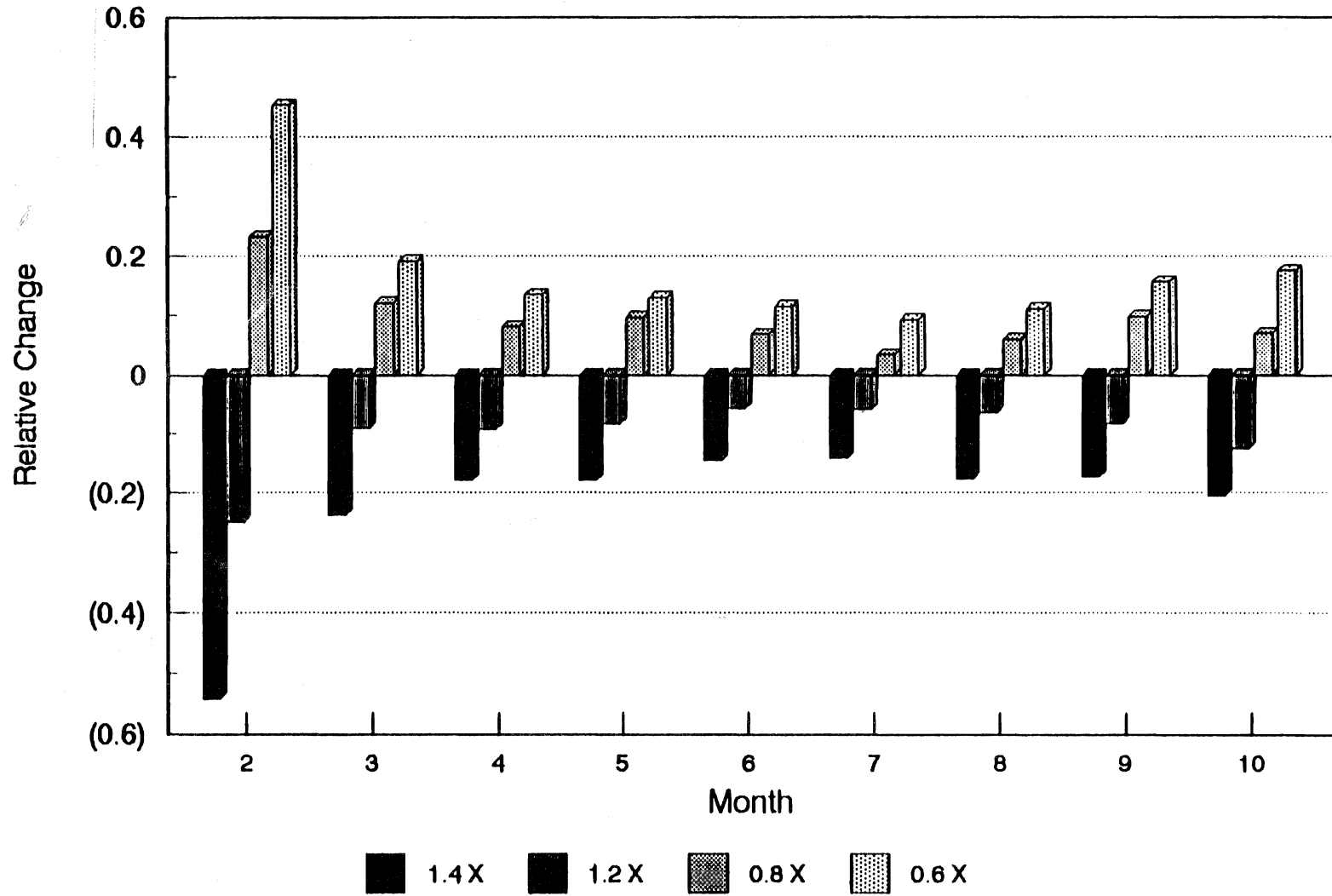


Figure 14

**Relative Change in Average Monthly
Saturation Vapor Pressure
Evaporation Sensitivity Analysis**

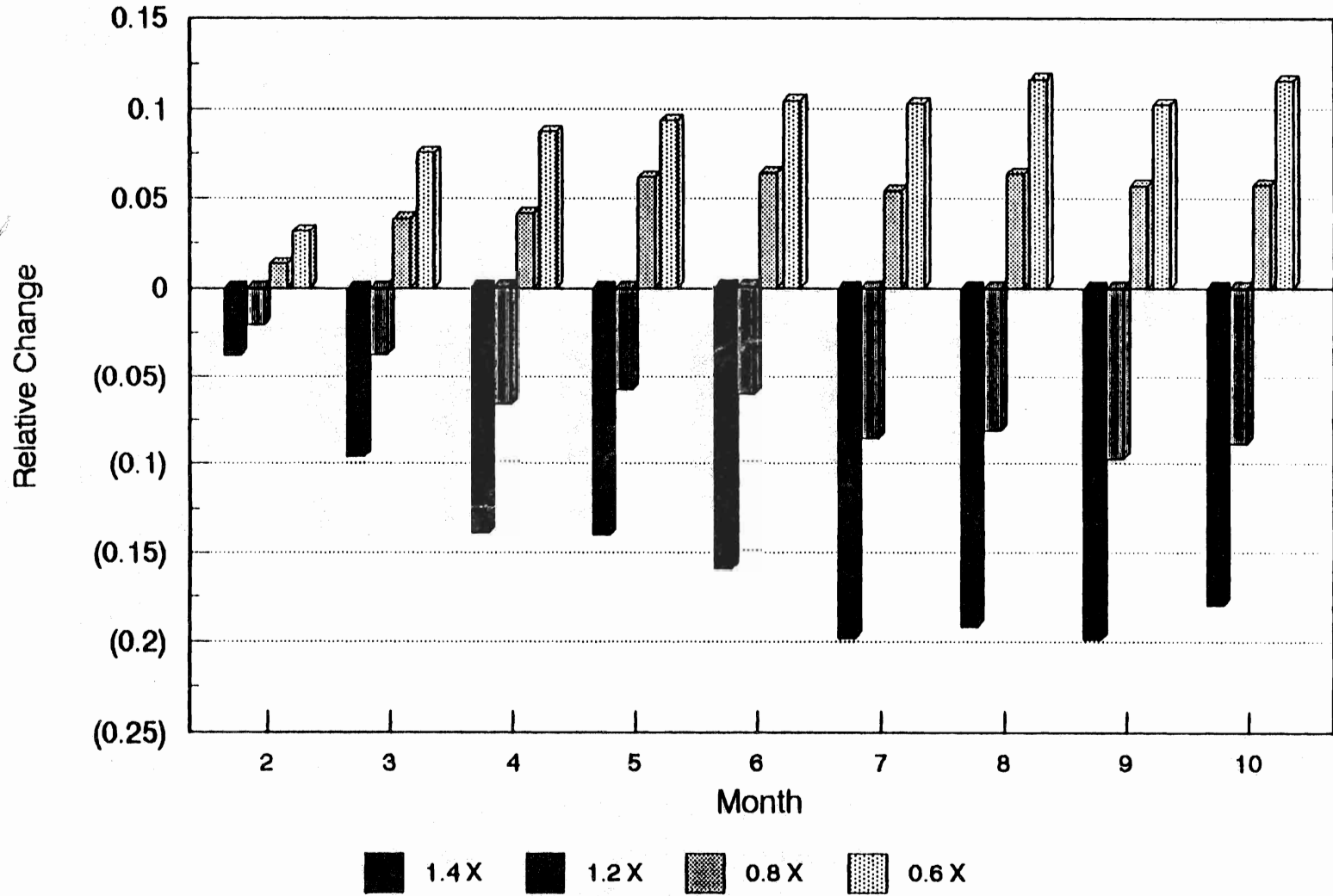


Figure 15

**Relative Change in Average Monthly
Mass of Evaporative Water Loss
Evaporation Sensitivity Analysis**

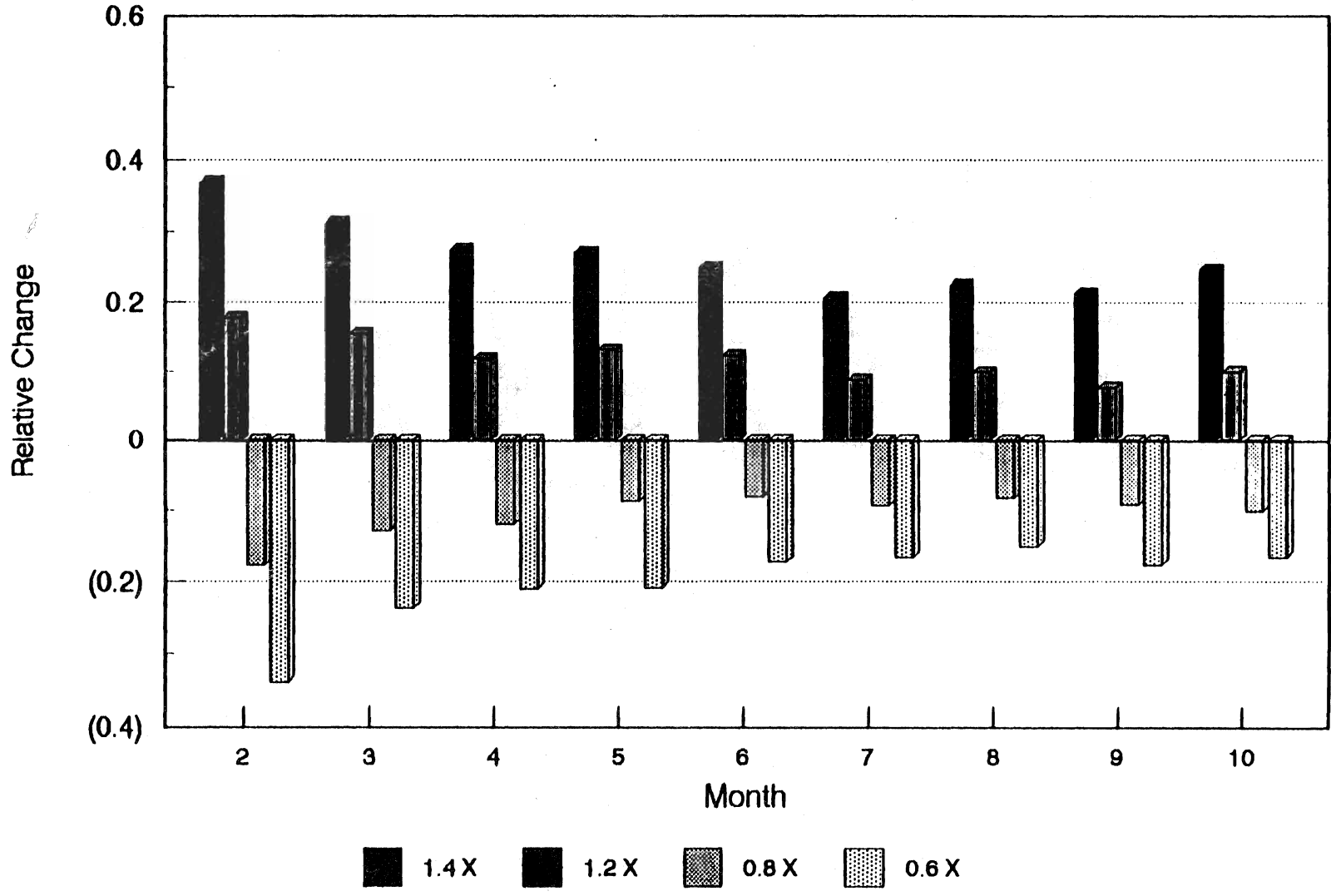


Figure 16

Temperature Plot of Mono Lake

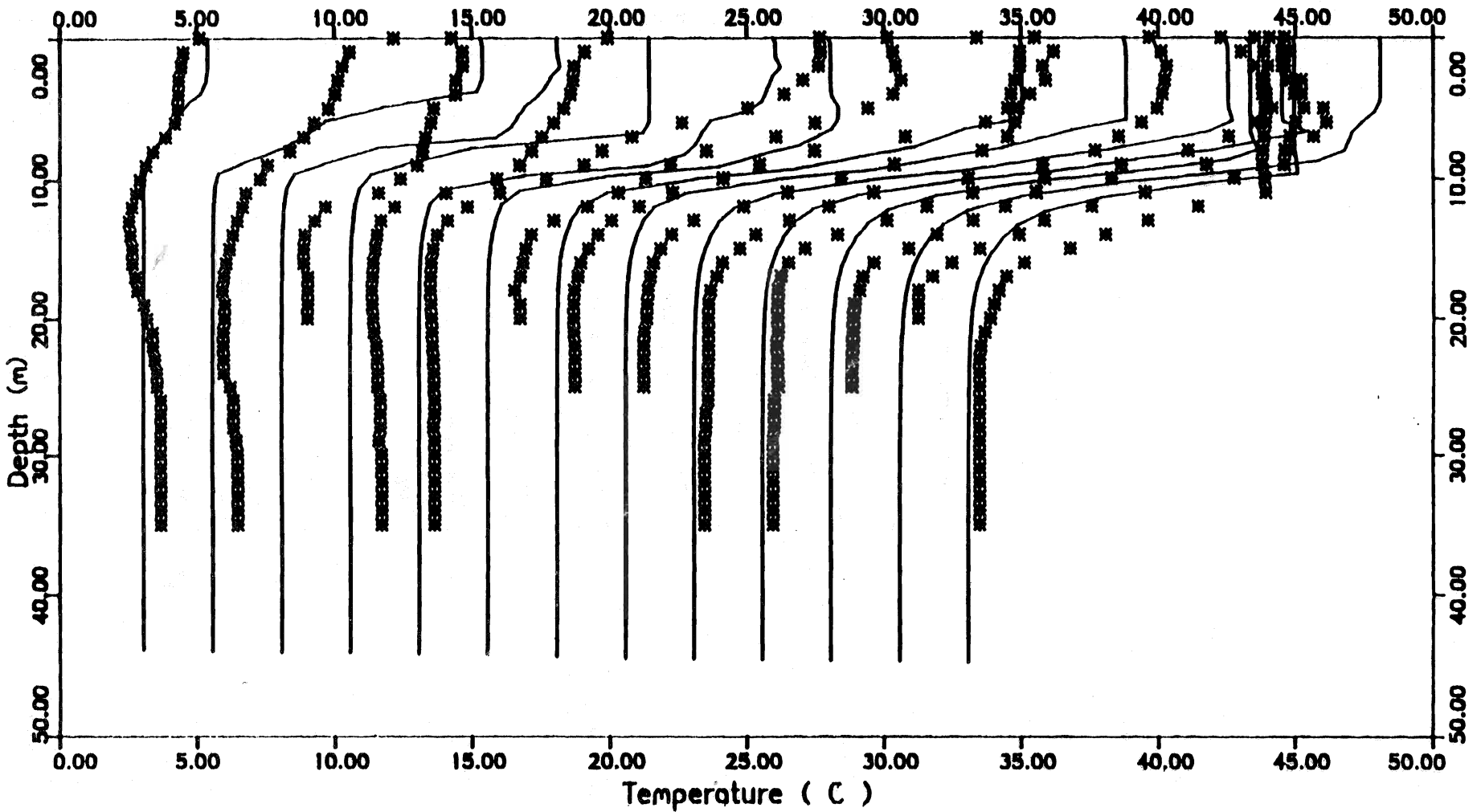


Figure 17

Julian dates of profiles in order:

- | | | | | | | |
|-------|-------|-------|-------|-------|-------|-------|
| 83084 | 83124 | 83158 | 83185 | 83214 | 83238 | 83291 |
| 83109 | 83137 | 83166 | 83195 | 83228 | 83255 | |

Offset between each Temperature plot is : 2.50 degrees C

Temperature Plot of Mono Lake

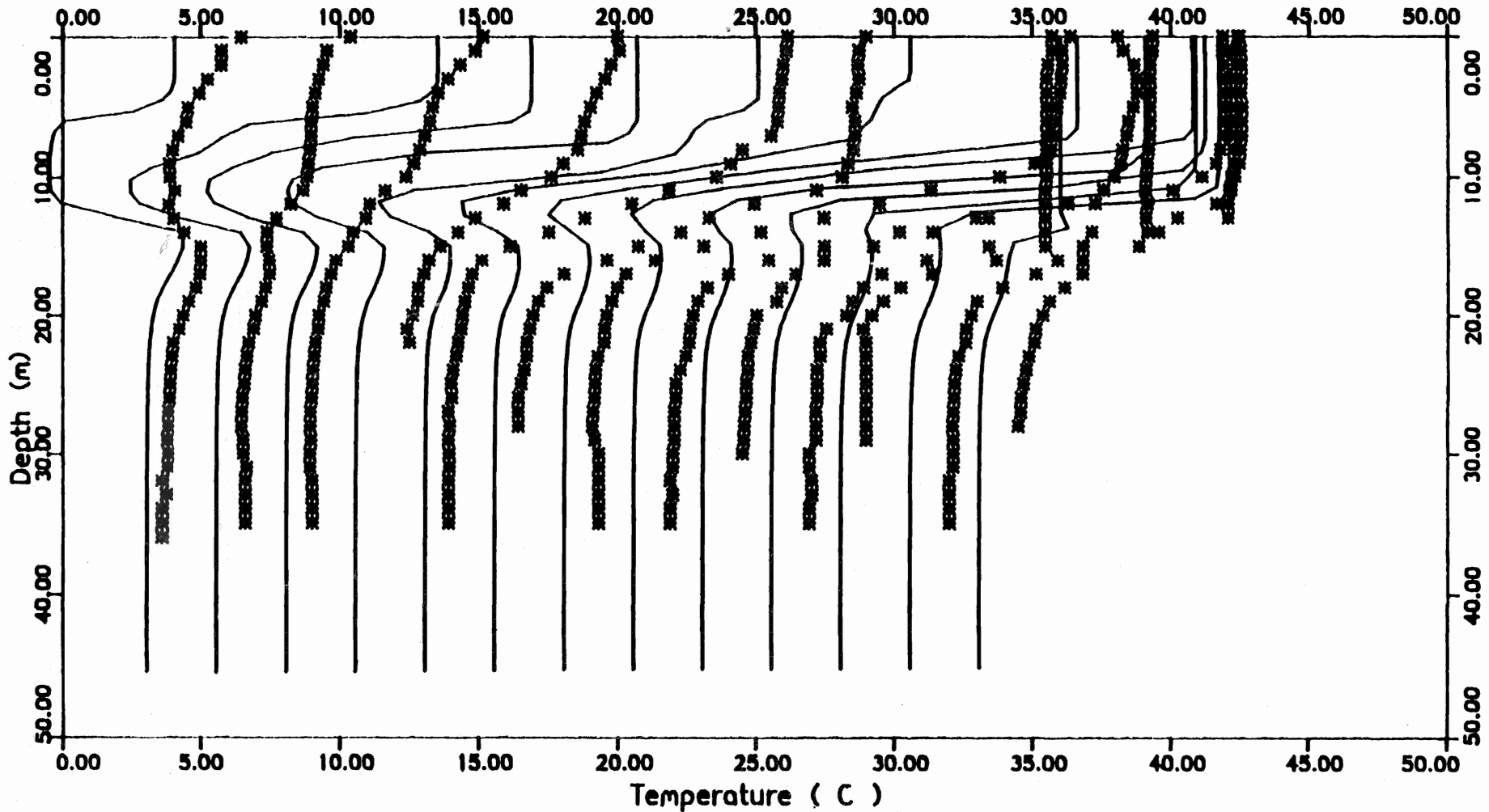


Figure 18

Julian dates of profiles in order:

84066 84113 84156 84198 84233 84269 84333
 84093 84131 84171 84219 84248 84297

Offset between each Temperature plot is : 2.50 degrees C

Temperature Plot of Mono Lake

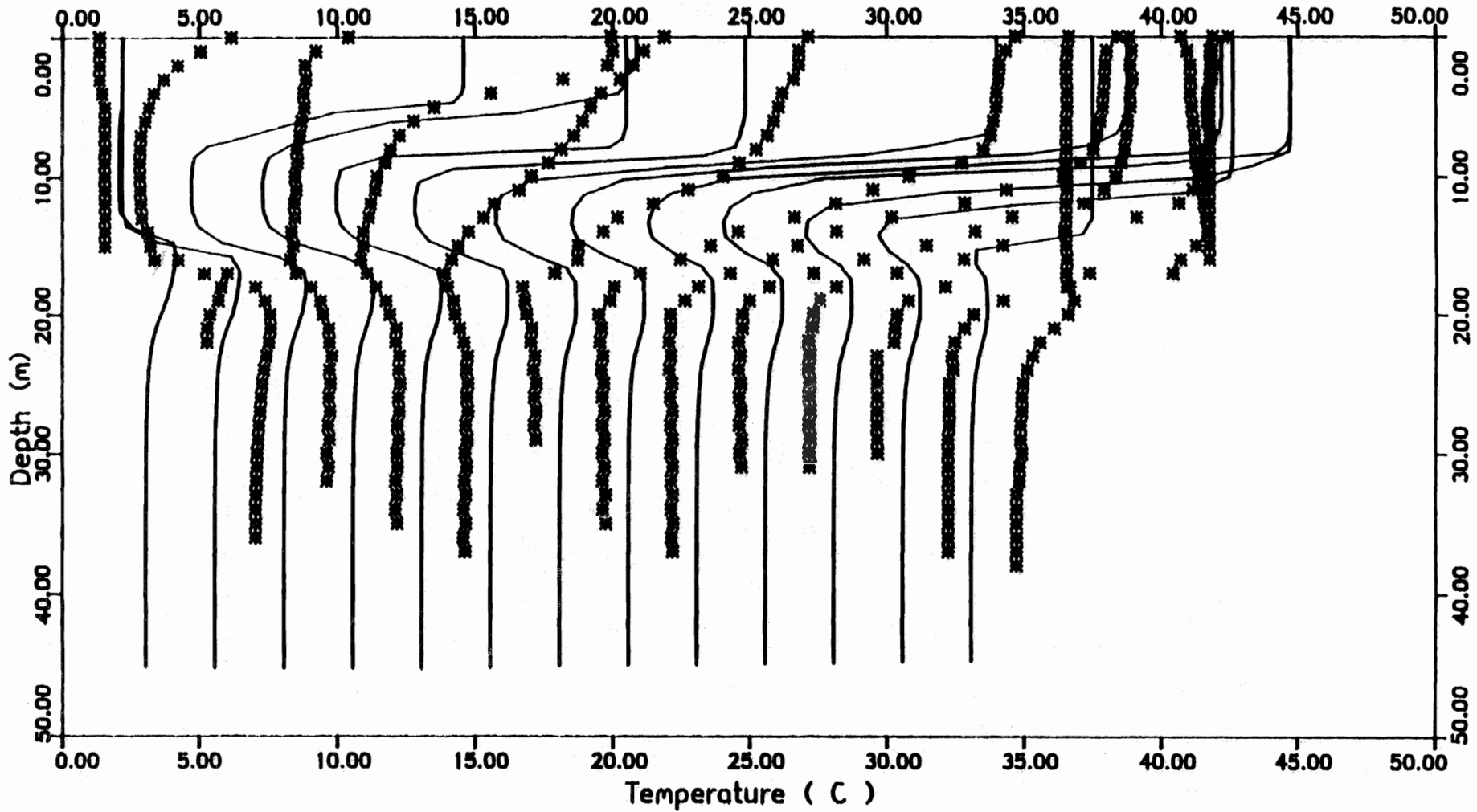


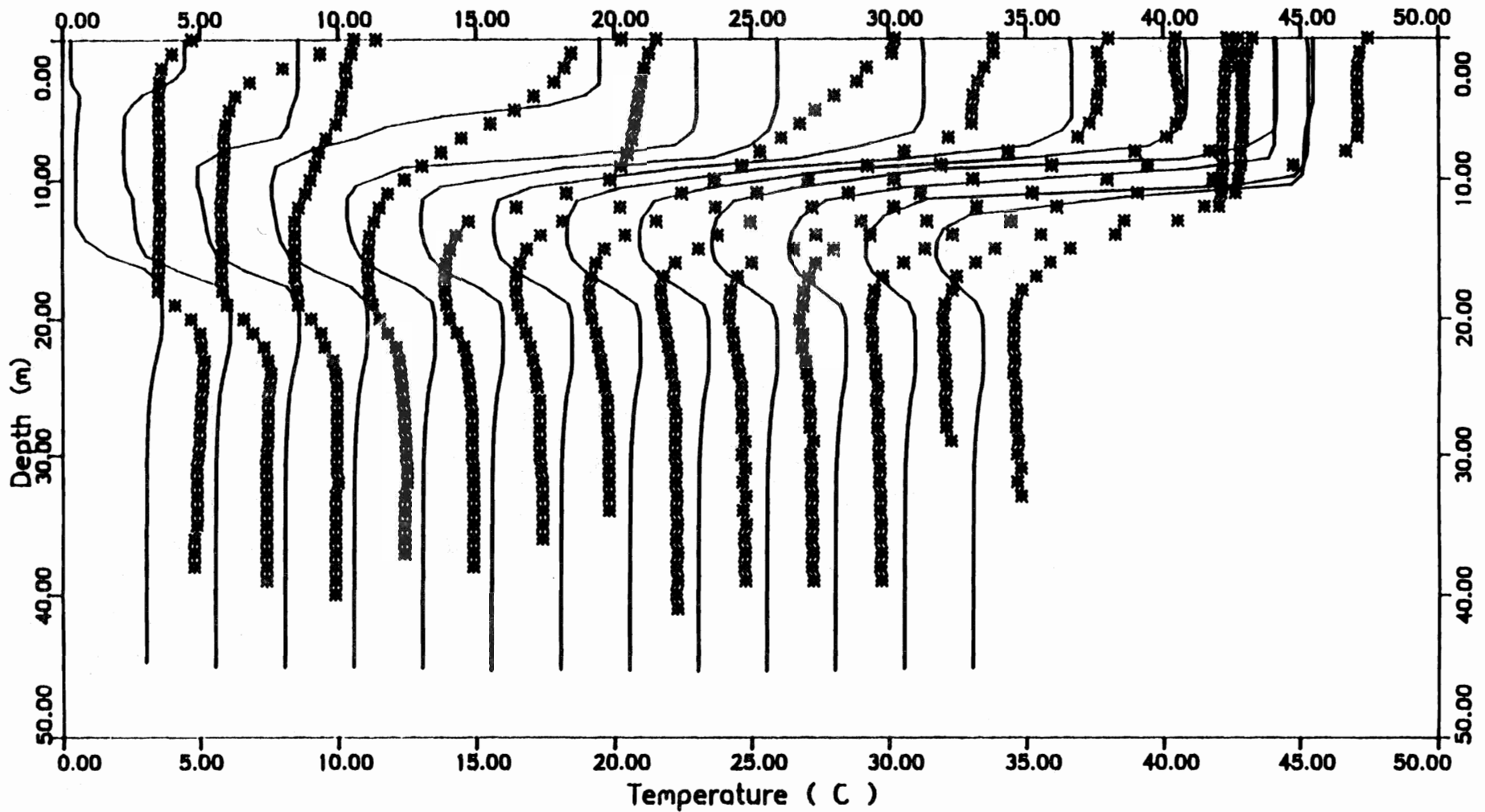
Figure 19

Julian dates of profiles in order:

- | | | | | | | |
|-------|-------|-------|-------|-------|-------|-------|
| 85007 | 85089 | 85120 | 85177 | 85213 | 85257 | 85330 |
| 85047 | 85103 | 85144 | 85193 | 85226 | 85283 | |

Offset between each Temperature plot is : 2.50 degrees C

Temperature Plot of Mono Lake



Julian dates of profiles in order:

86025 86073 86132 86163 86190 86233 86286
 86056 86101 86148 86178 86205 86262

Offset between each Temperature plot is : 2.50 degrees C

Figure 20

Temperature Plot of Mono Lake

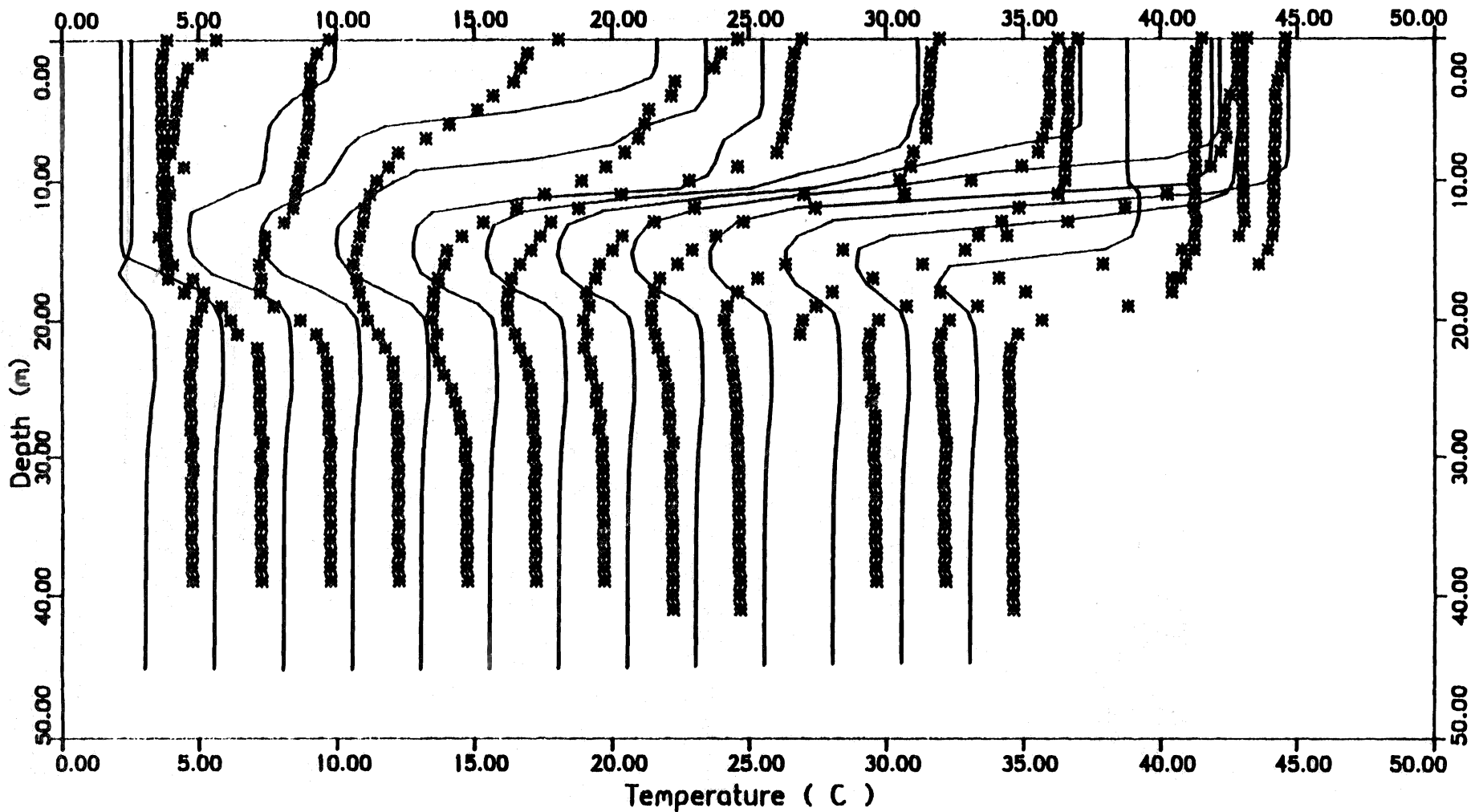


Figure 21

Julian dates of profiles in order:

87002 87076 87126 87169 87203 87257 87322

87038 87104 87149 87180 87234 87287

Offset between each Temperature plot is : 2.50 degrees C

Temperature Plot of Mono Lake

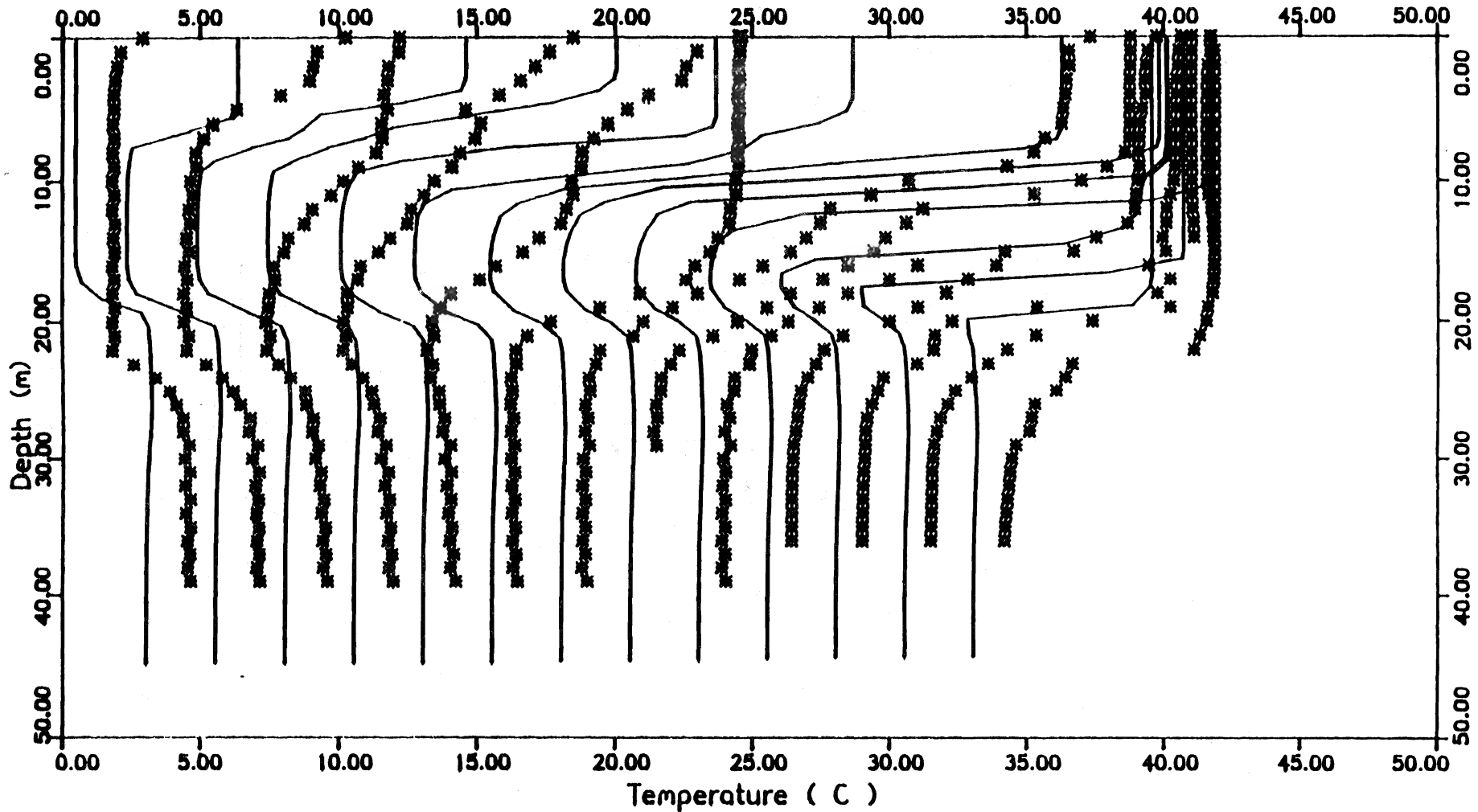


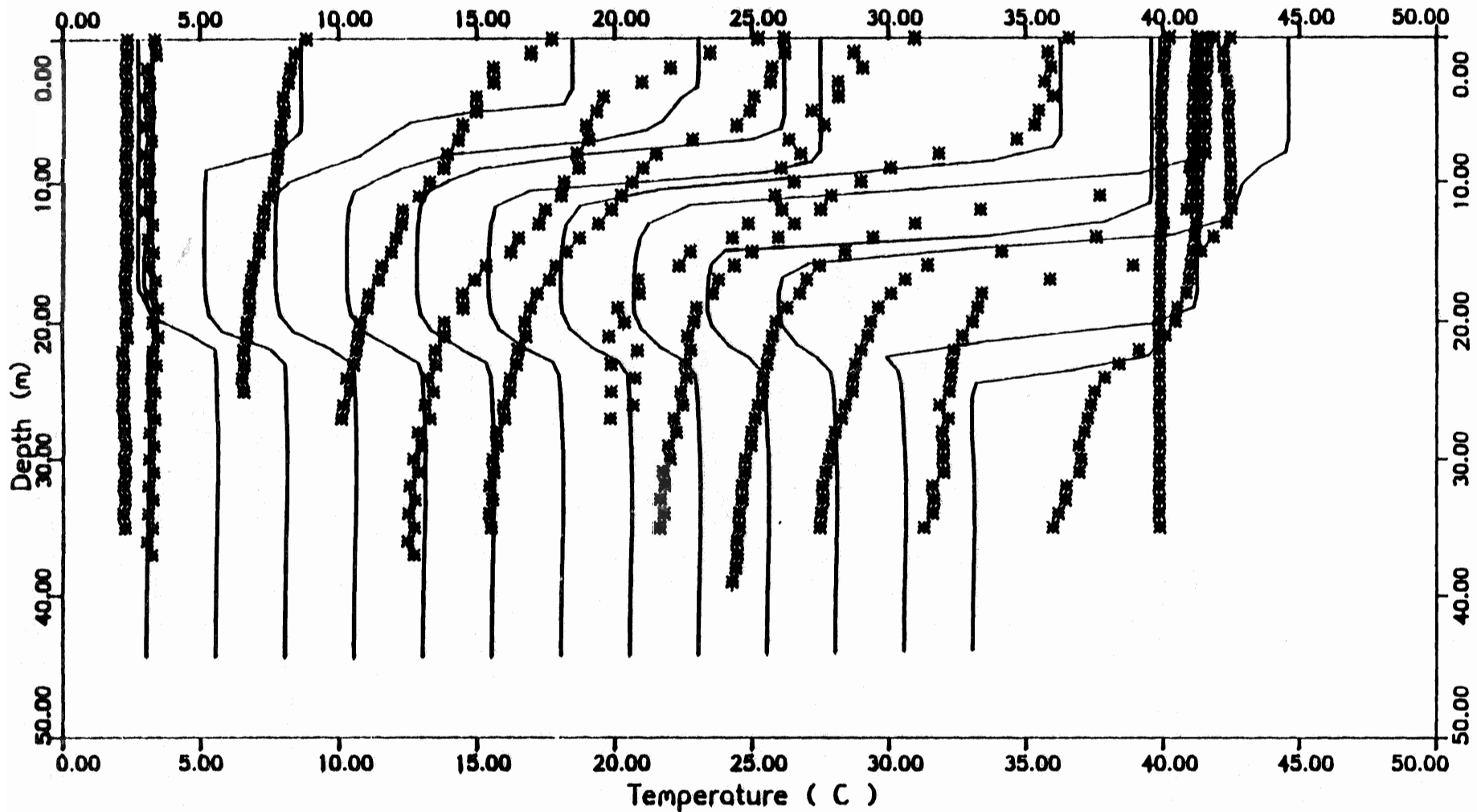
Figure 22

Julian dates of profiles in order:

88034 88088 88135 88196 88230 88278 88315
 88067 88102 88160 88215 88257 88298

Offset between each Temperature plot is ; 2.50 degrees C

Temperature Plot of Mono Lake



Julian dates of profiles in order:

89015 89067 89124 89152 89207 89256 89321
89046 89095 89136 89177 89238 89291

Offset between each Temperature plot is : 2.50 degrees C

Figure 23

Temperature Plot of Mono Lake

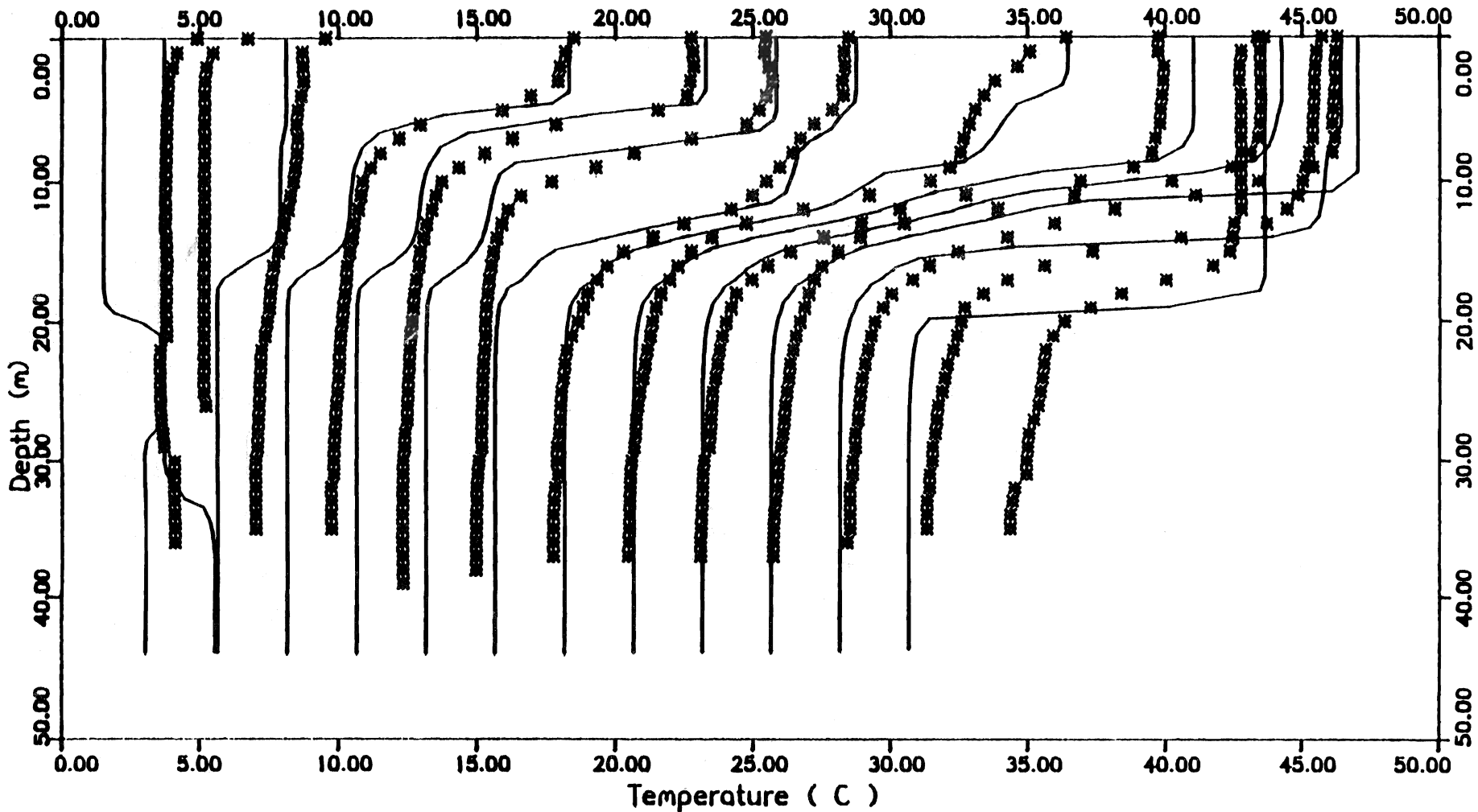


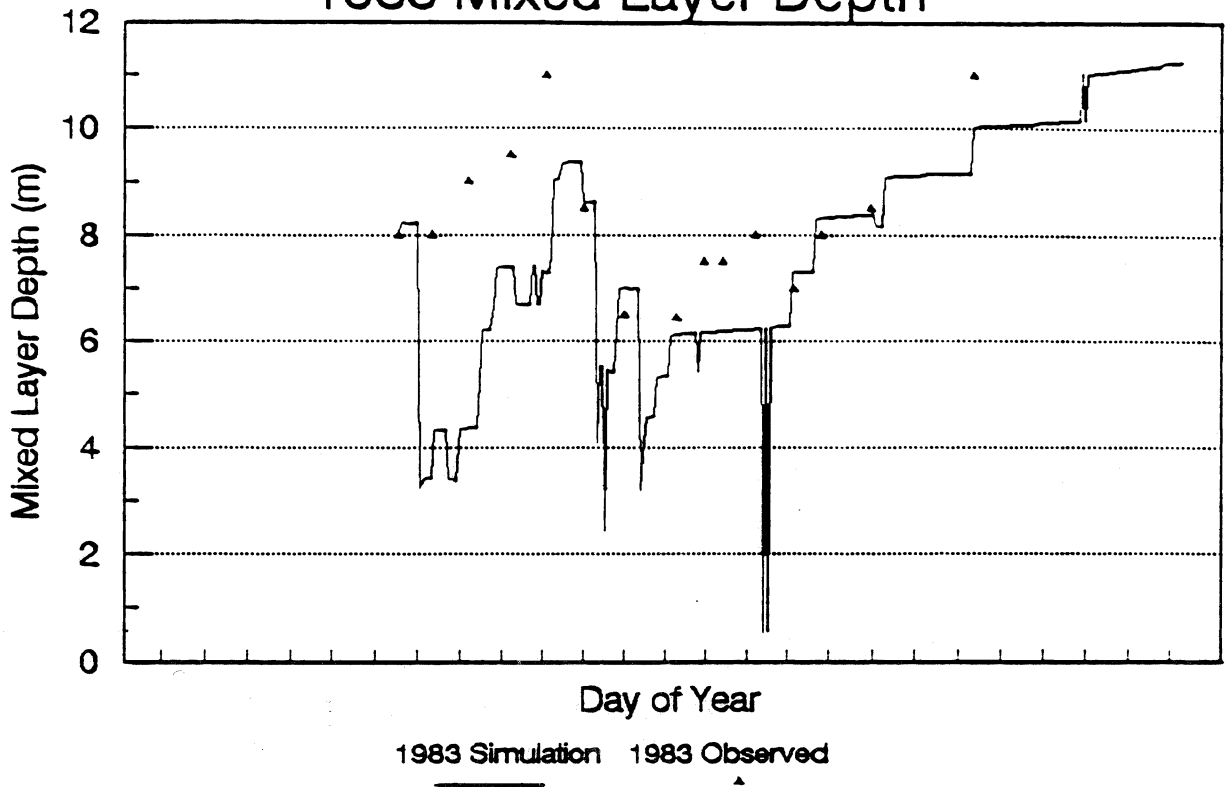
Figure 24

Julian dates of profiles in order:

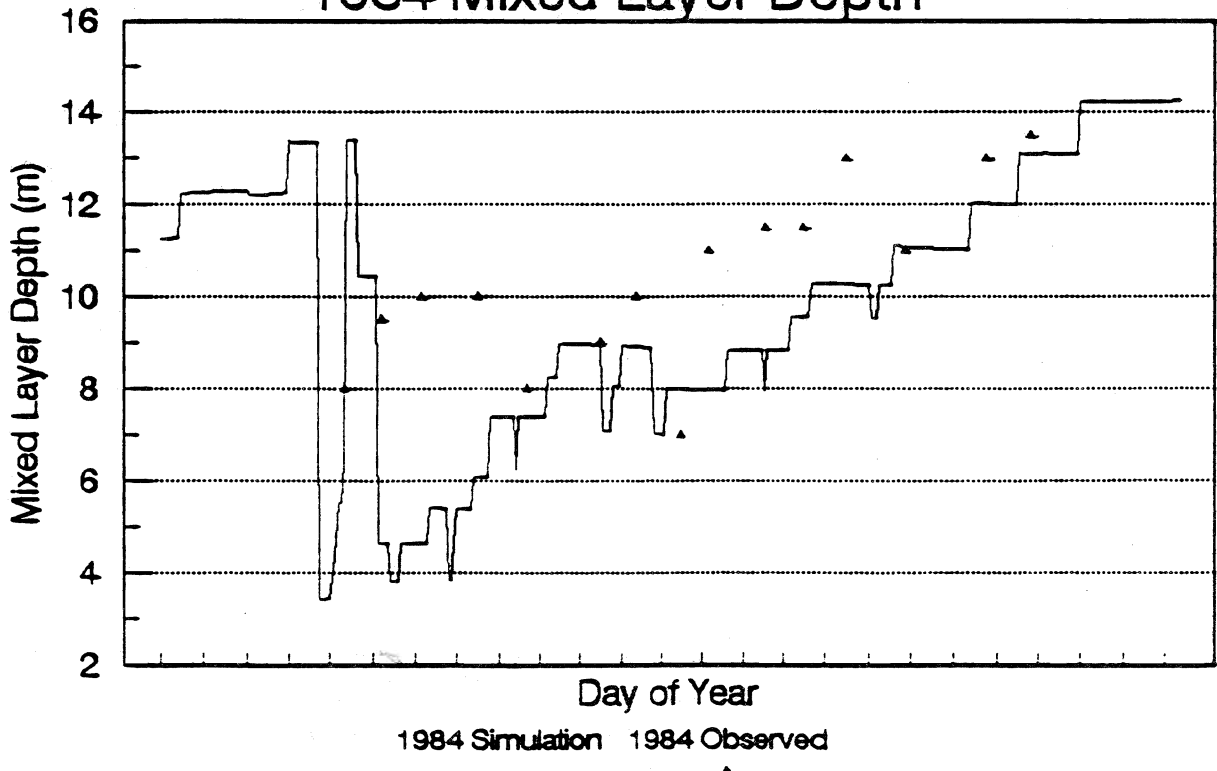
90027 90073 90112 90155 90193 90223 90295
90046 90099 90129 90172 90208 90250

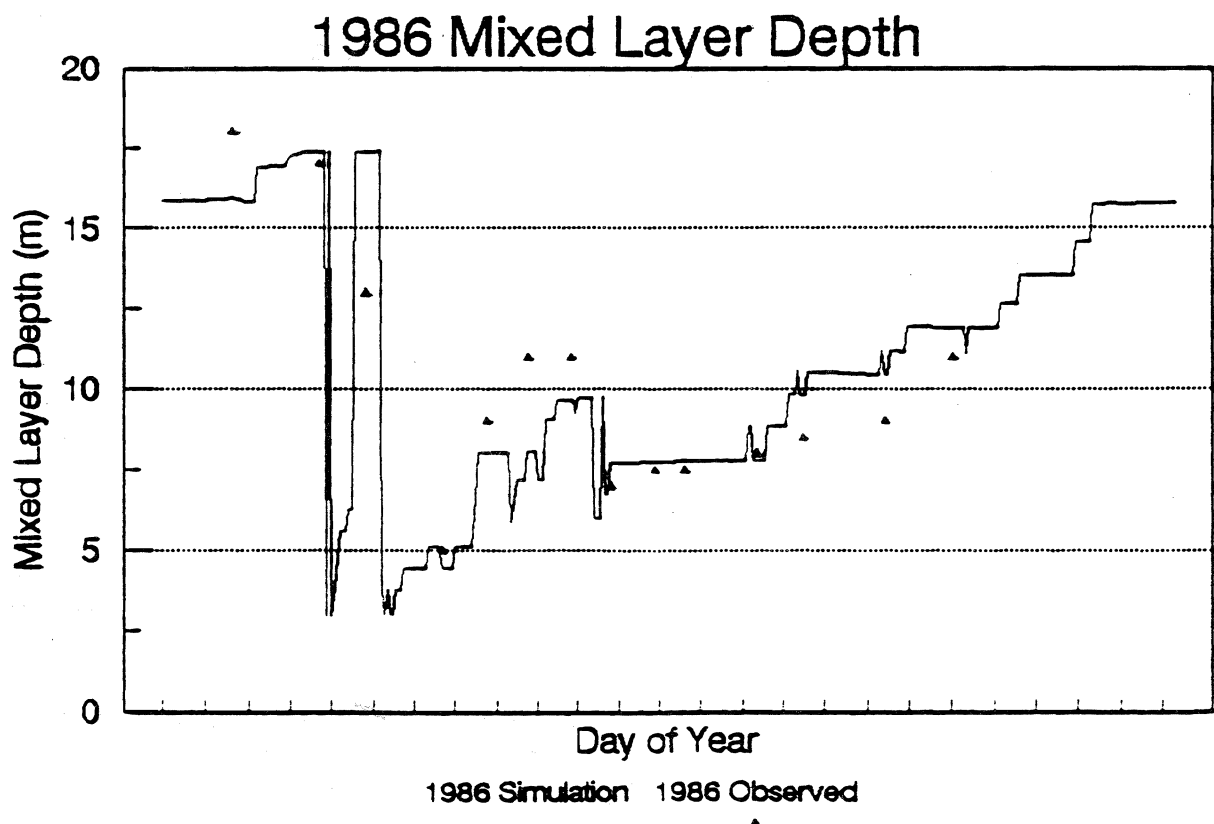
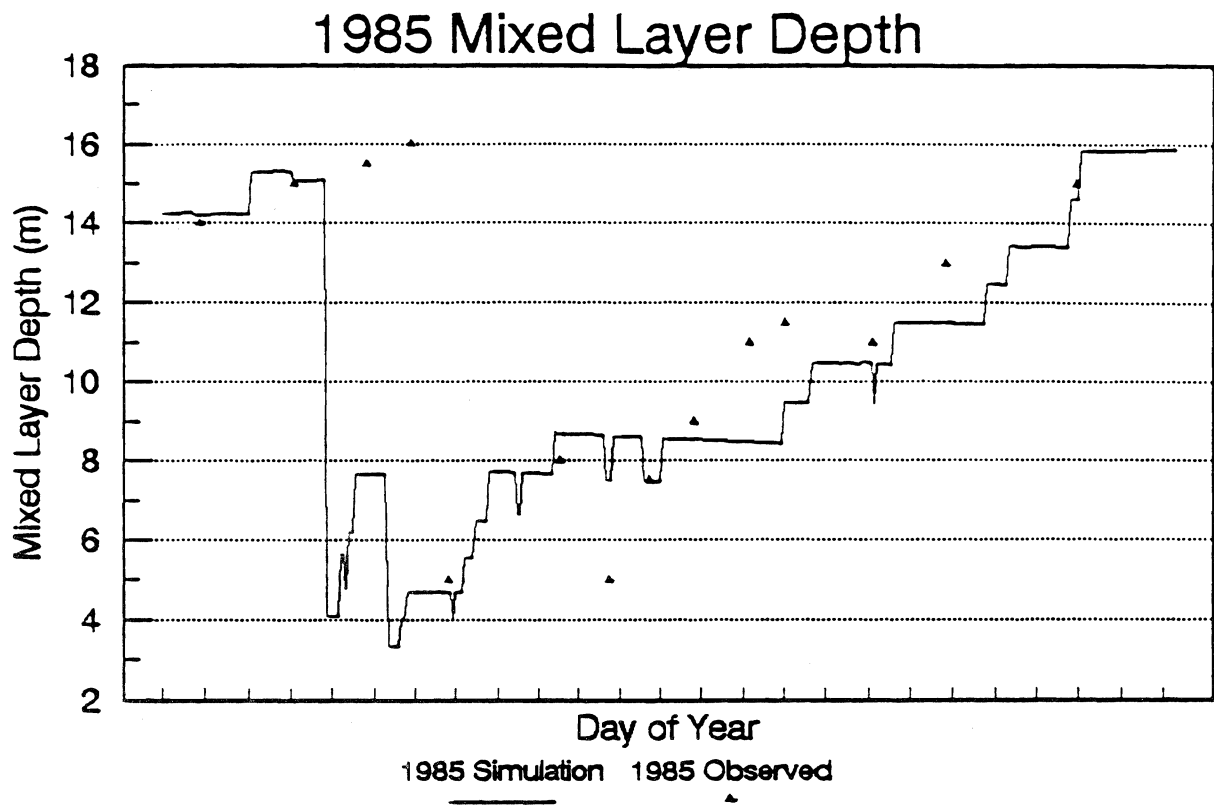
Offset between each Temperature plot is : 2.50 degrees C

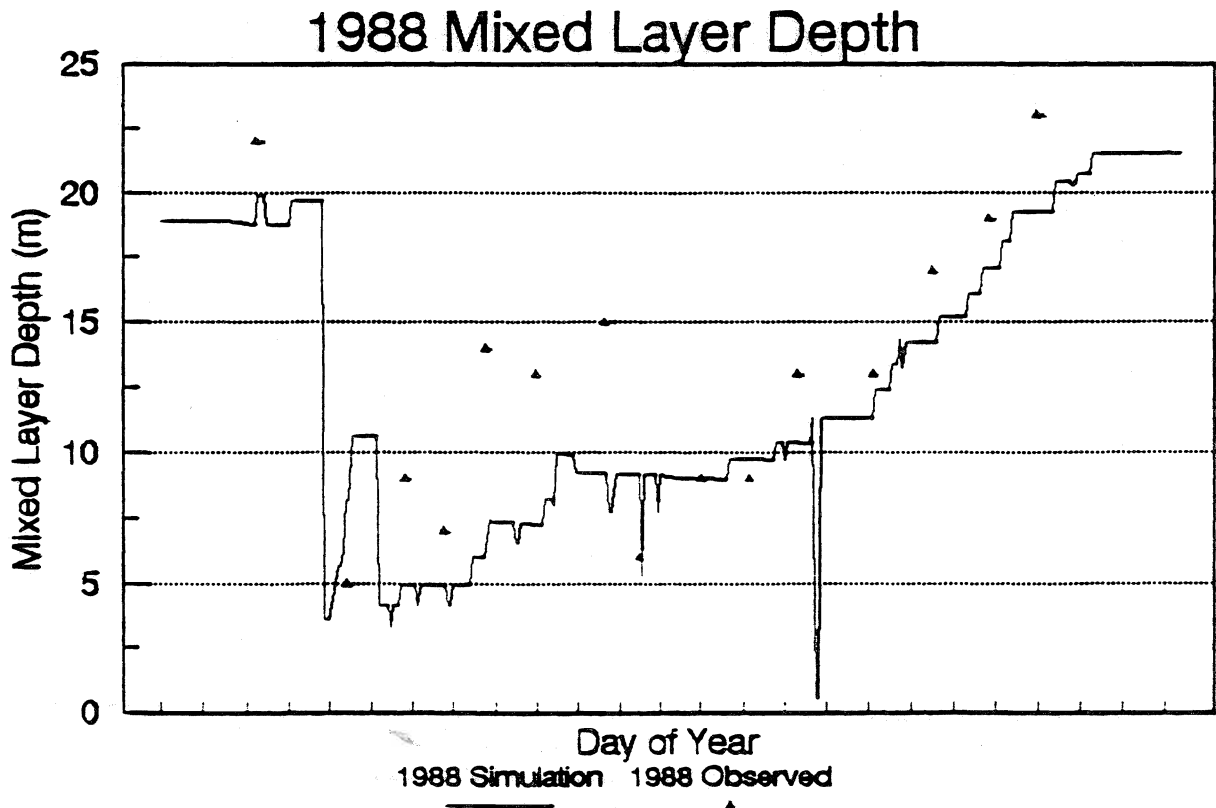
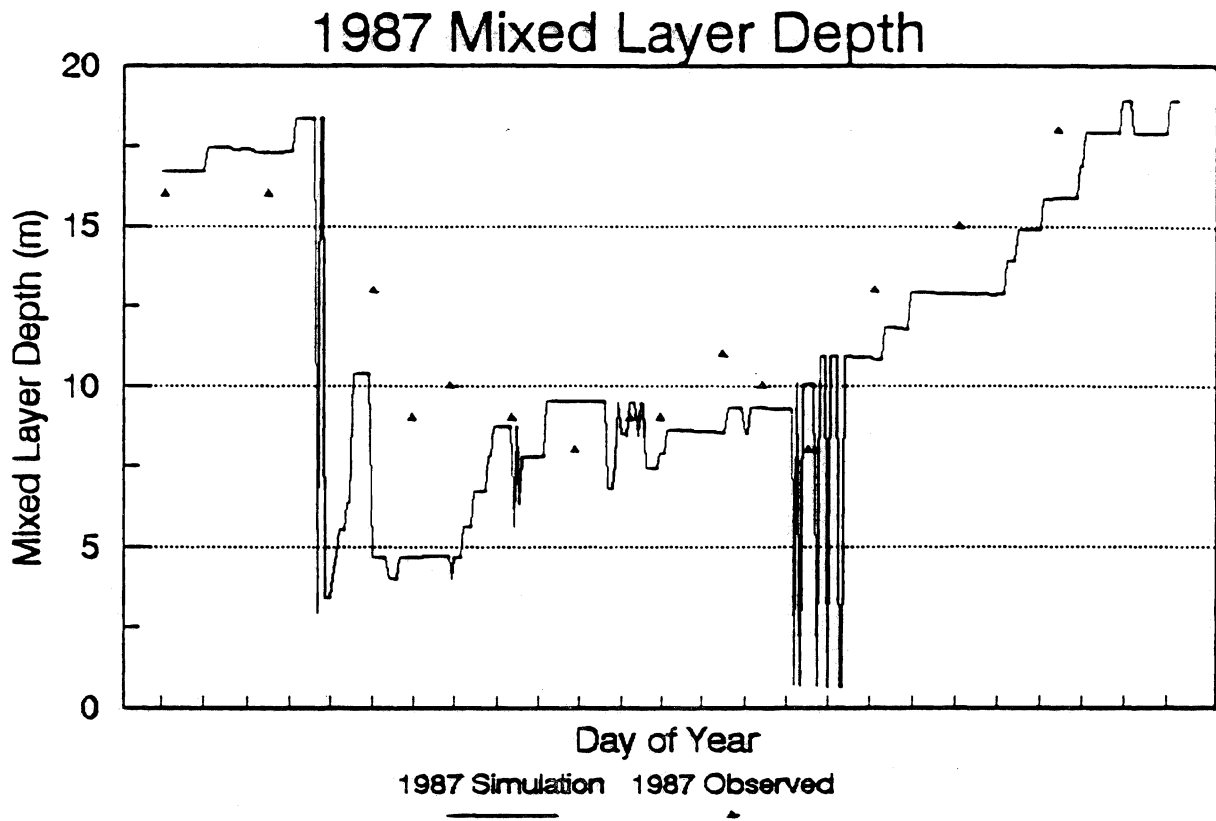
1983 Mixed Layer Depth

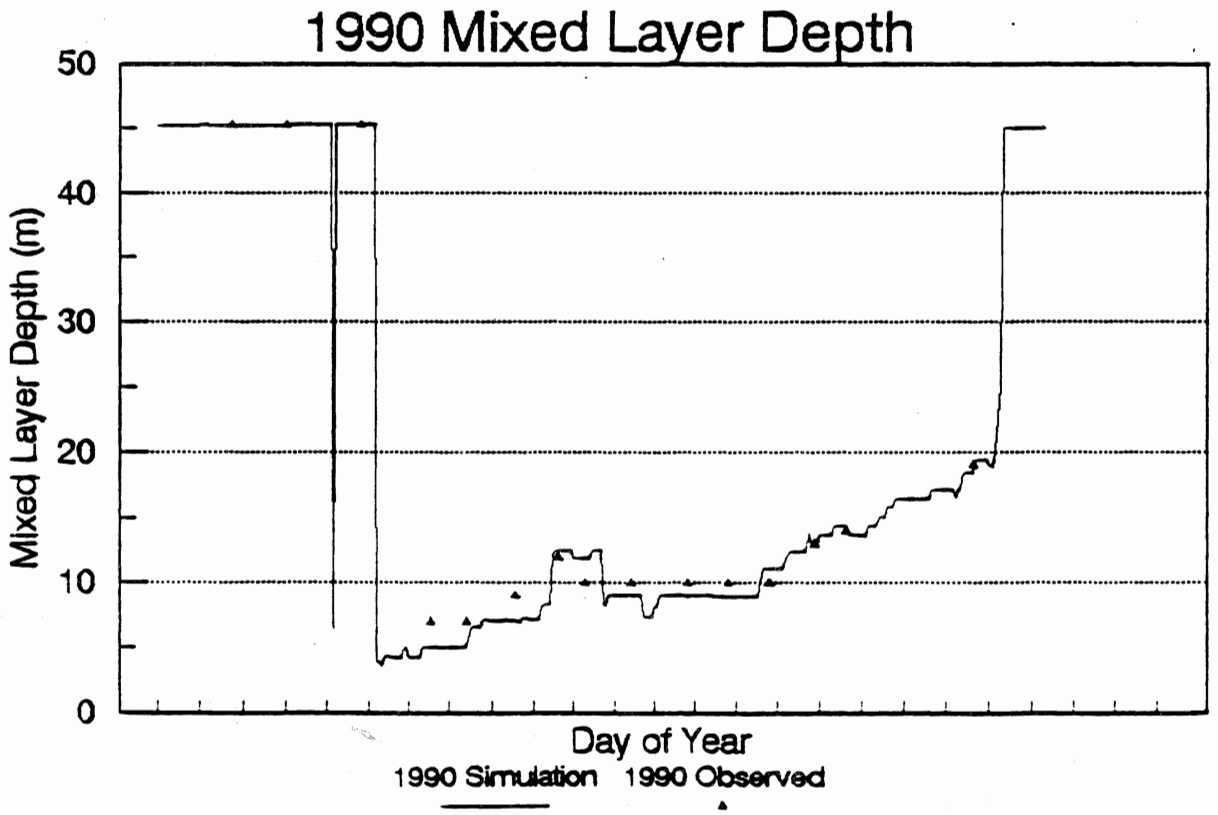
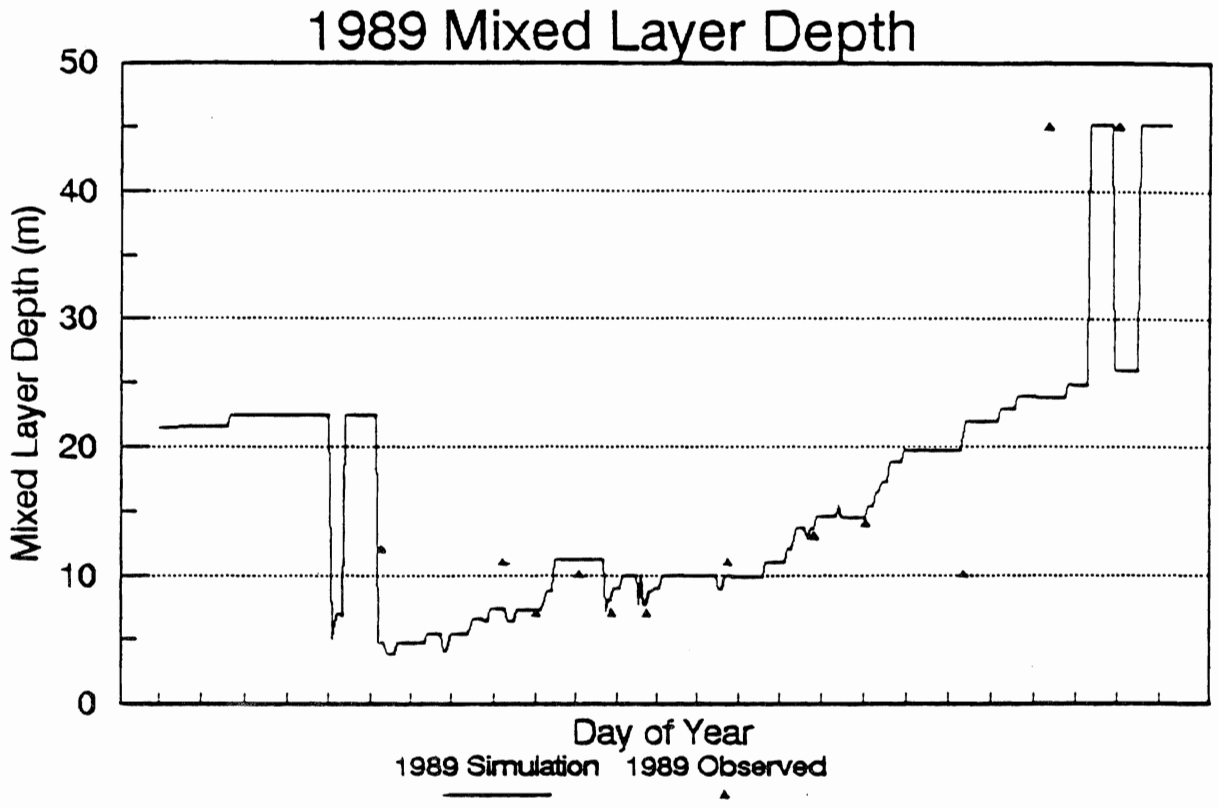


1984 Mixed Layer Depth

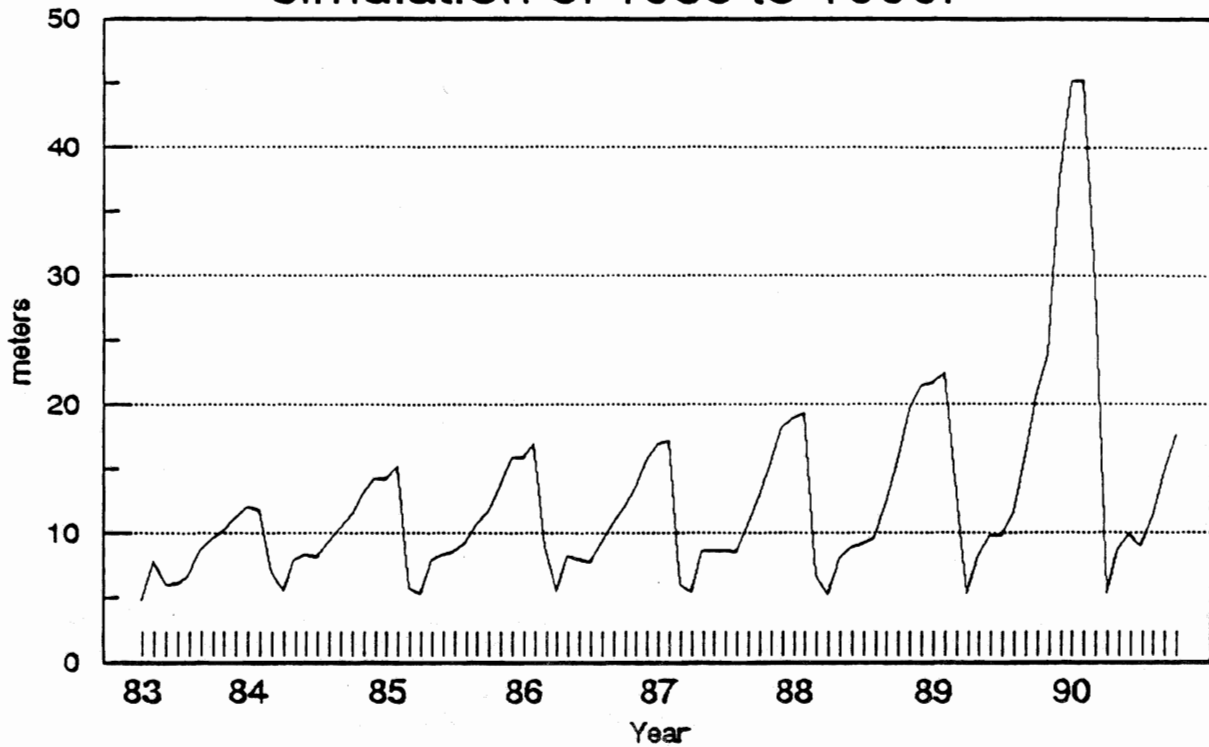




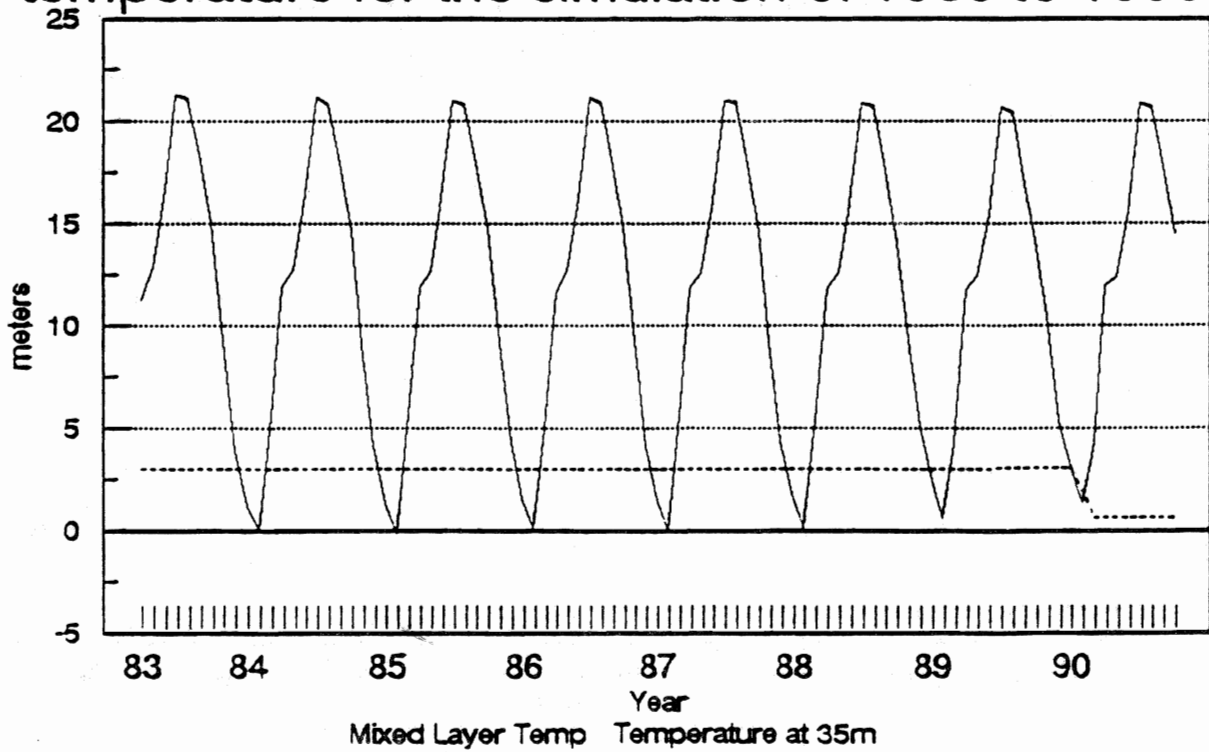




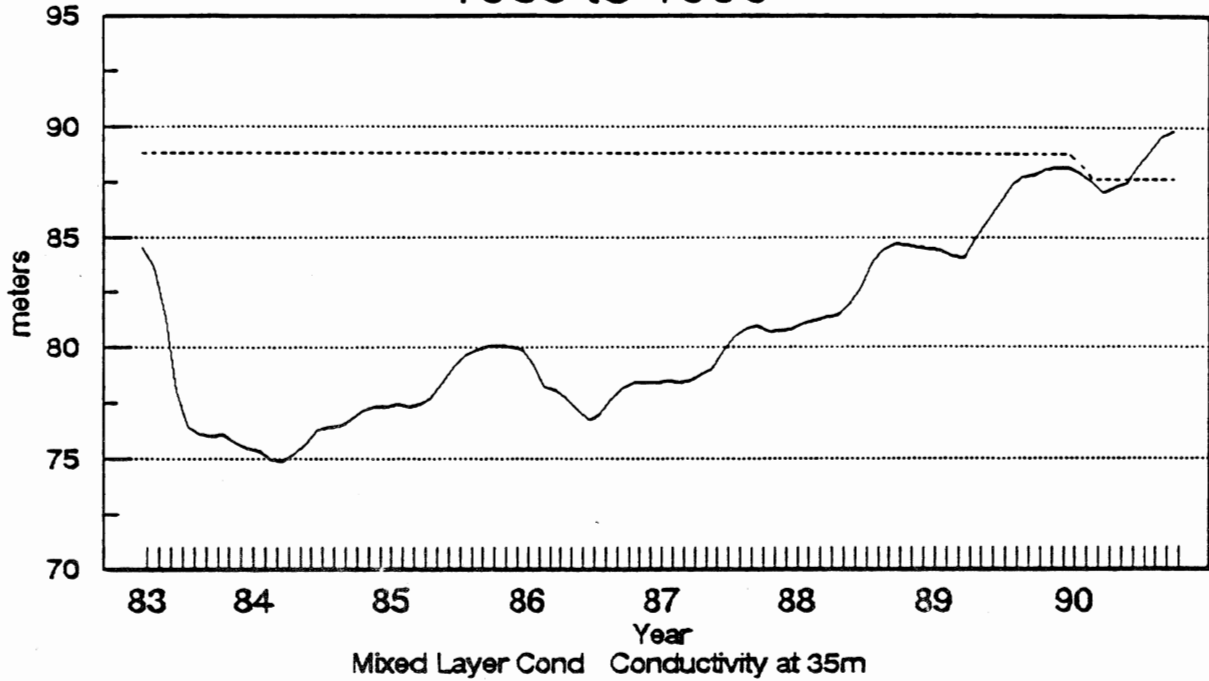
Monthly averaged mixed layer depth for simulation of 1983 to 1990.



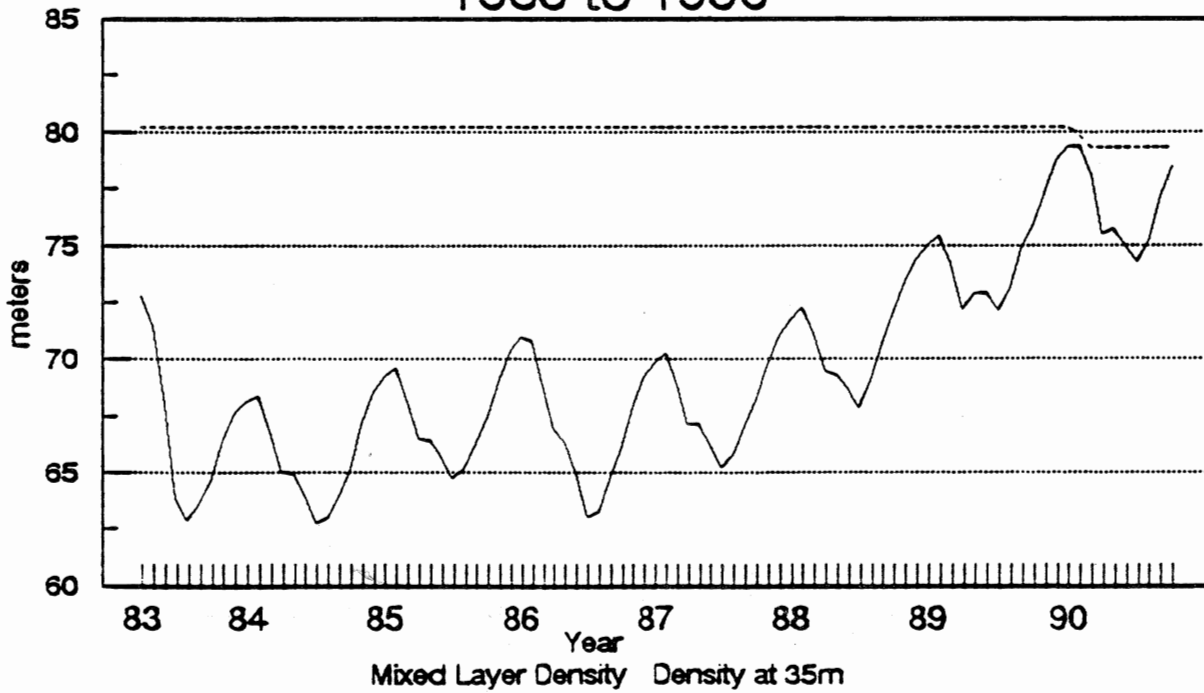
Monthly averaged mixed layer and 35 m temperature for the simulation of 1983 to 1990

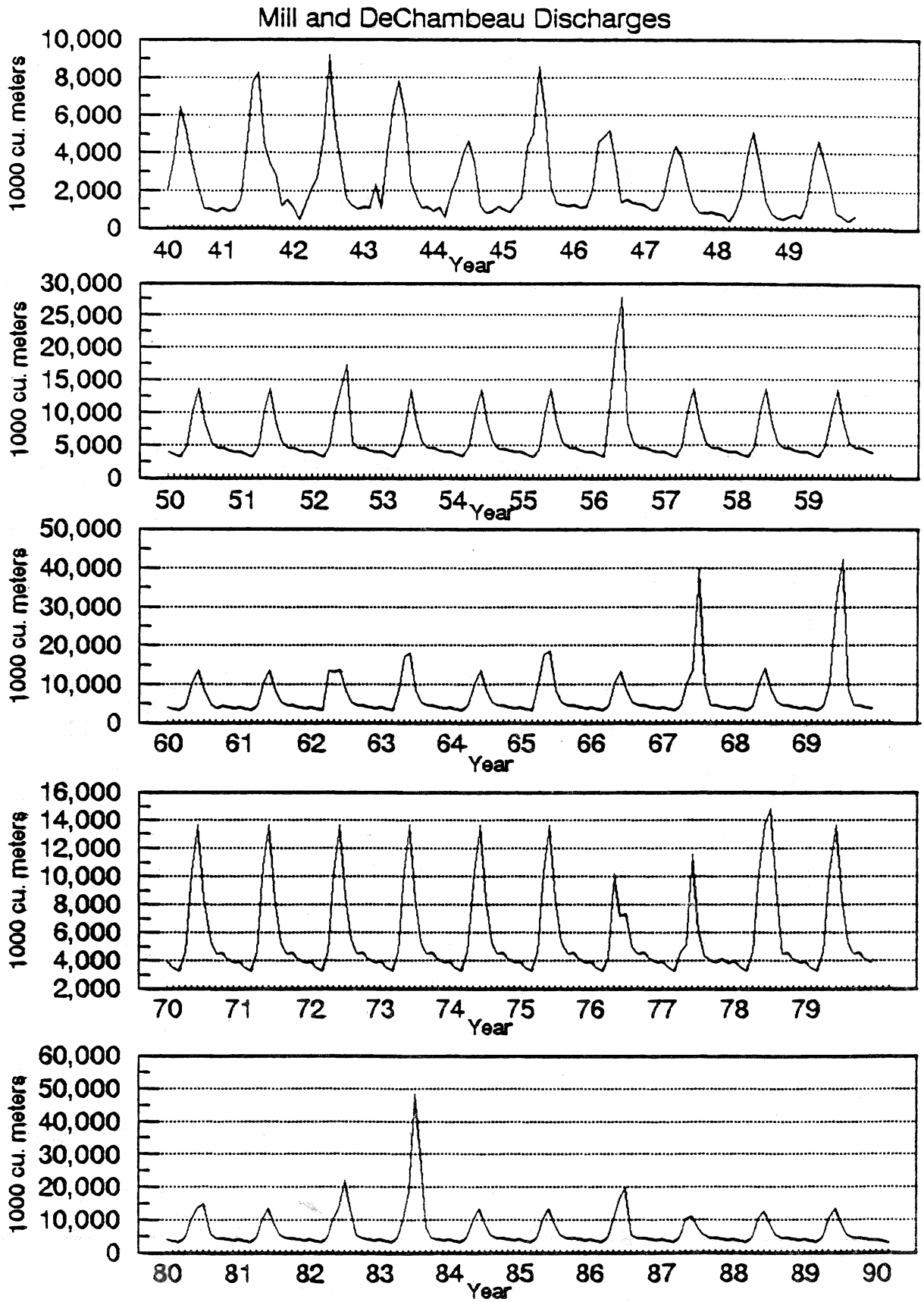


Monthly averaged mixed layer and 35 m corrected conductivity for the simulation of 1983 to 1990

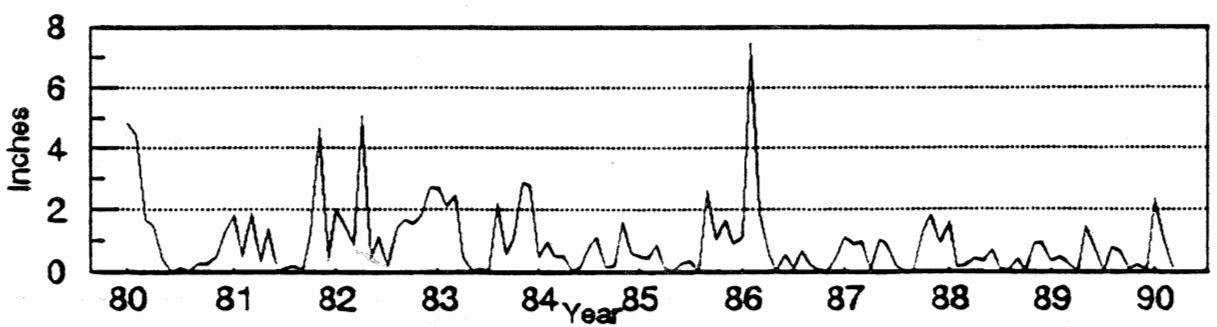
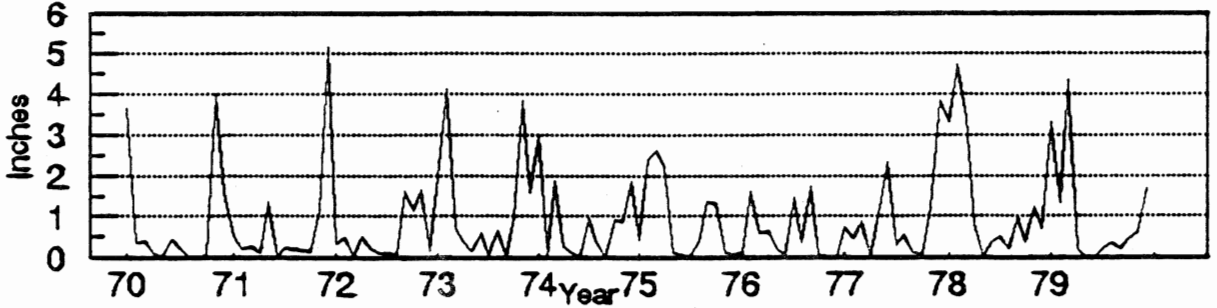
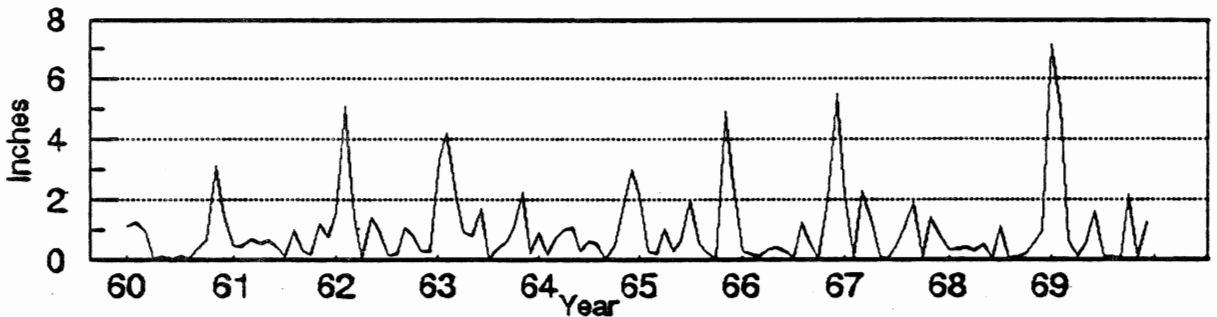
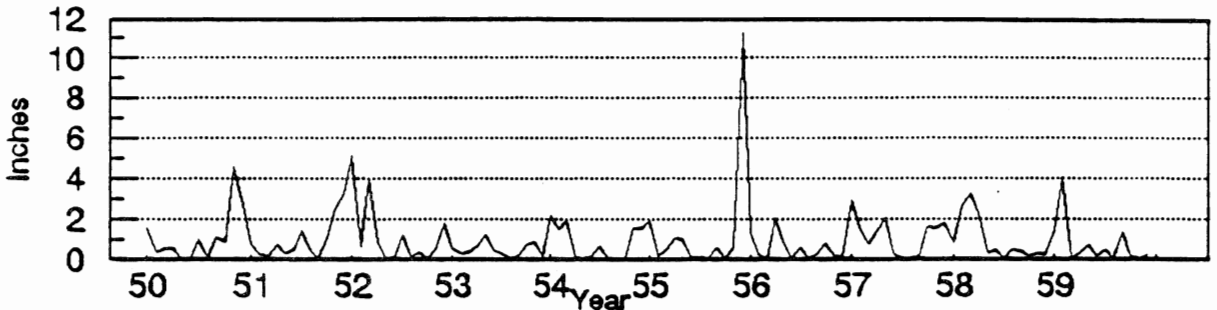
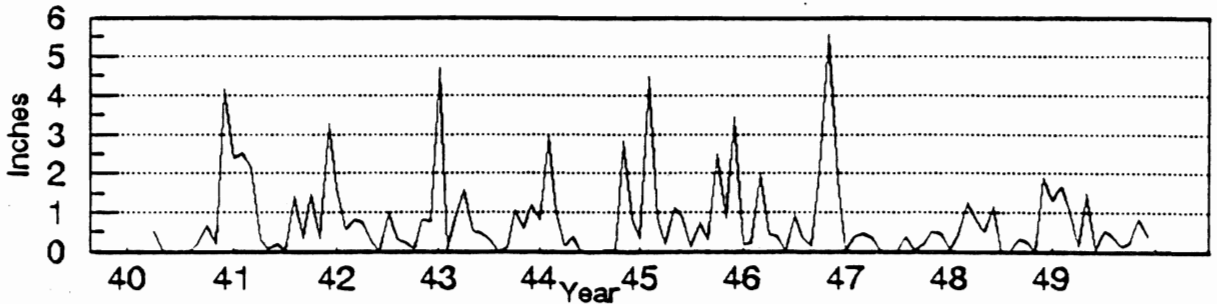


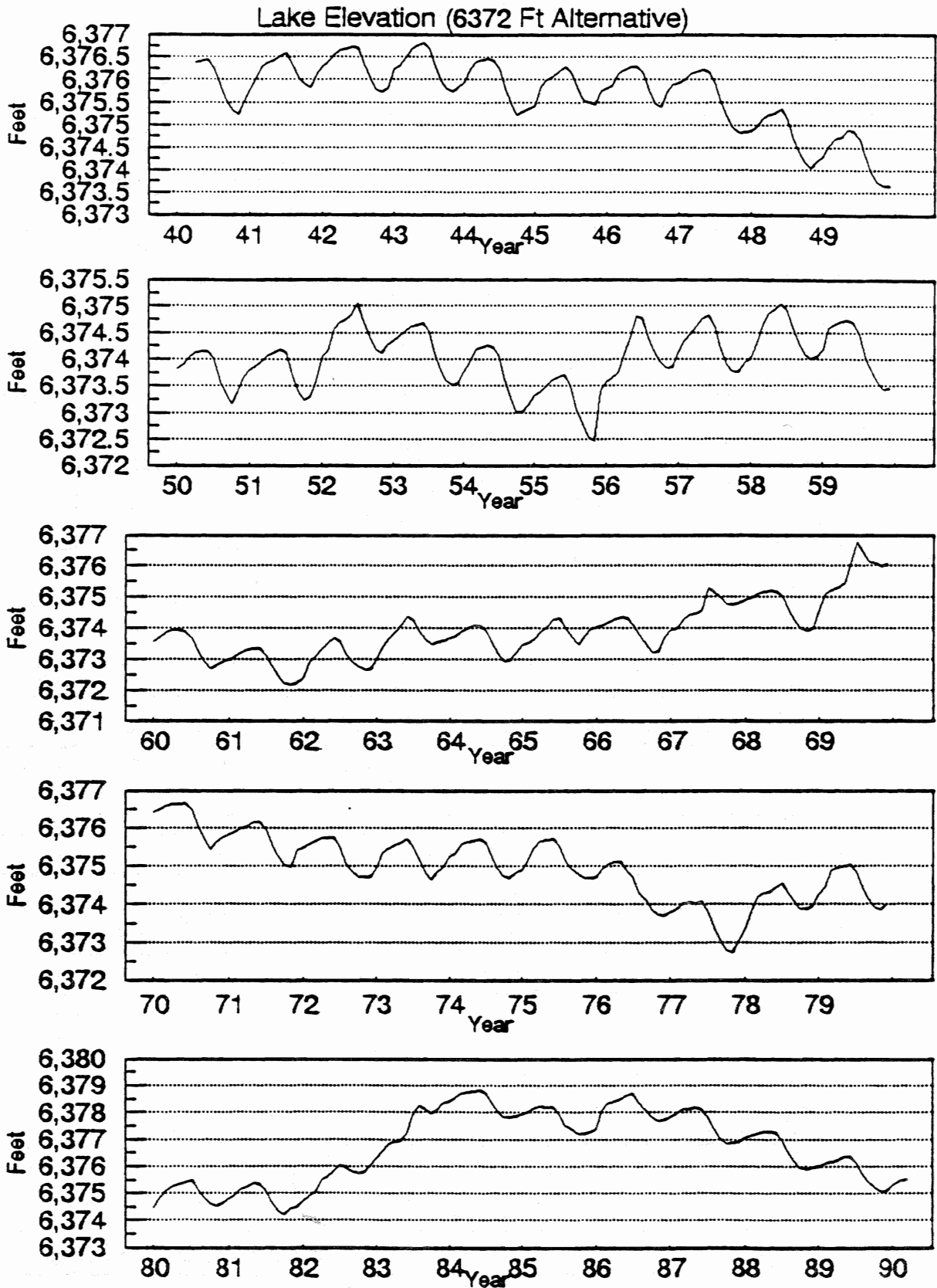
Monthly averaged mixed layer and 35 m density for the simulation of 1983 to 1990

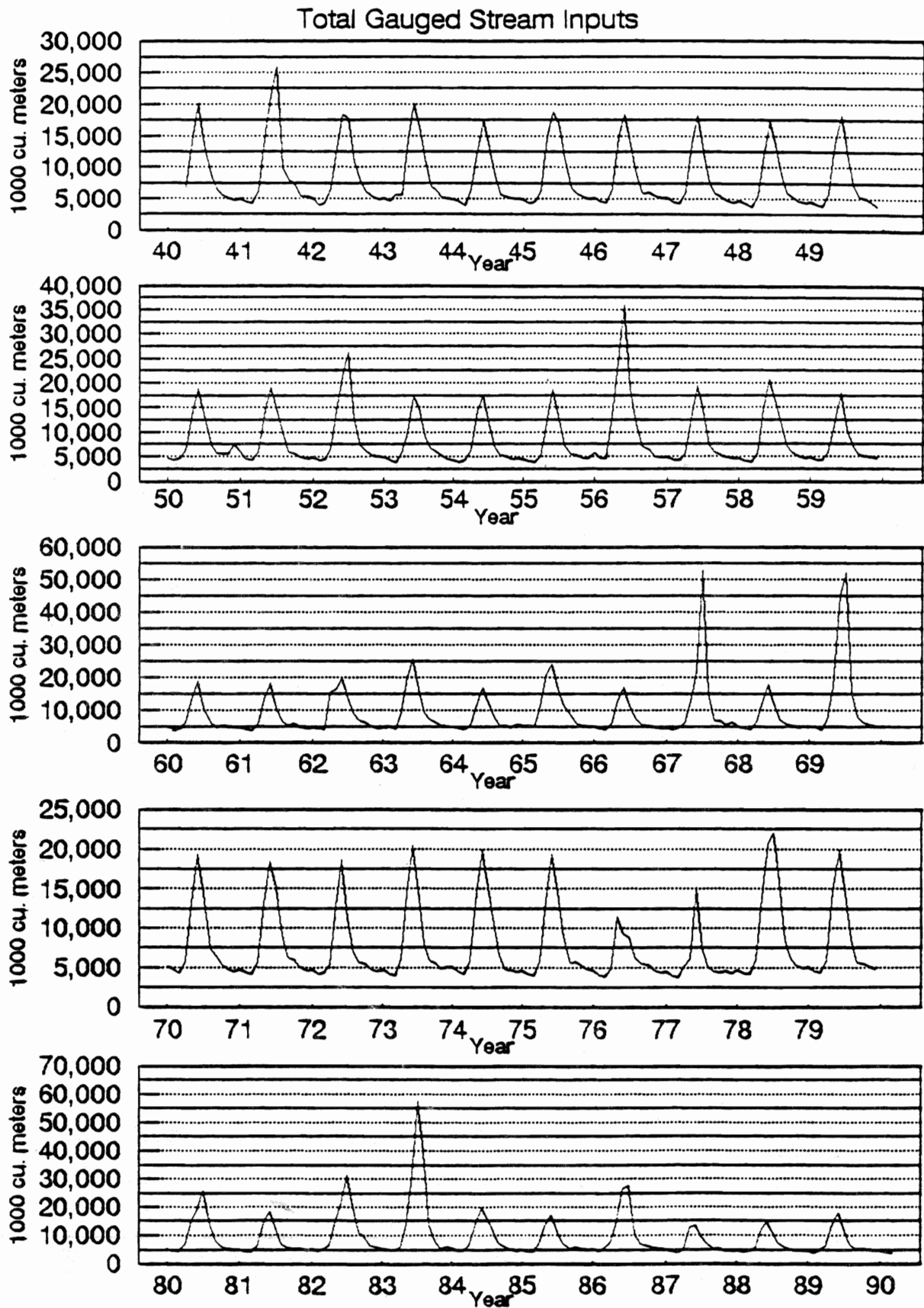


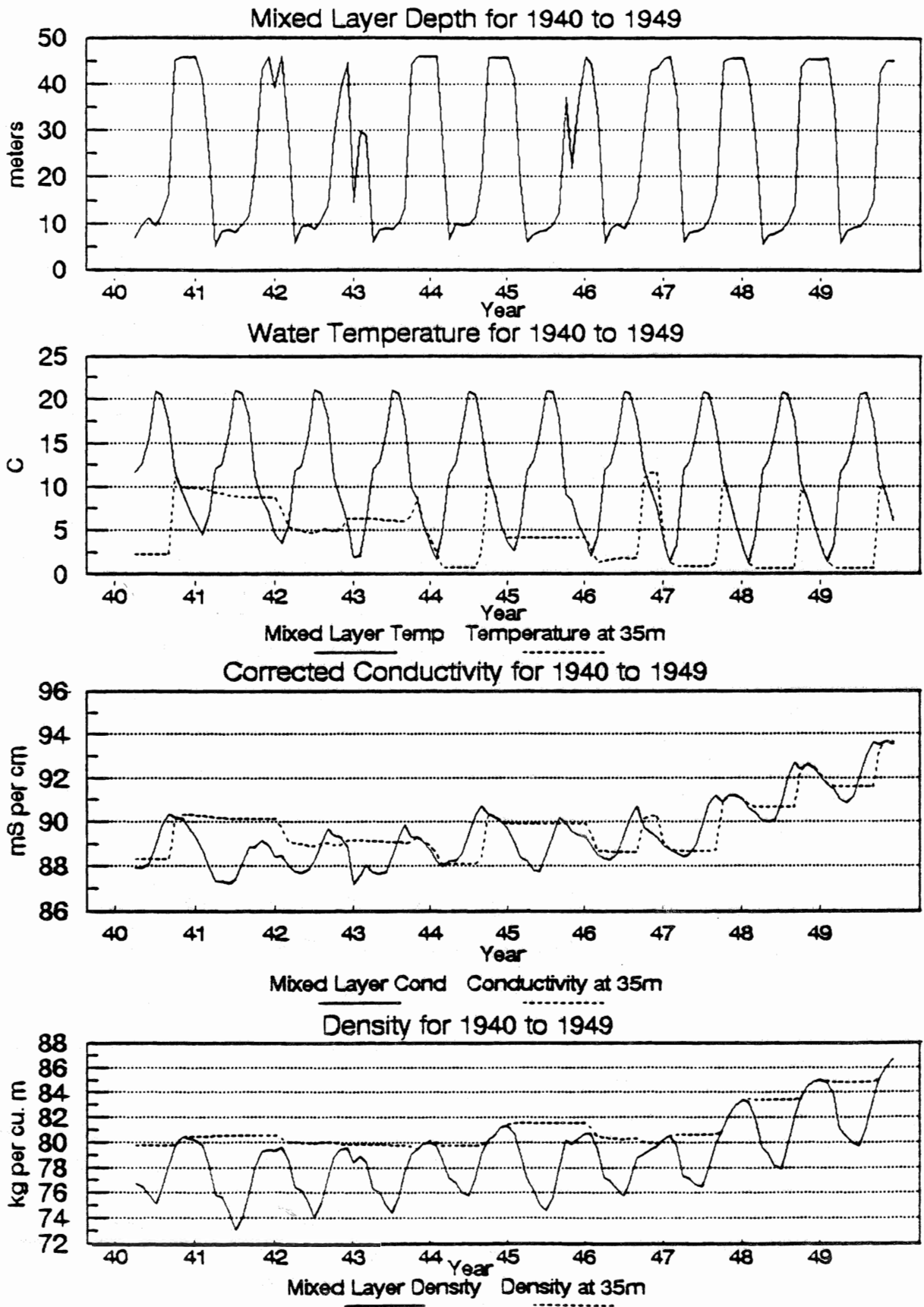


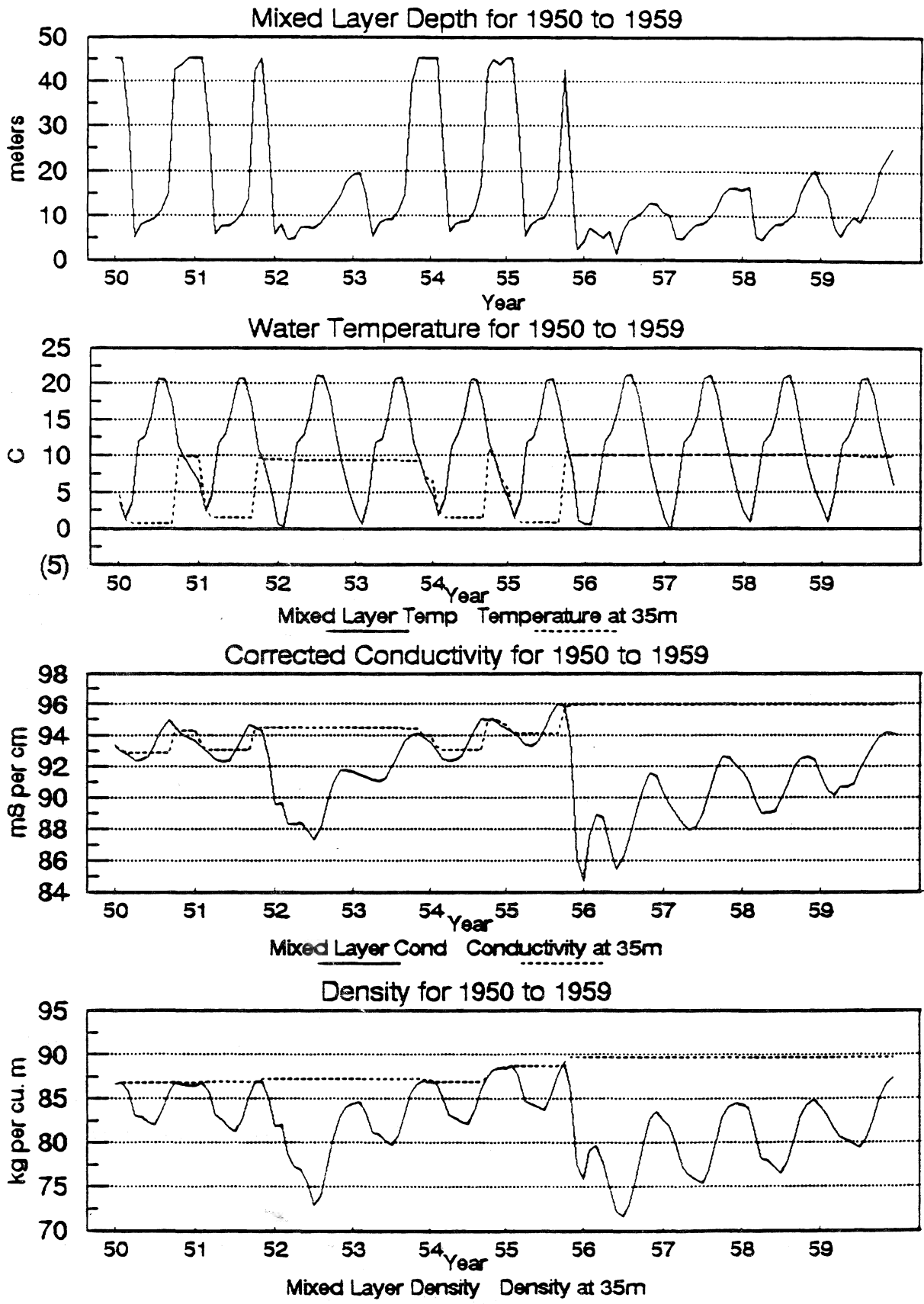
Precipitation

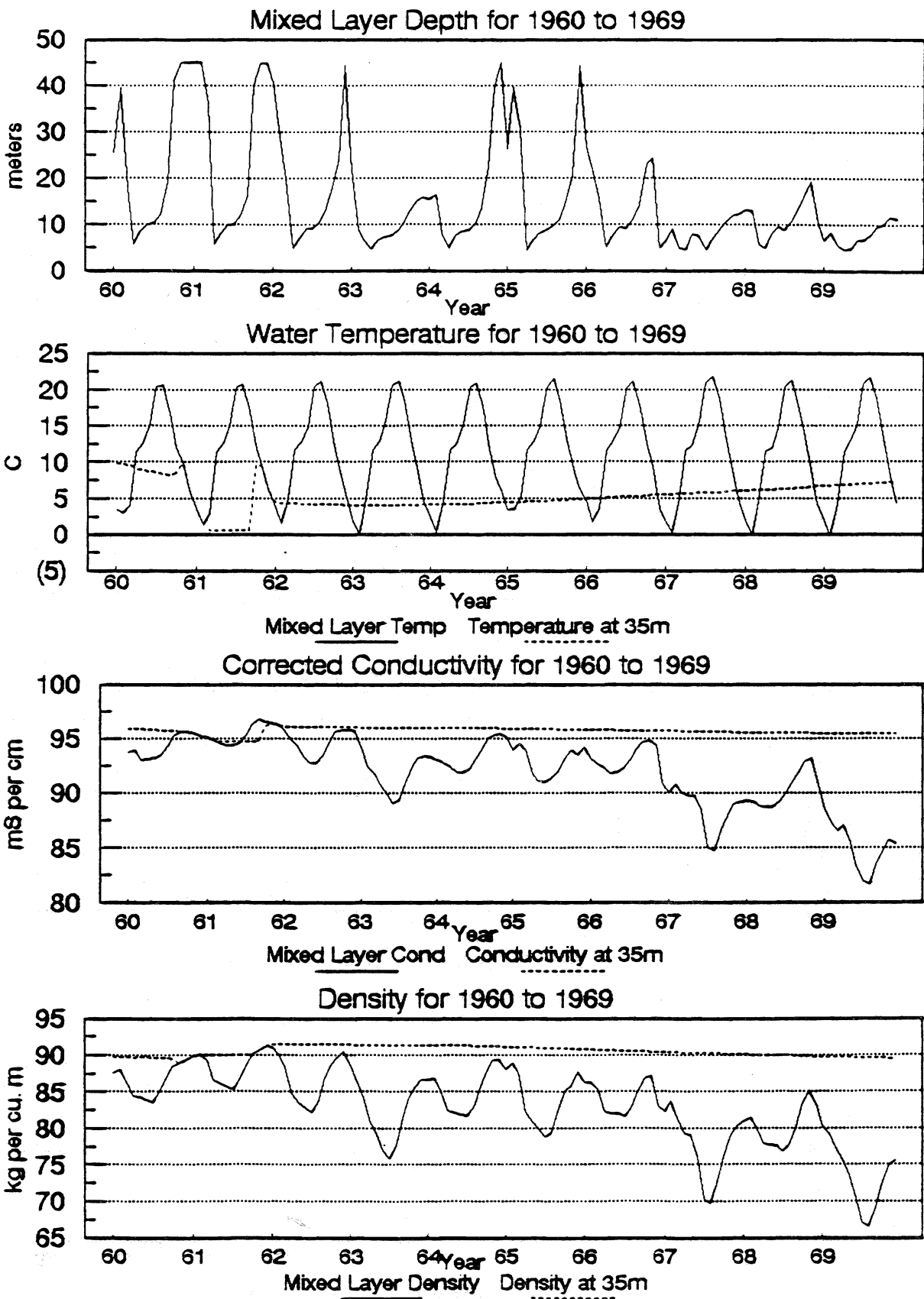


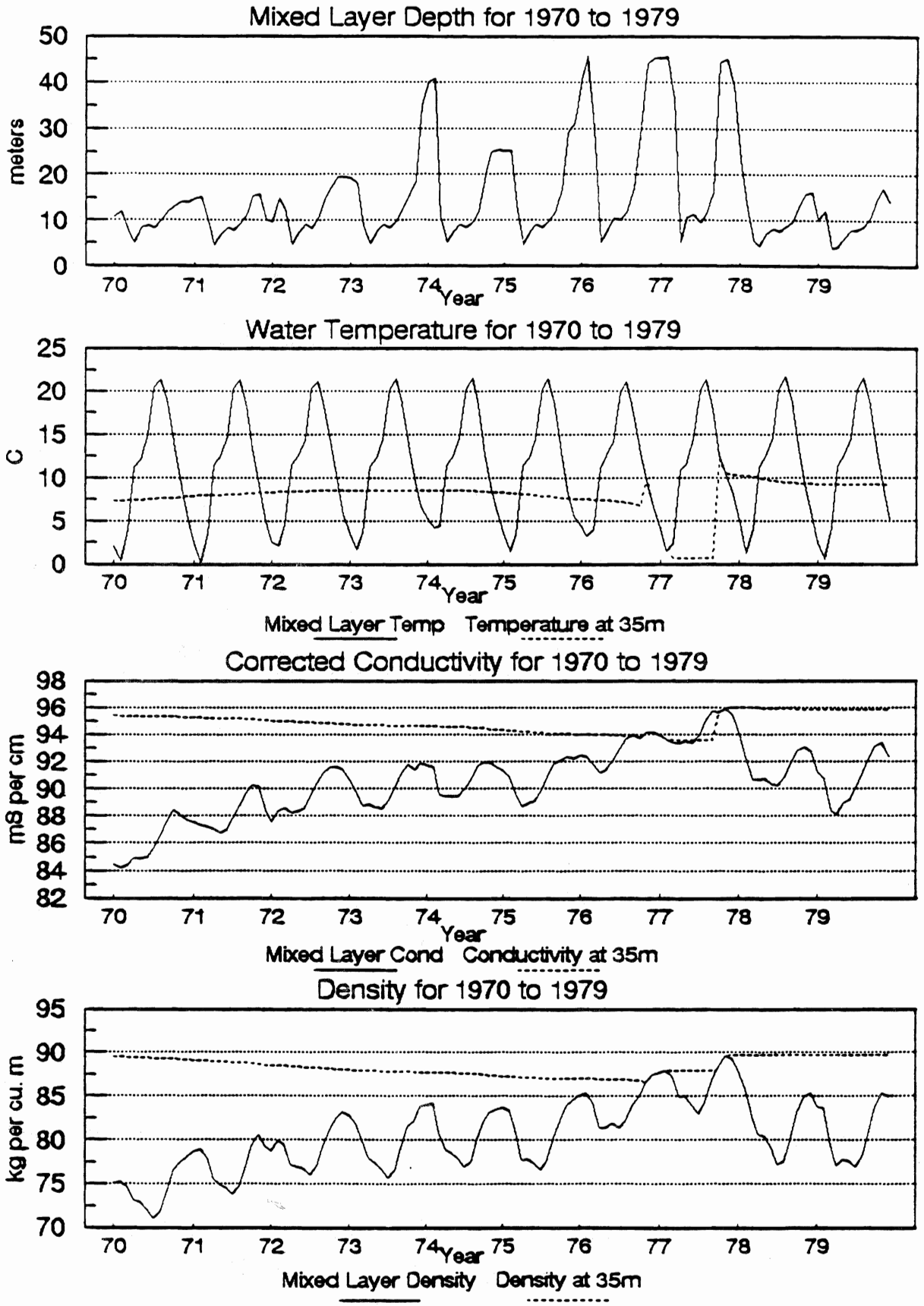


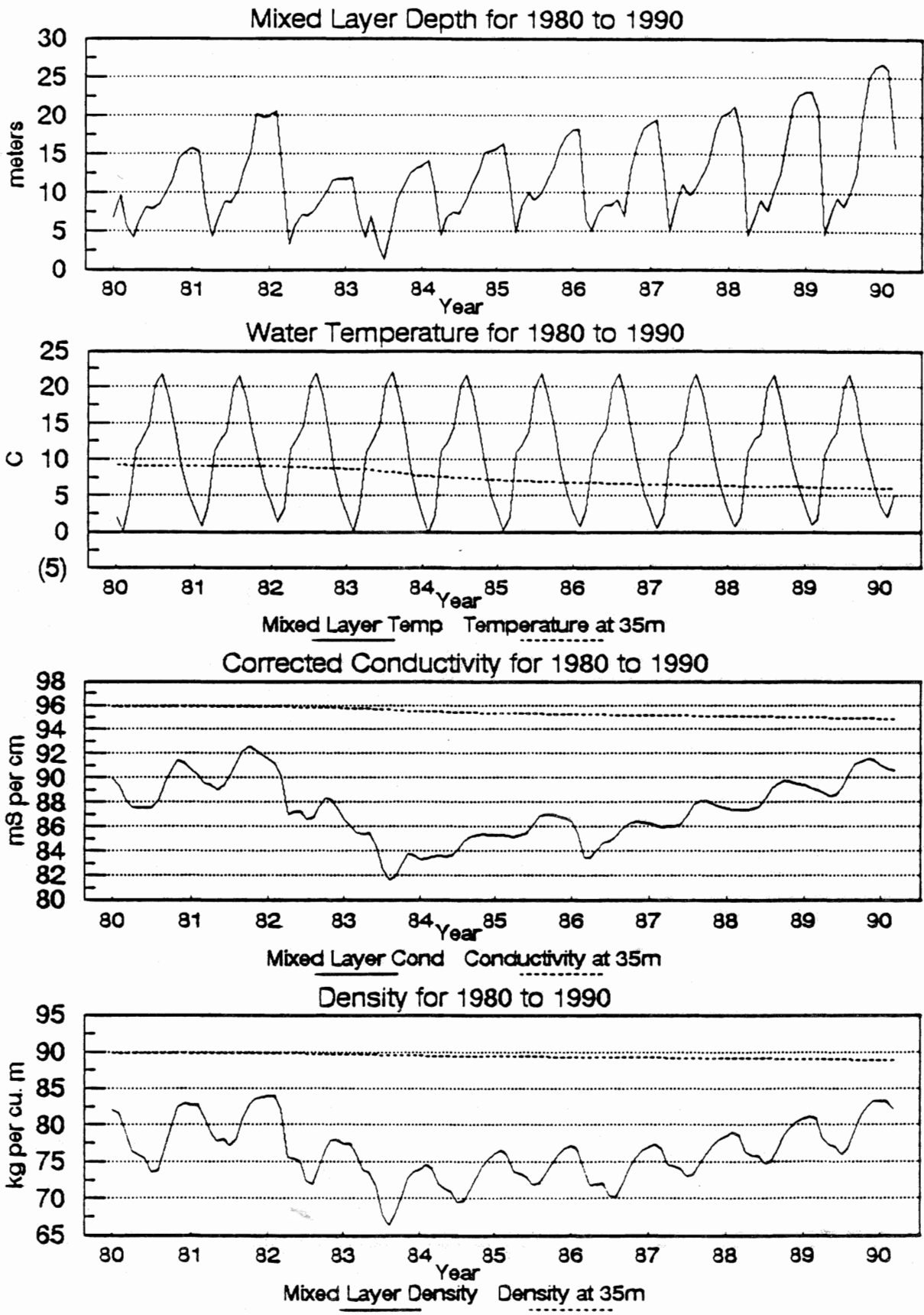




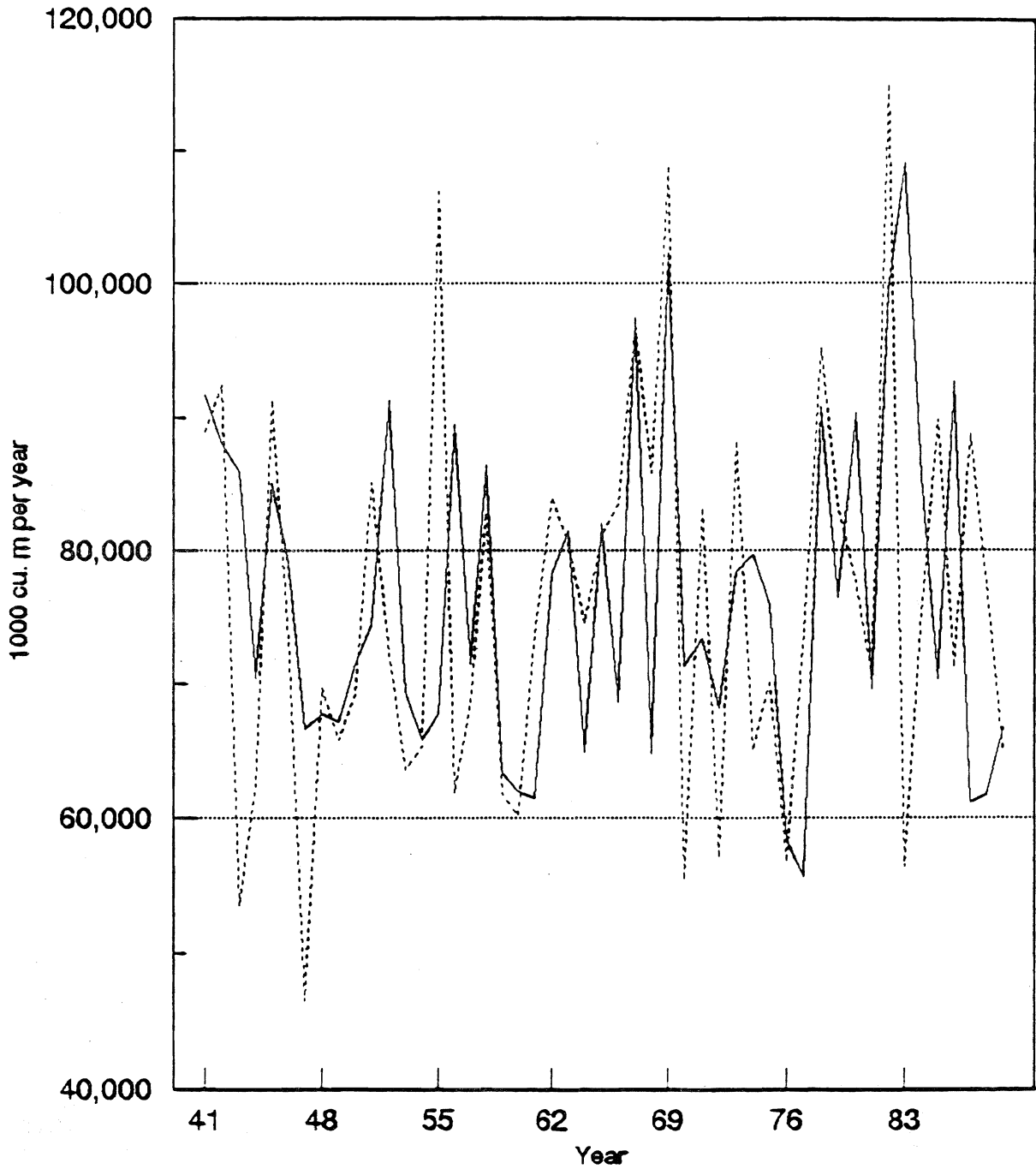








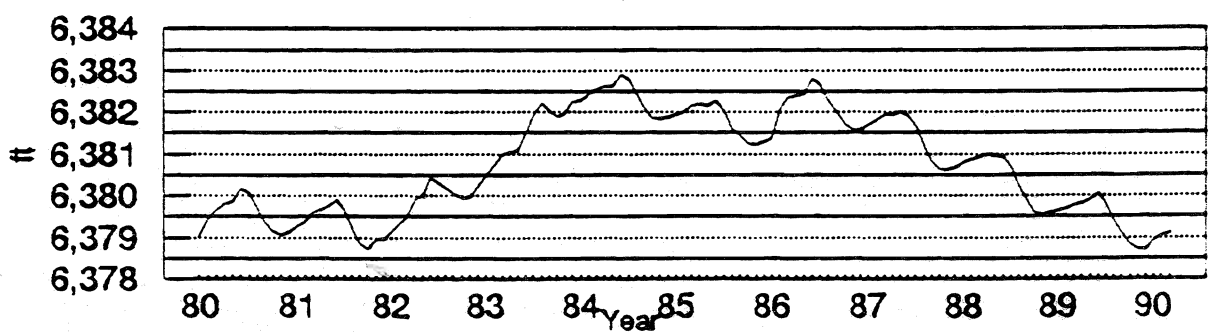
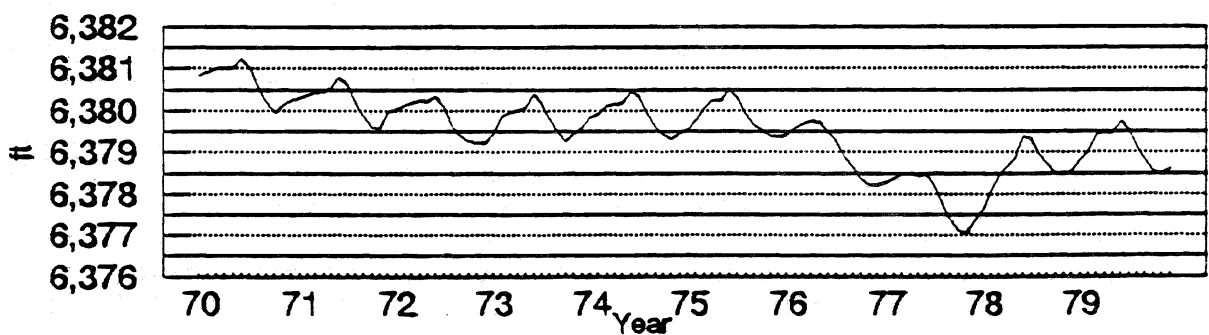
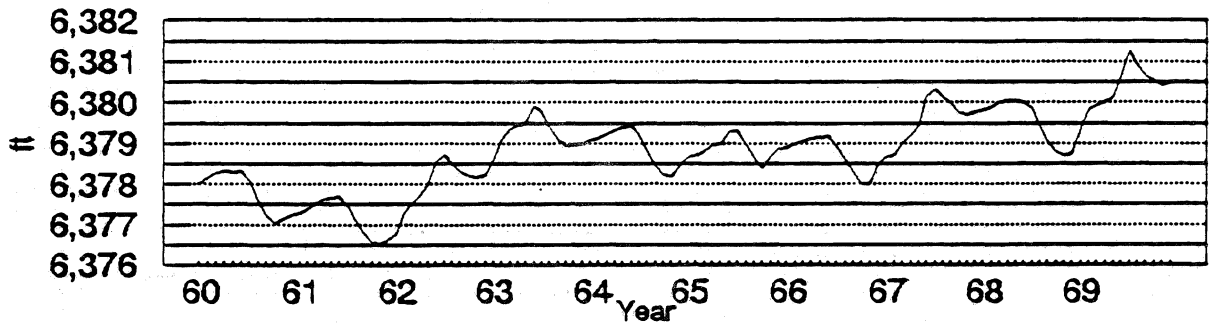
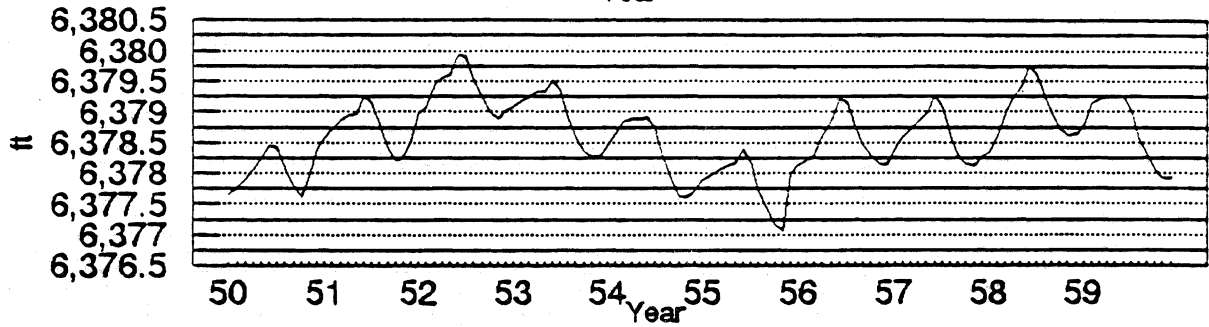
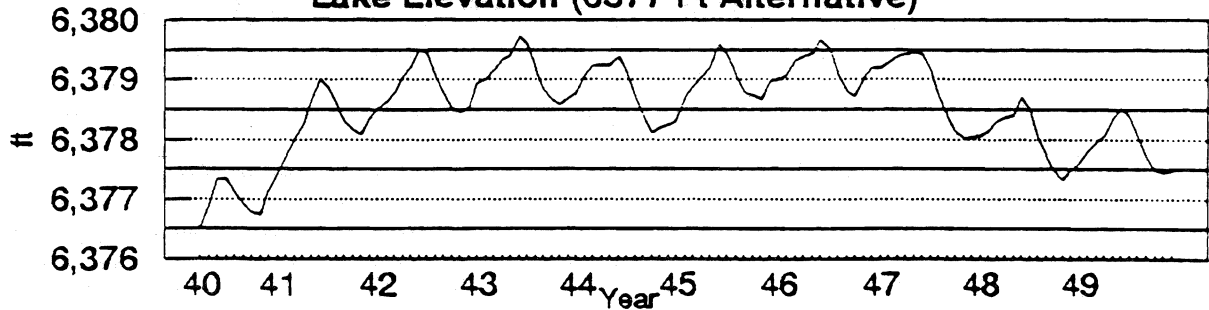
**Yearly Ungauged Stream Discharge and GroundWater
Estimates from DYRESM and LAAMP
1941 to 1989 (6372 ft Scenario)**

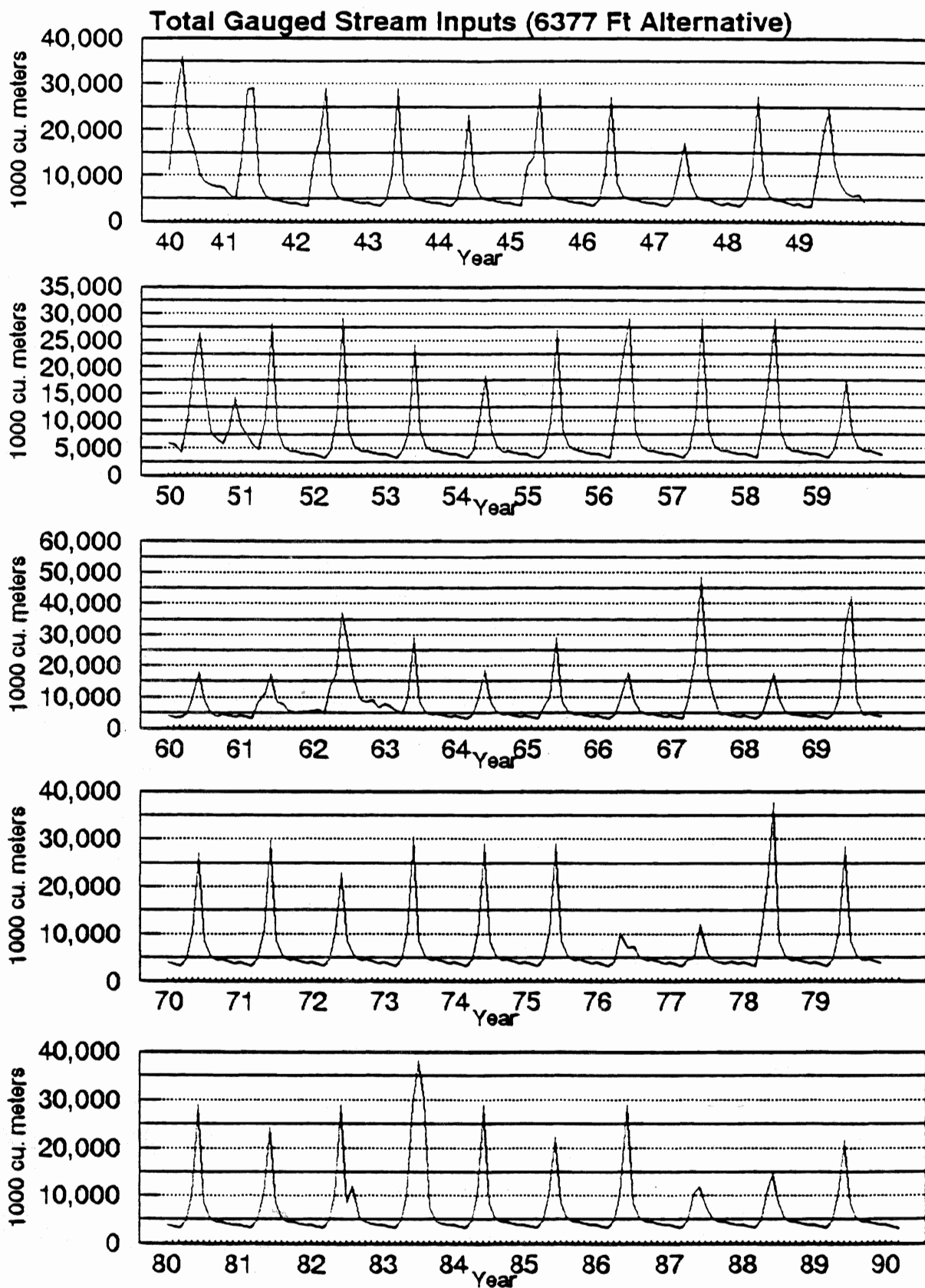


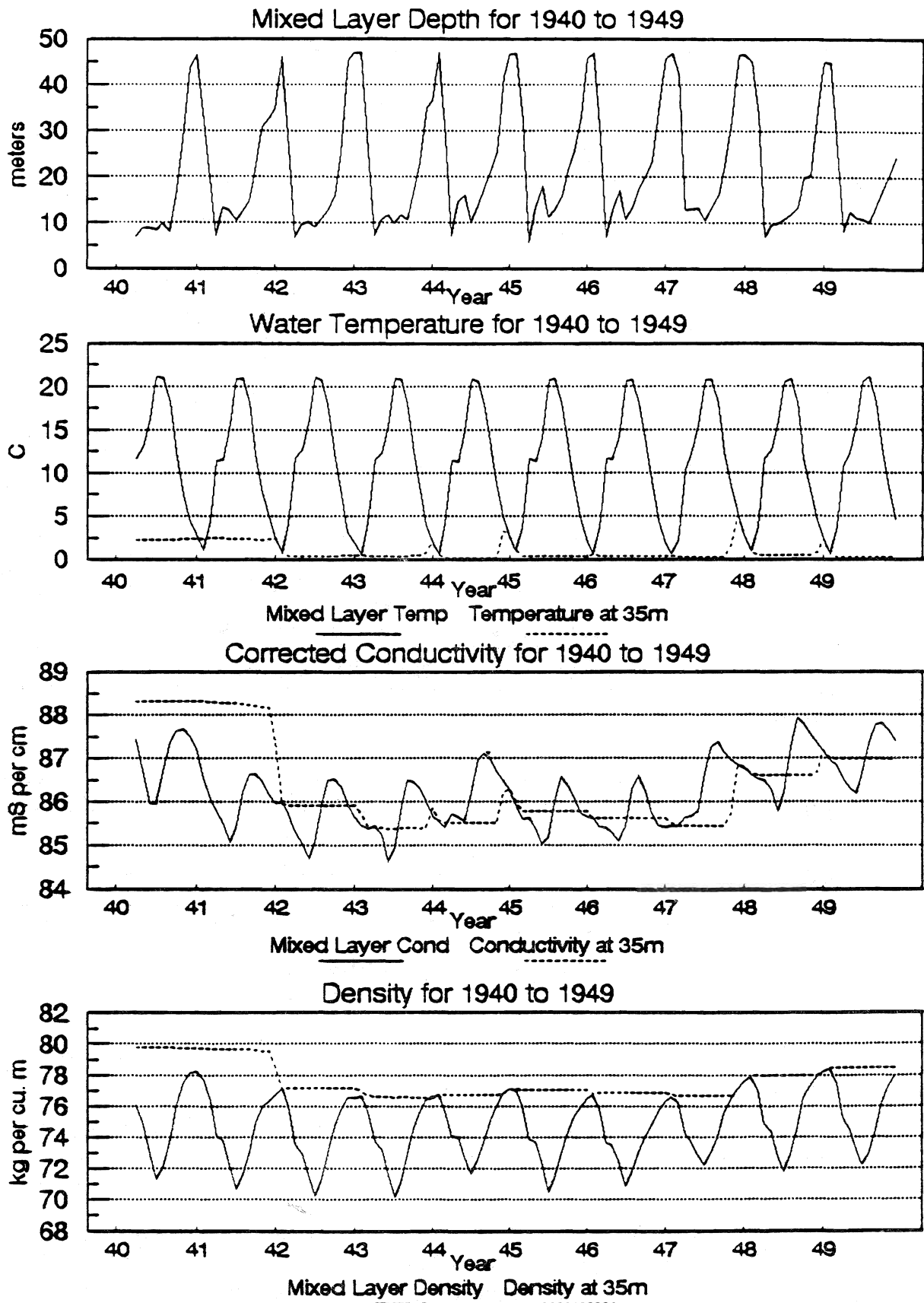
LAAMP DYRESM
76522 per year 76033 per year

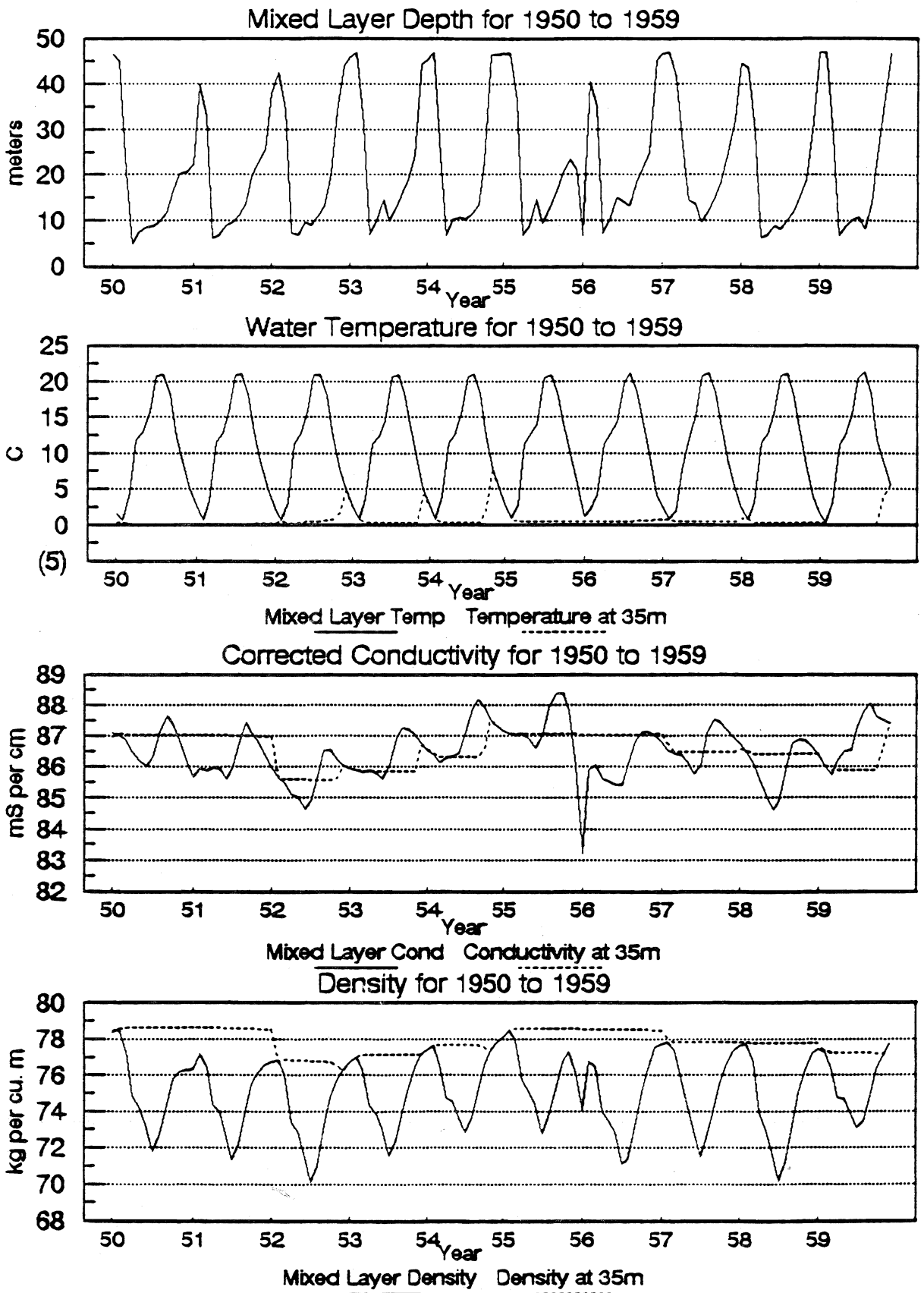
————— ······

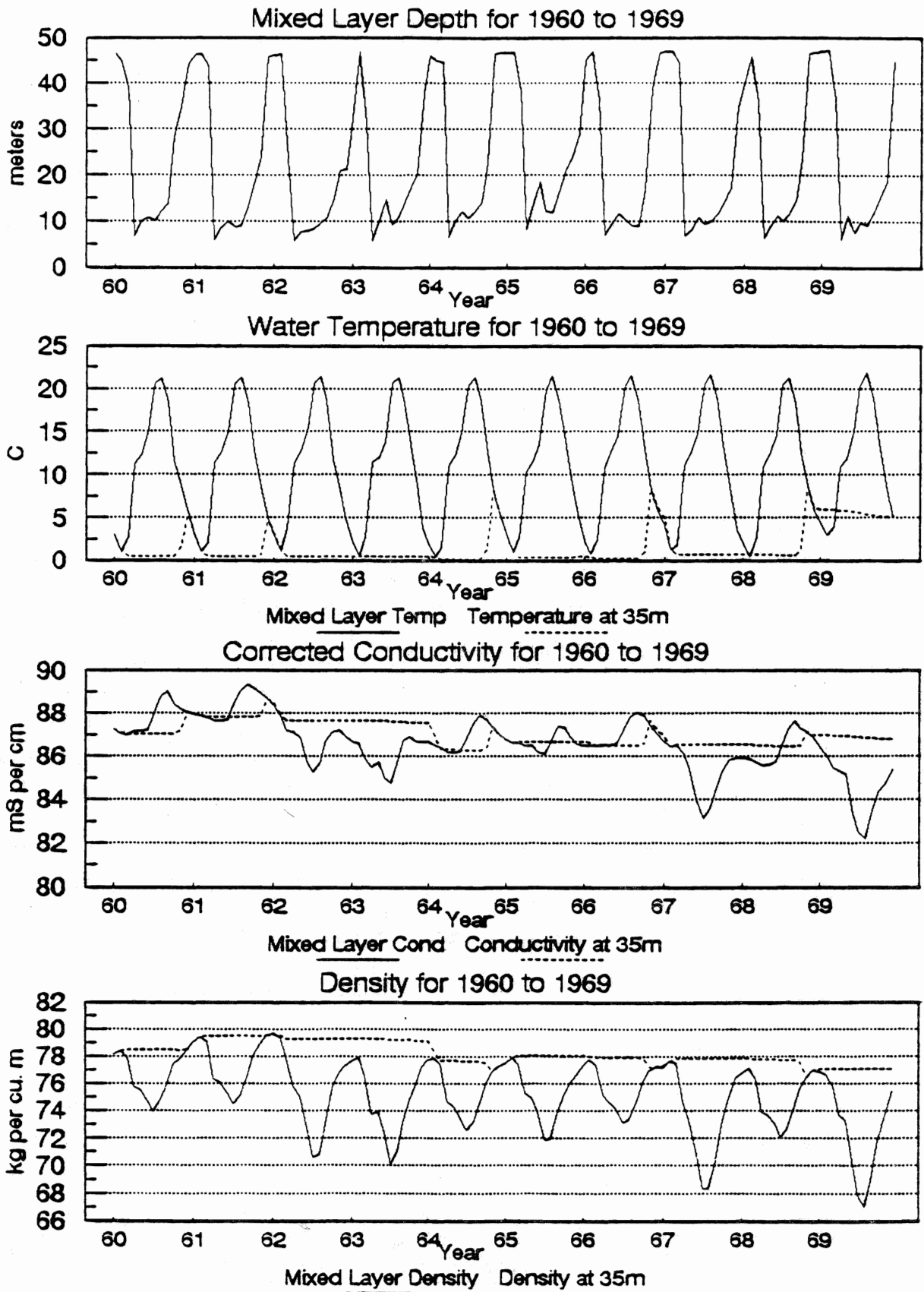
Lake Elevation (6377 Ft Alternative)

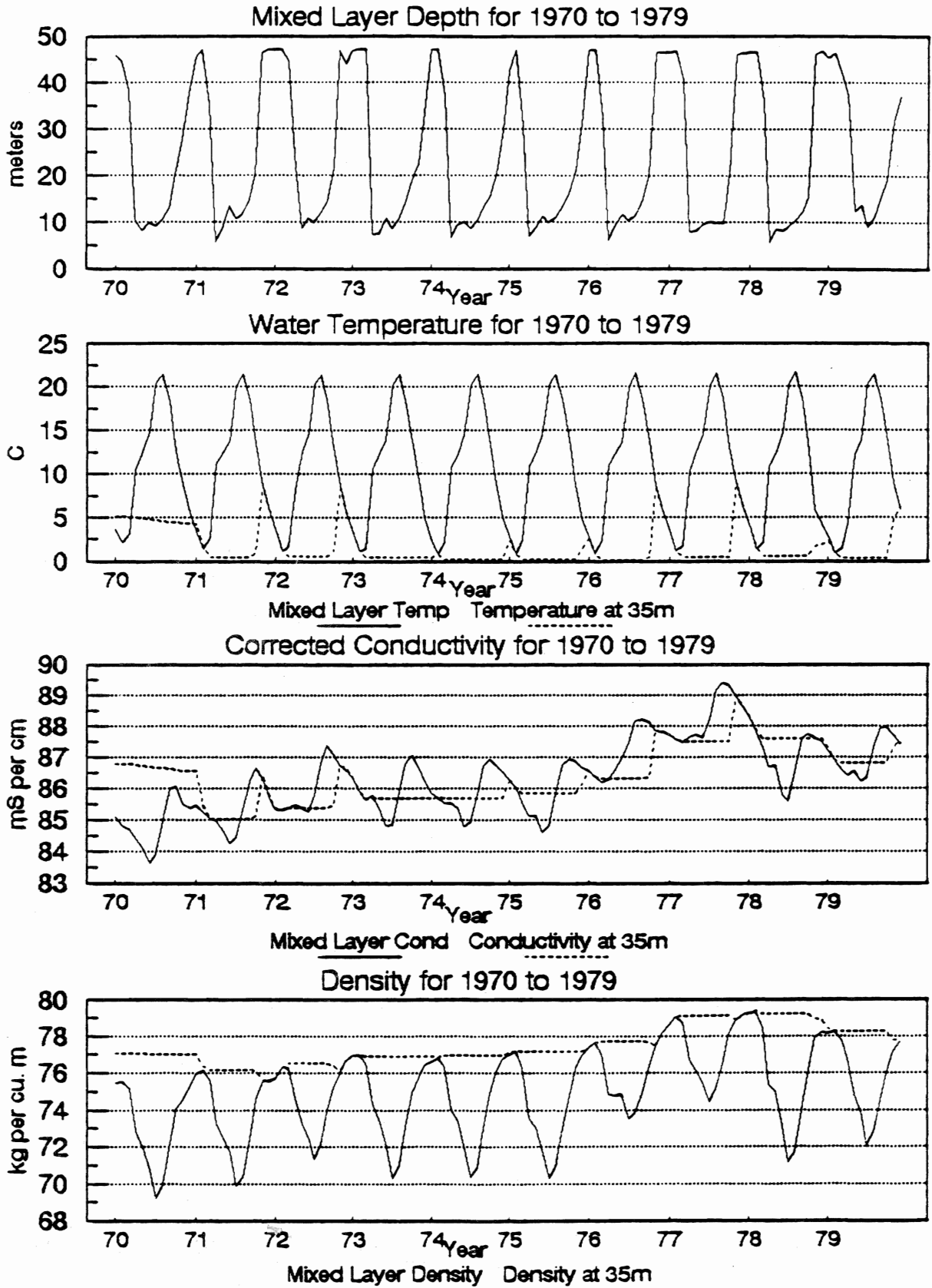


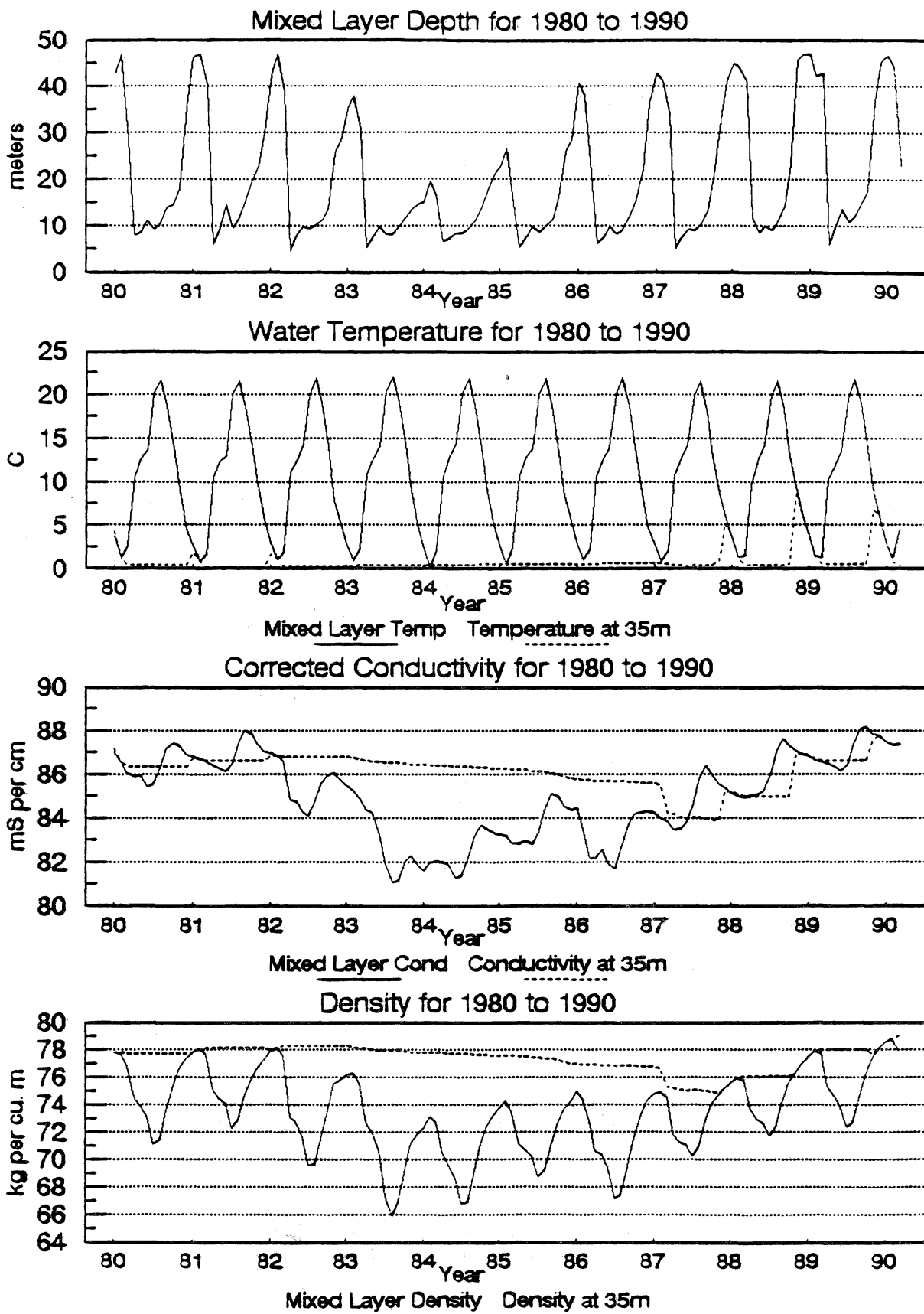




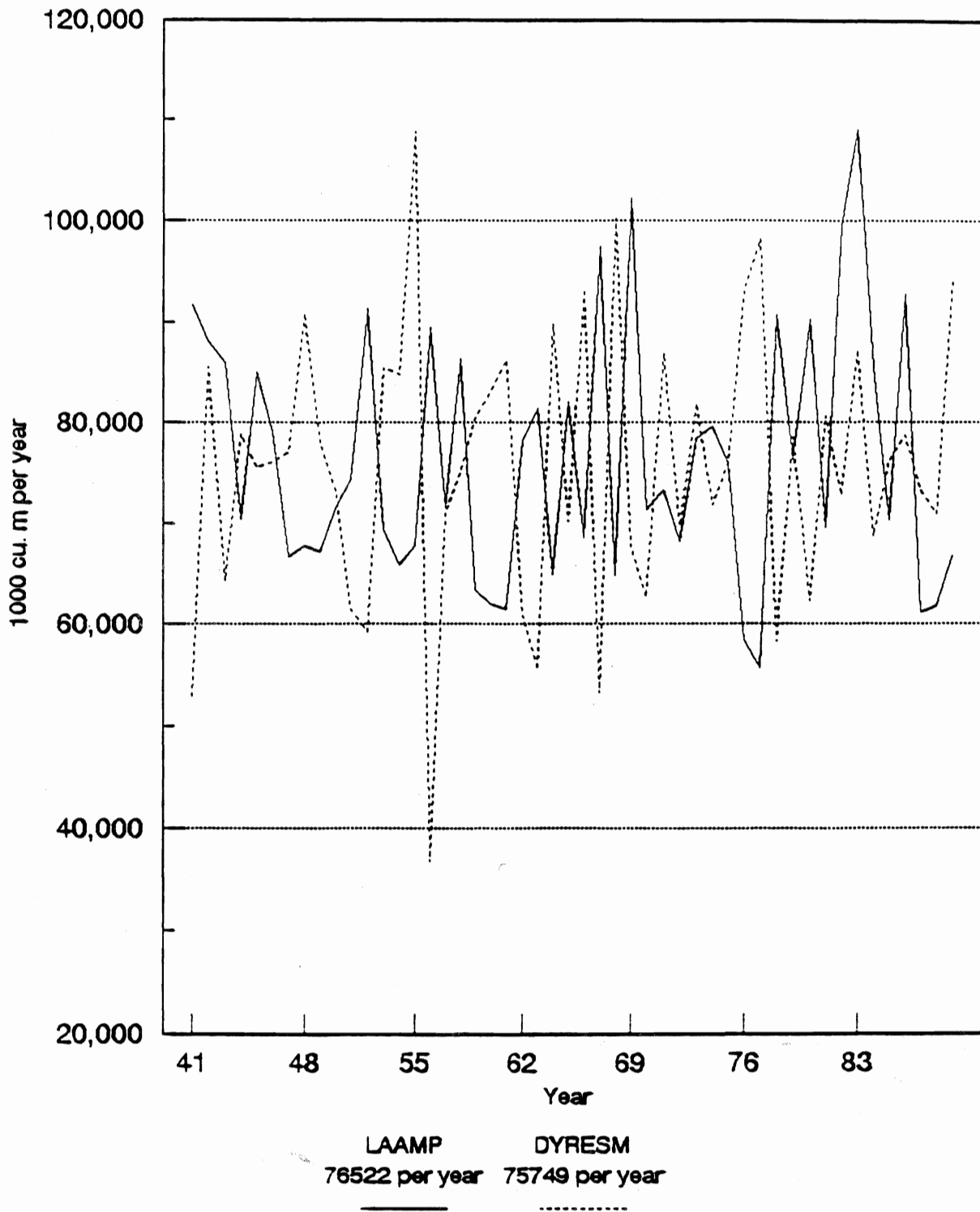




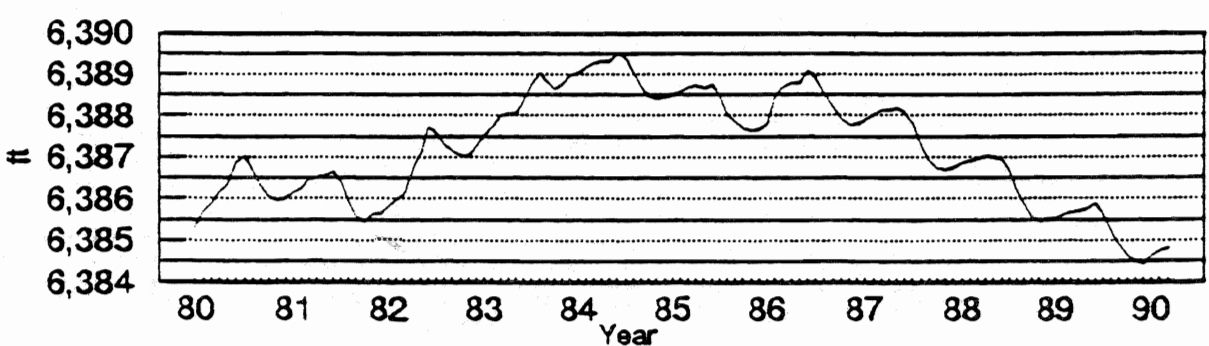
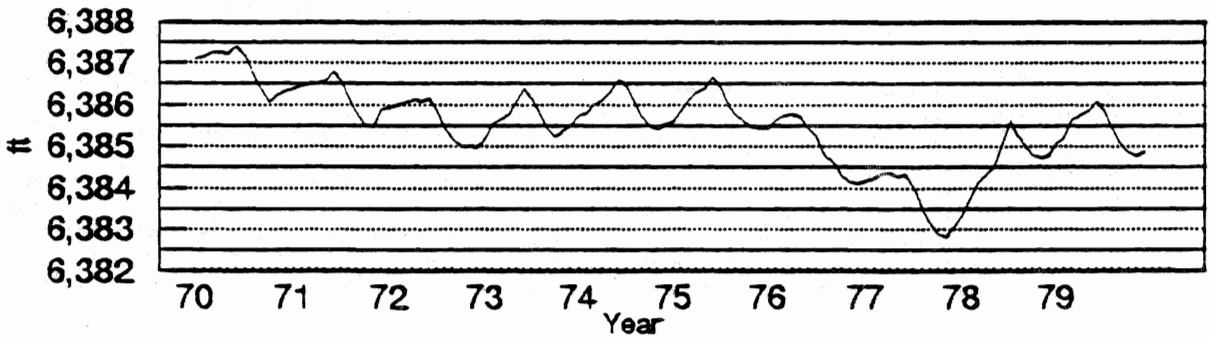
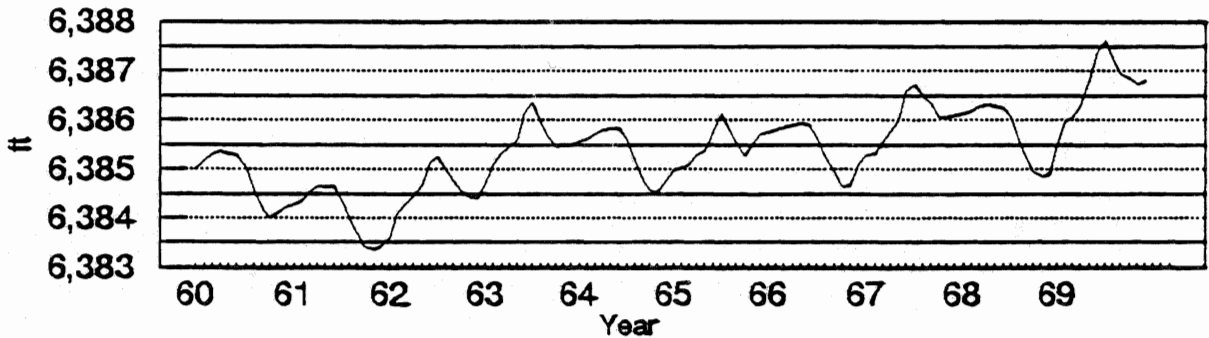
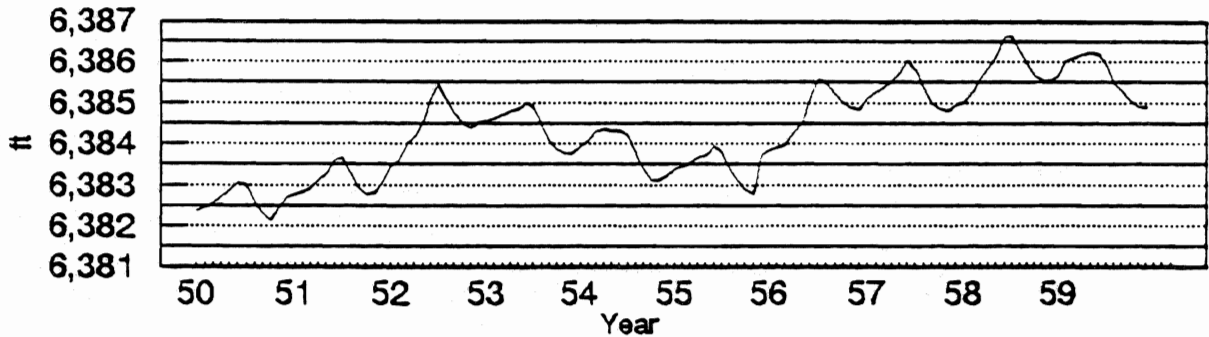
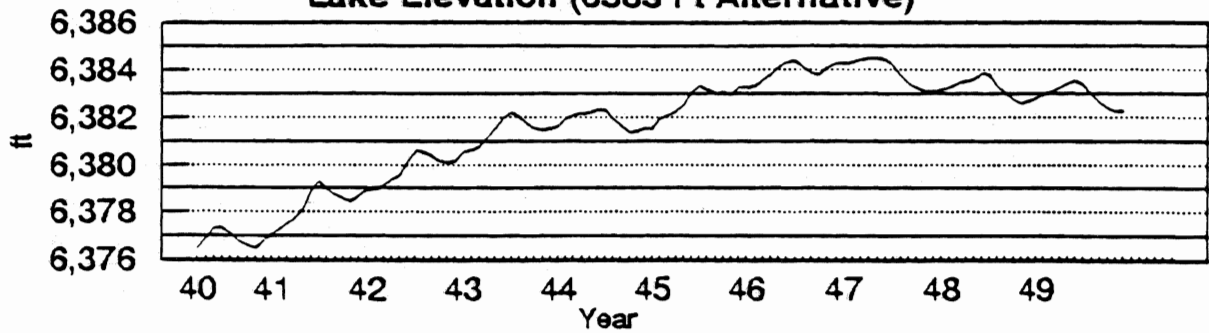




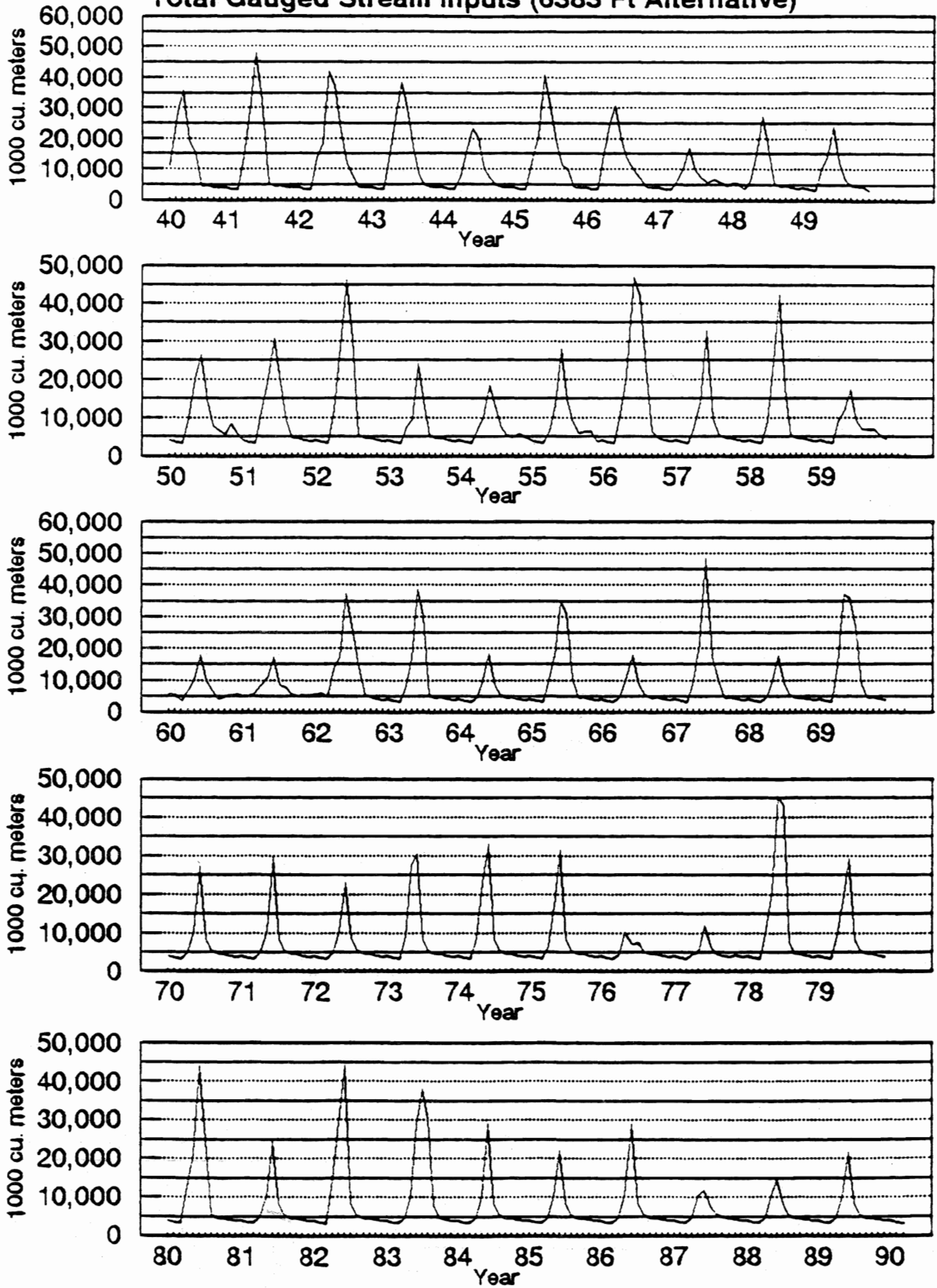
**Yearly Ungauged Stream Discharge and GroundWater
Estimates from DYRESM and LAAMP
1941 to 1989 (6377 ft Scenario)**

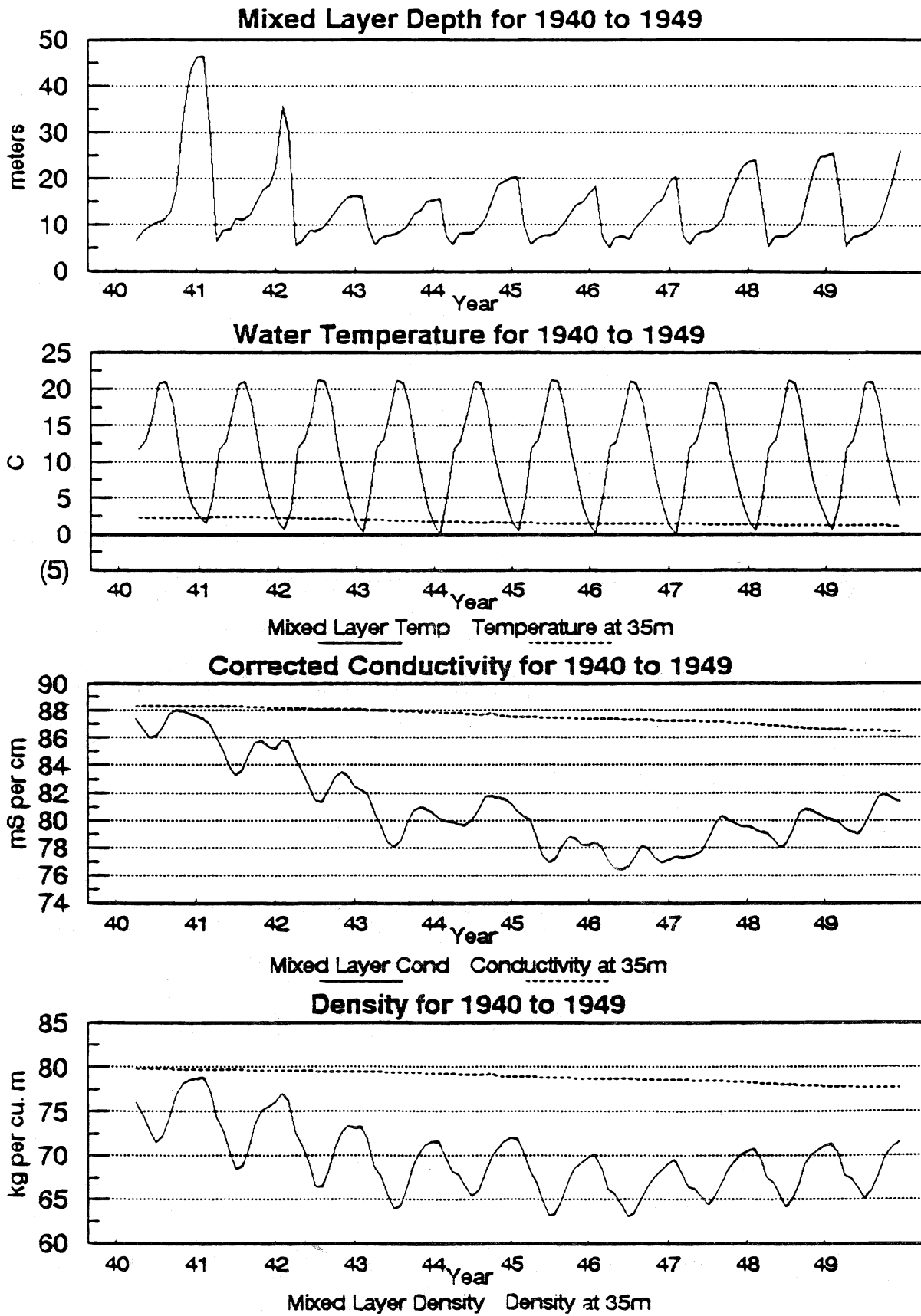


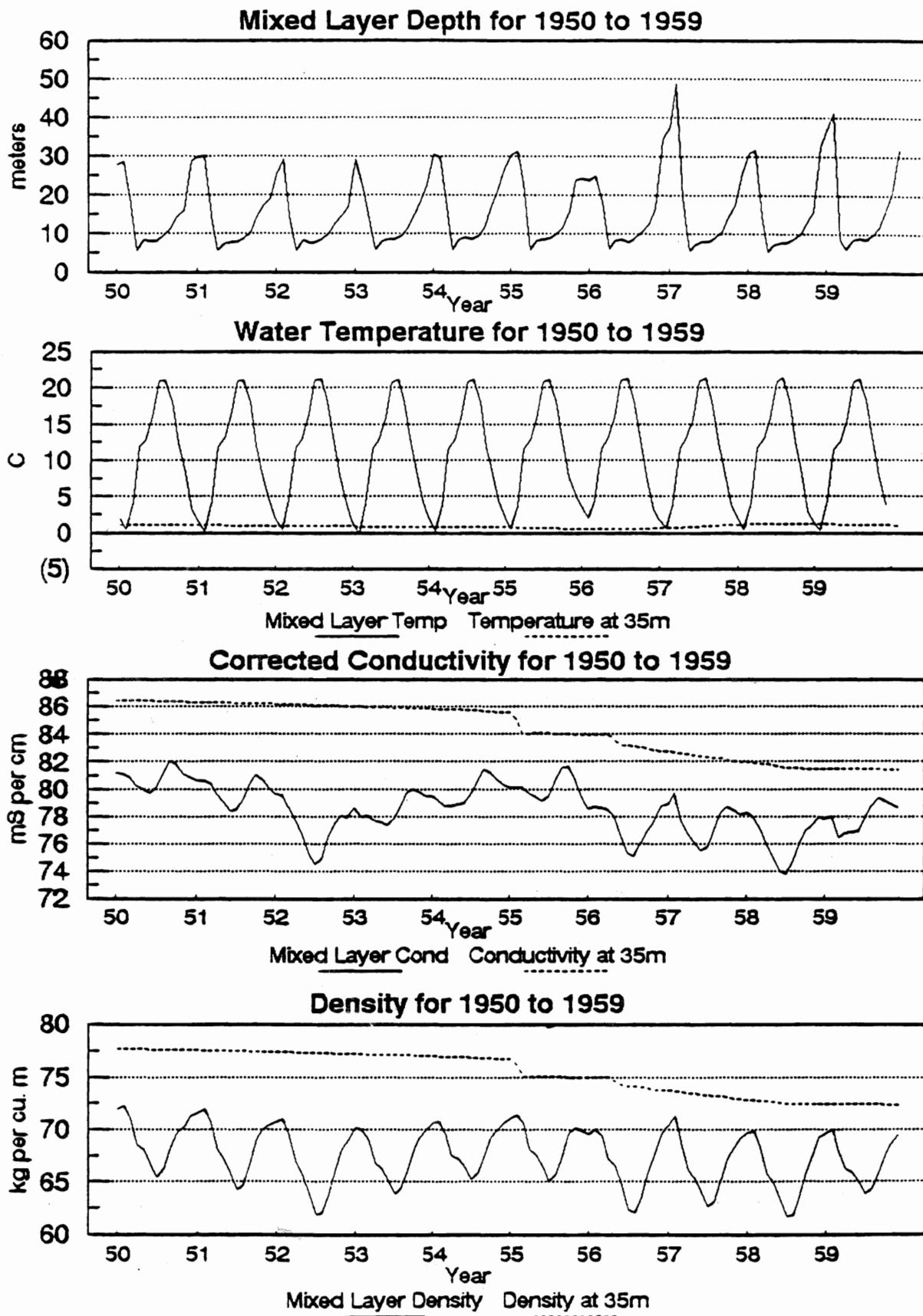
Lake Elevation (6383 Ft Alternative)

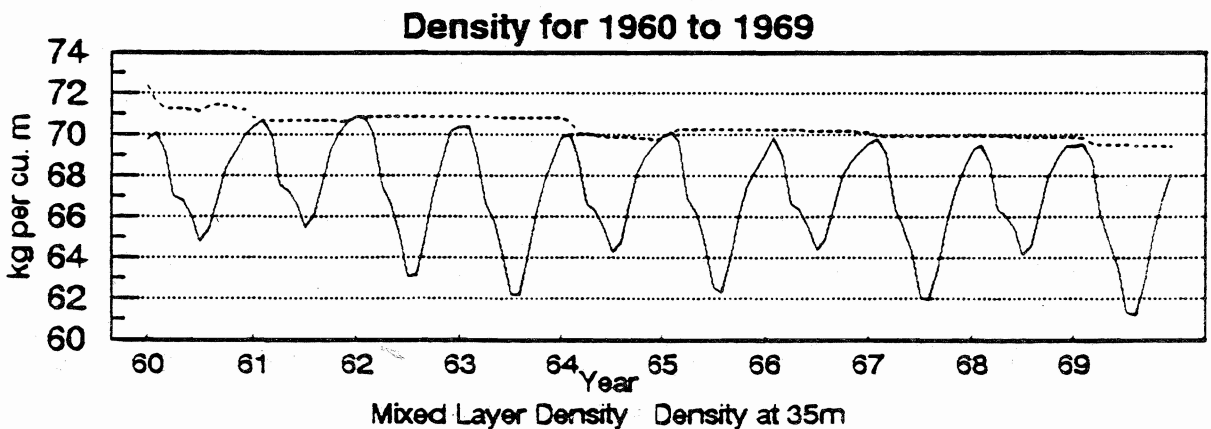
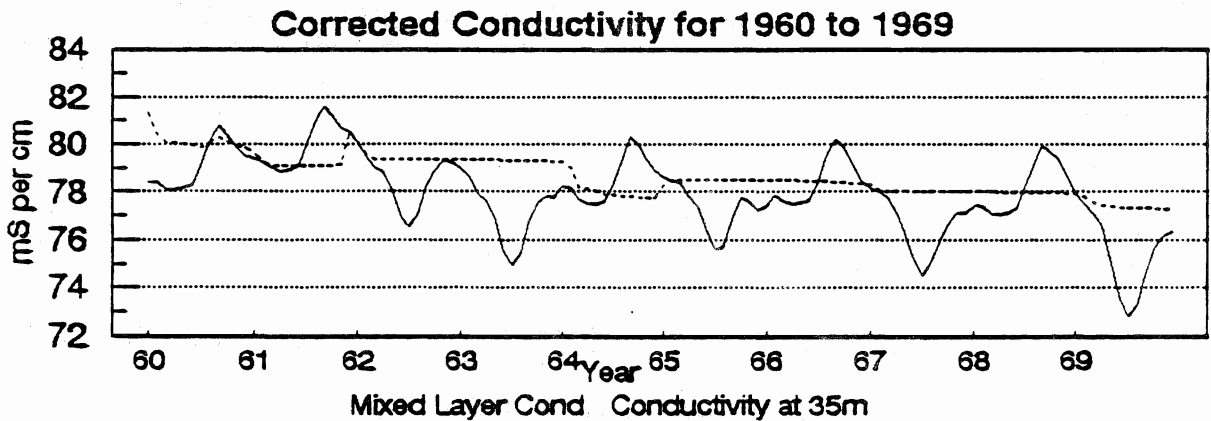
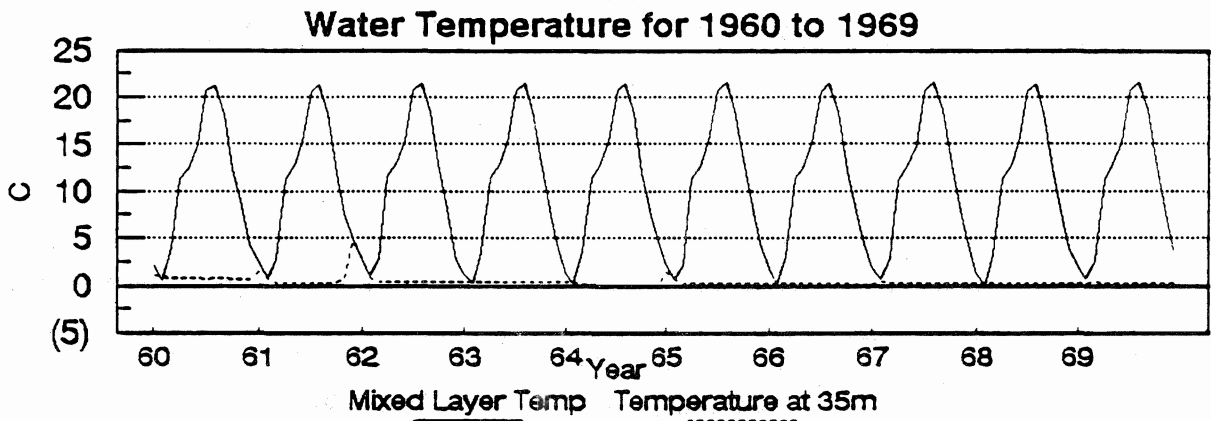
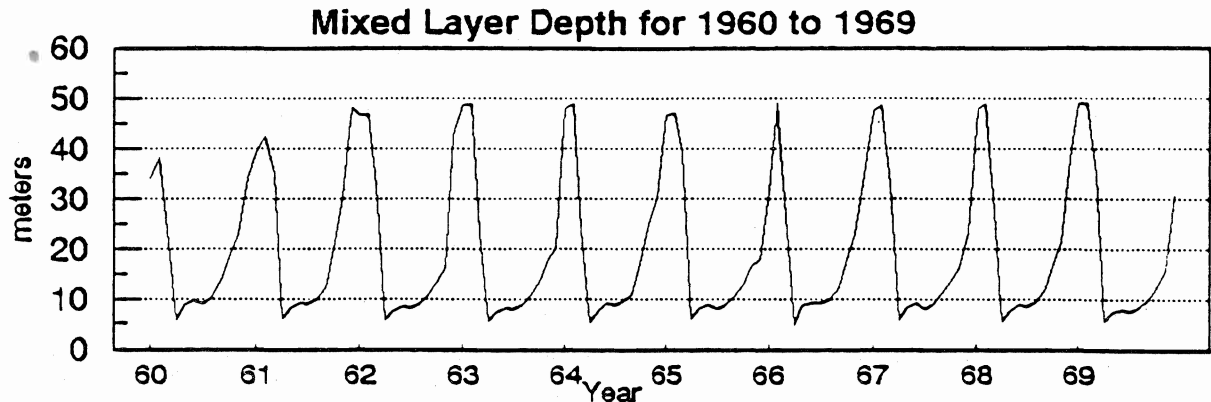


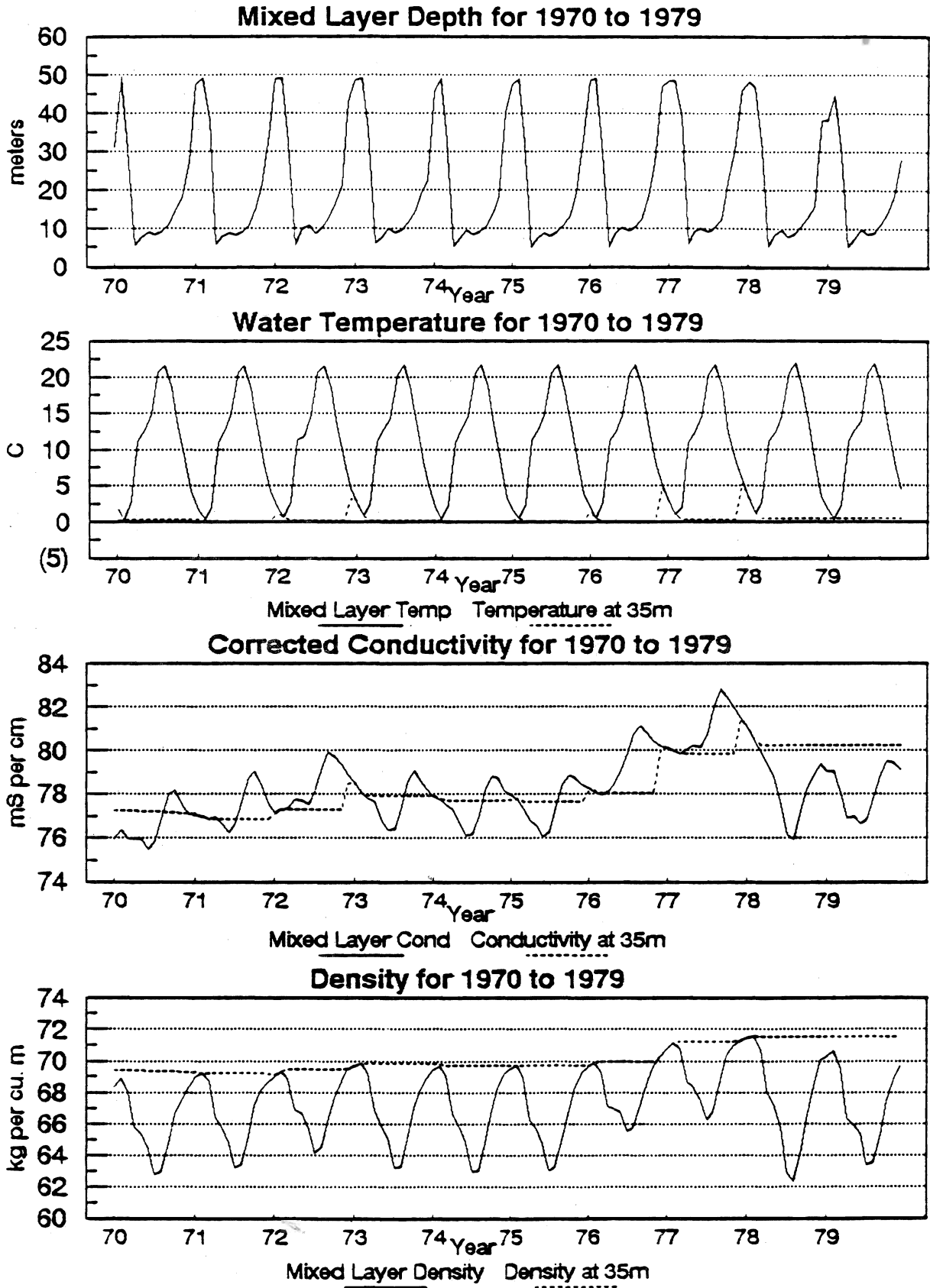
Total Gauged Stream Inputs (6383 Ft Alternative)

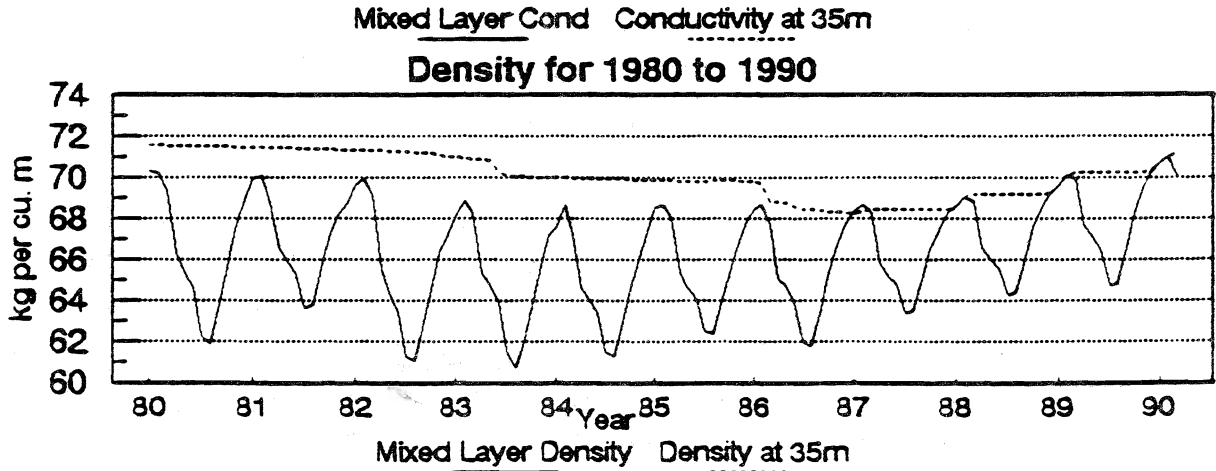
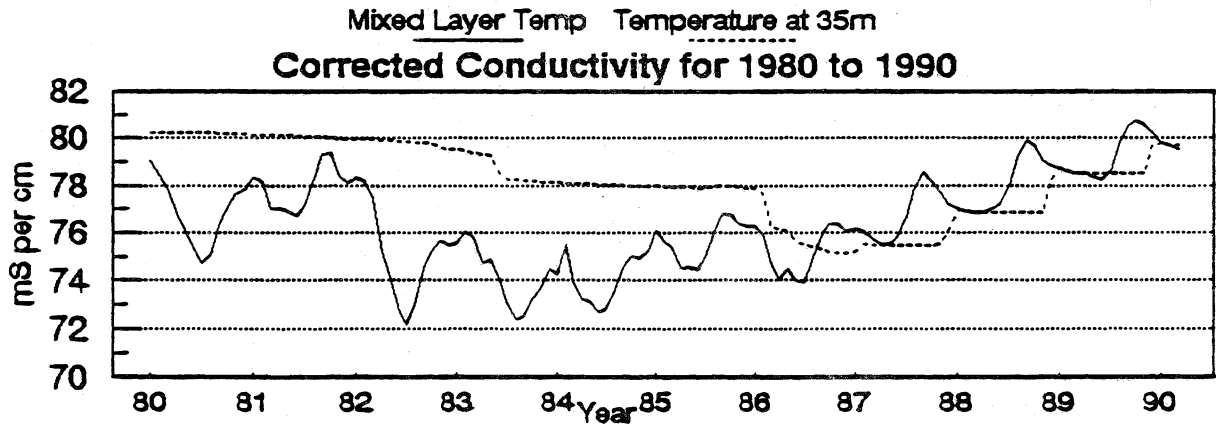
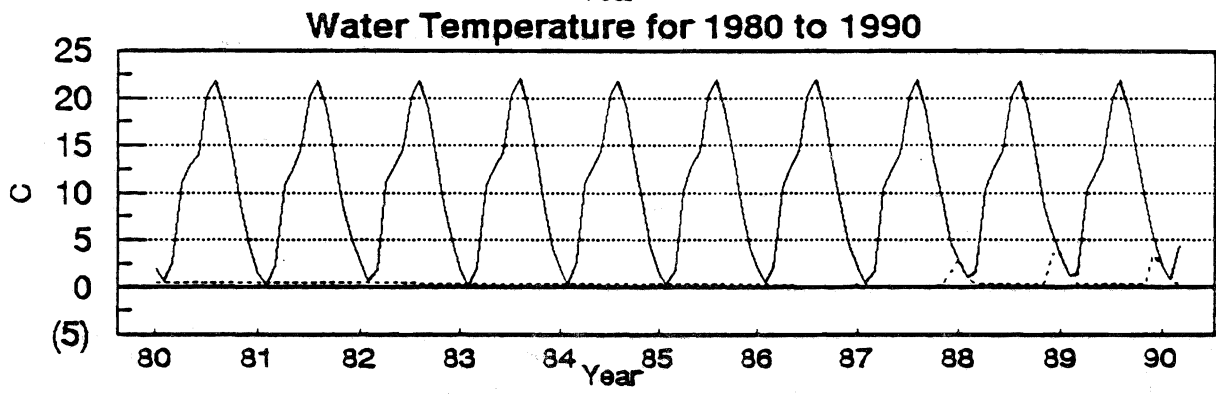
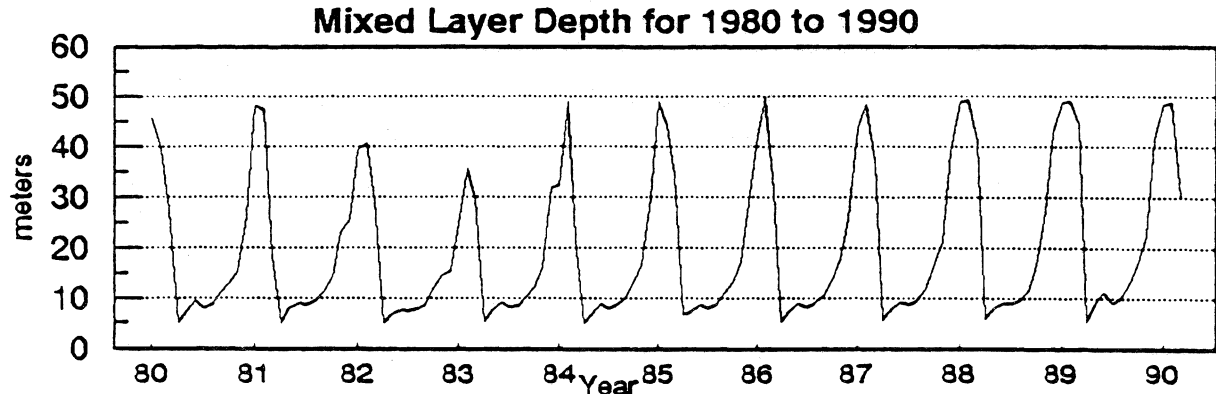




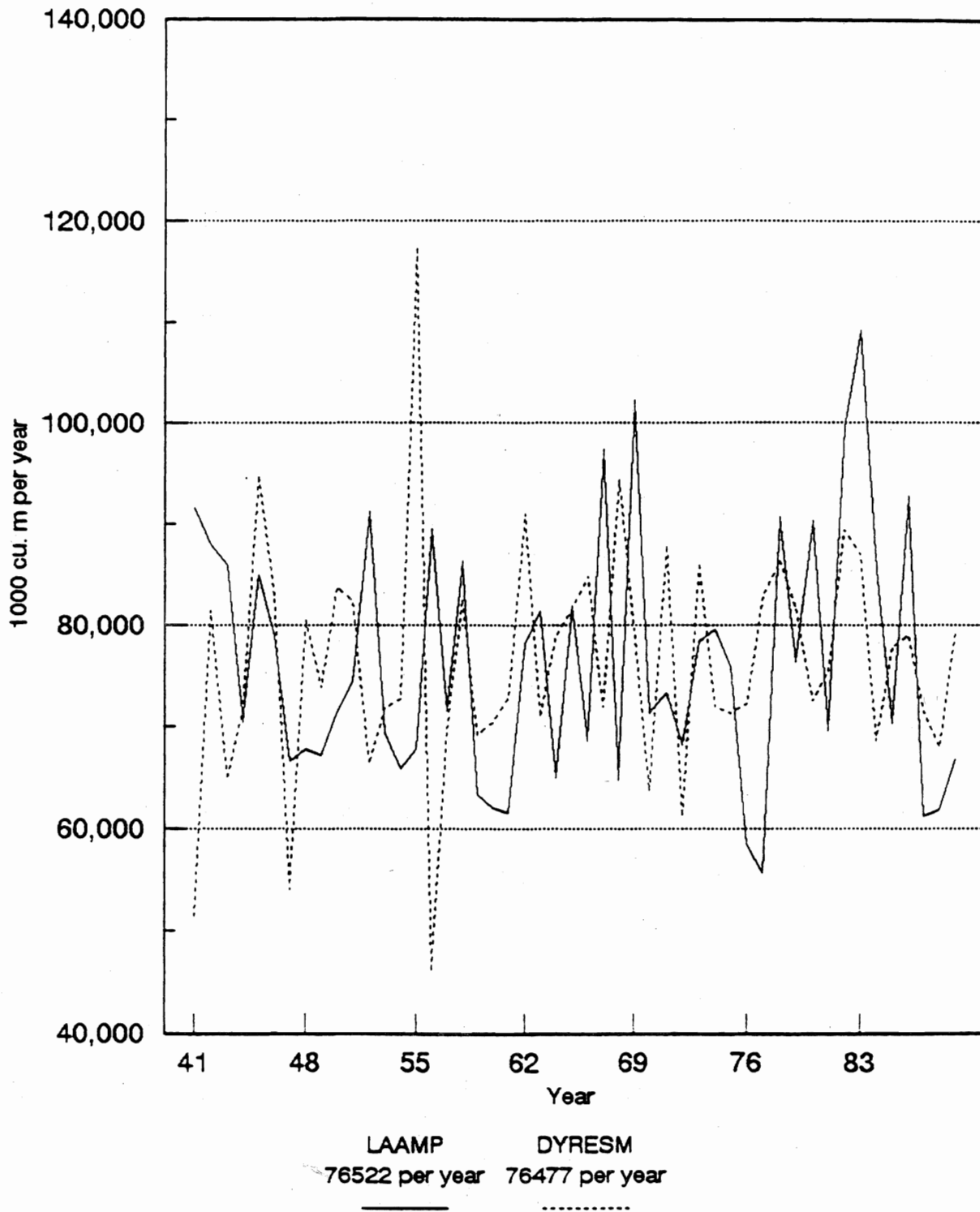




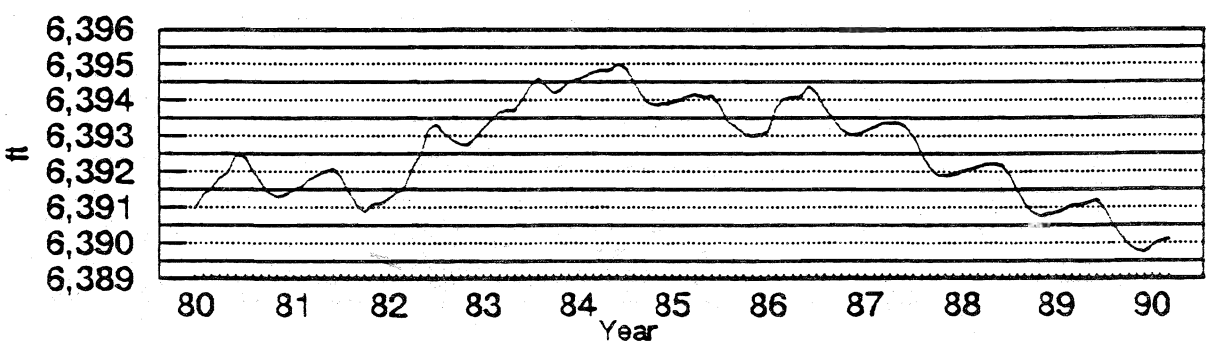
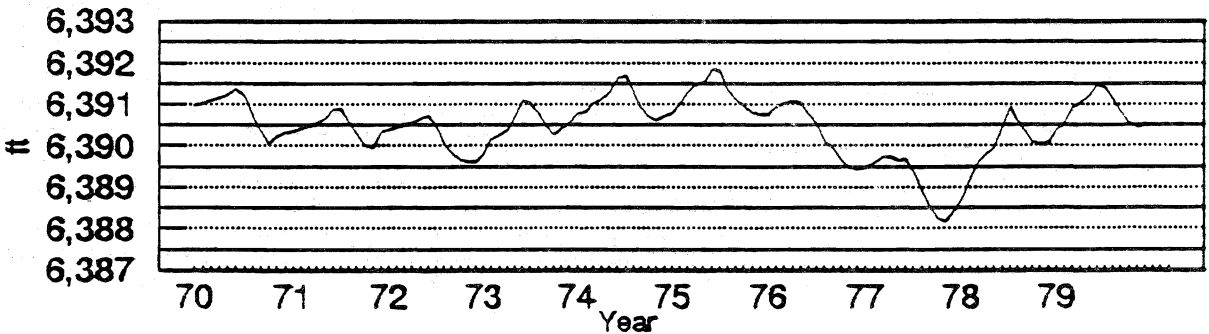
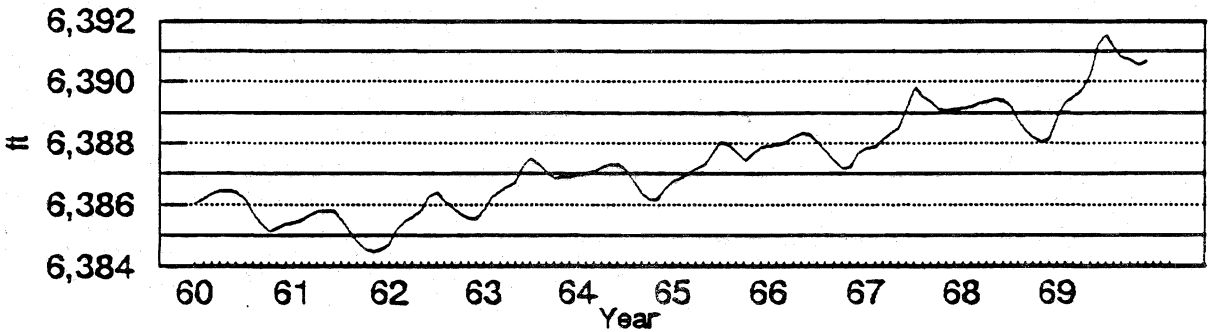
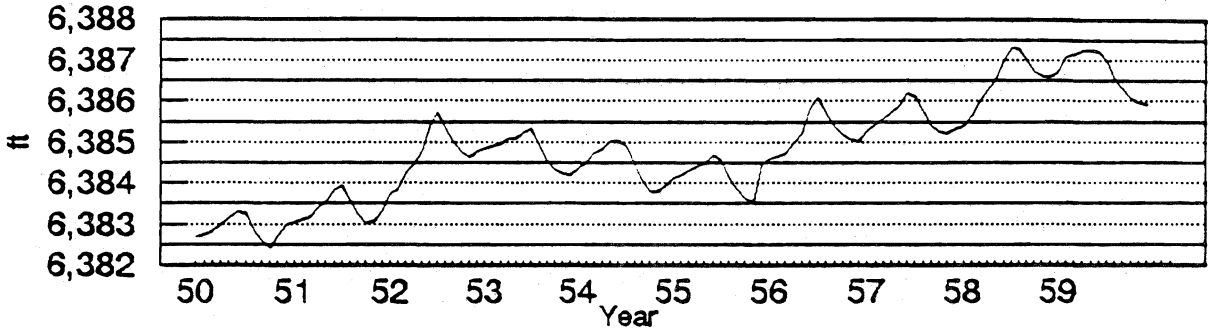
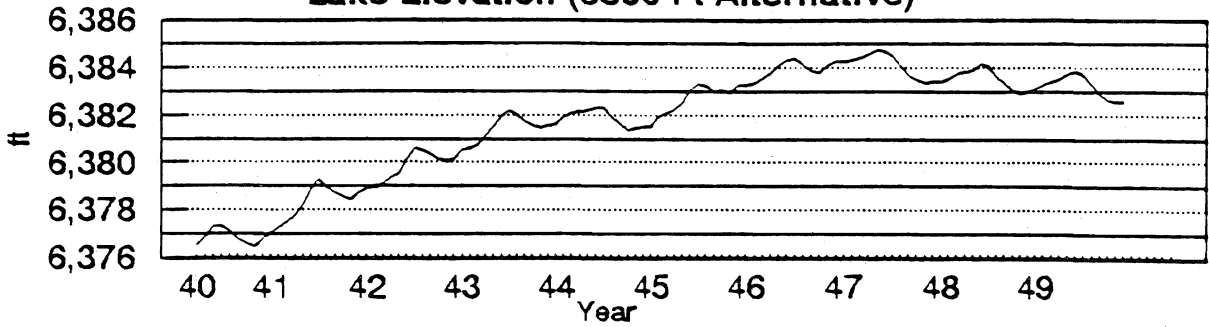


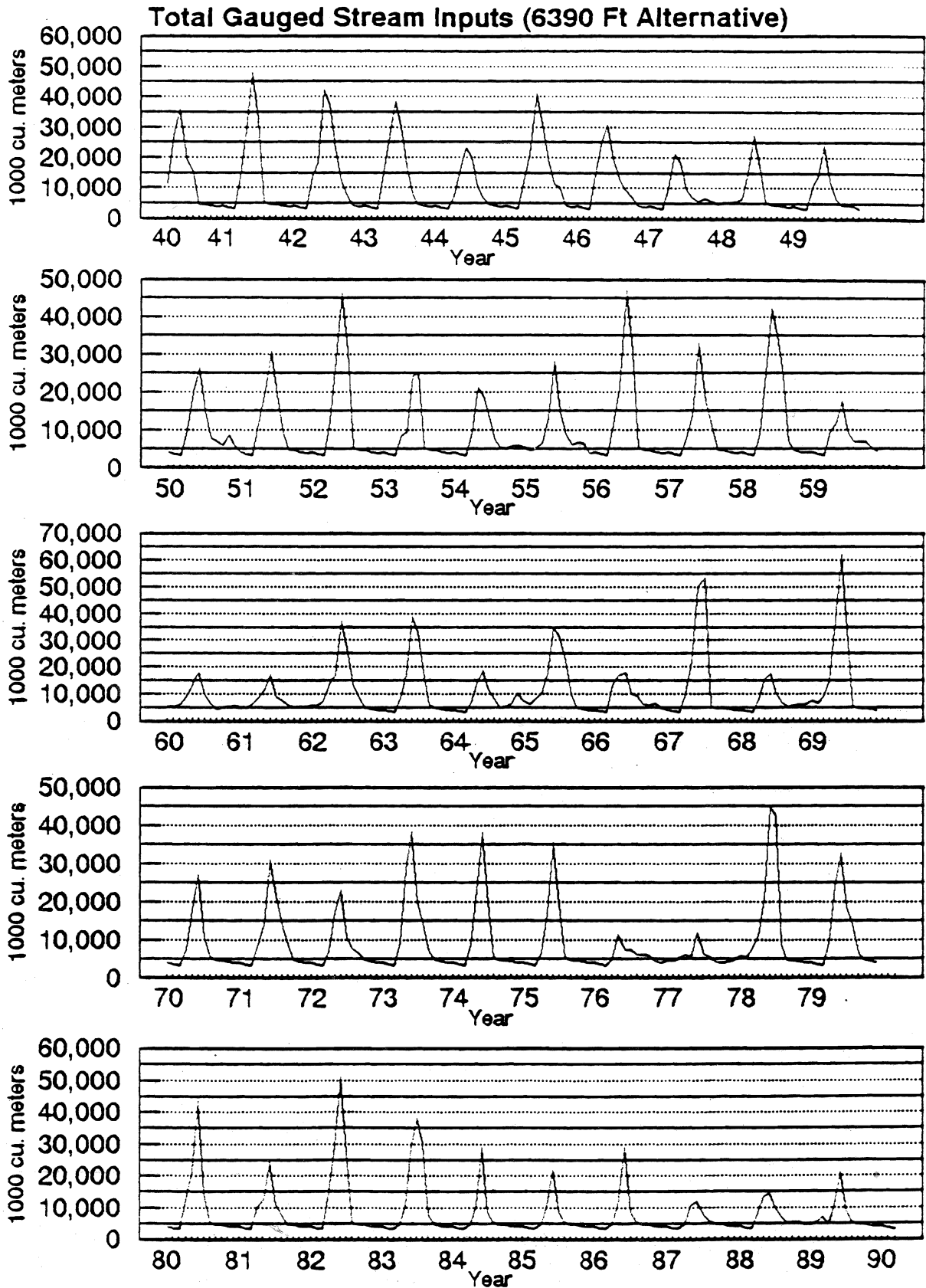


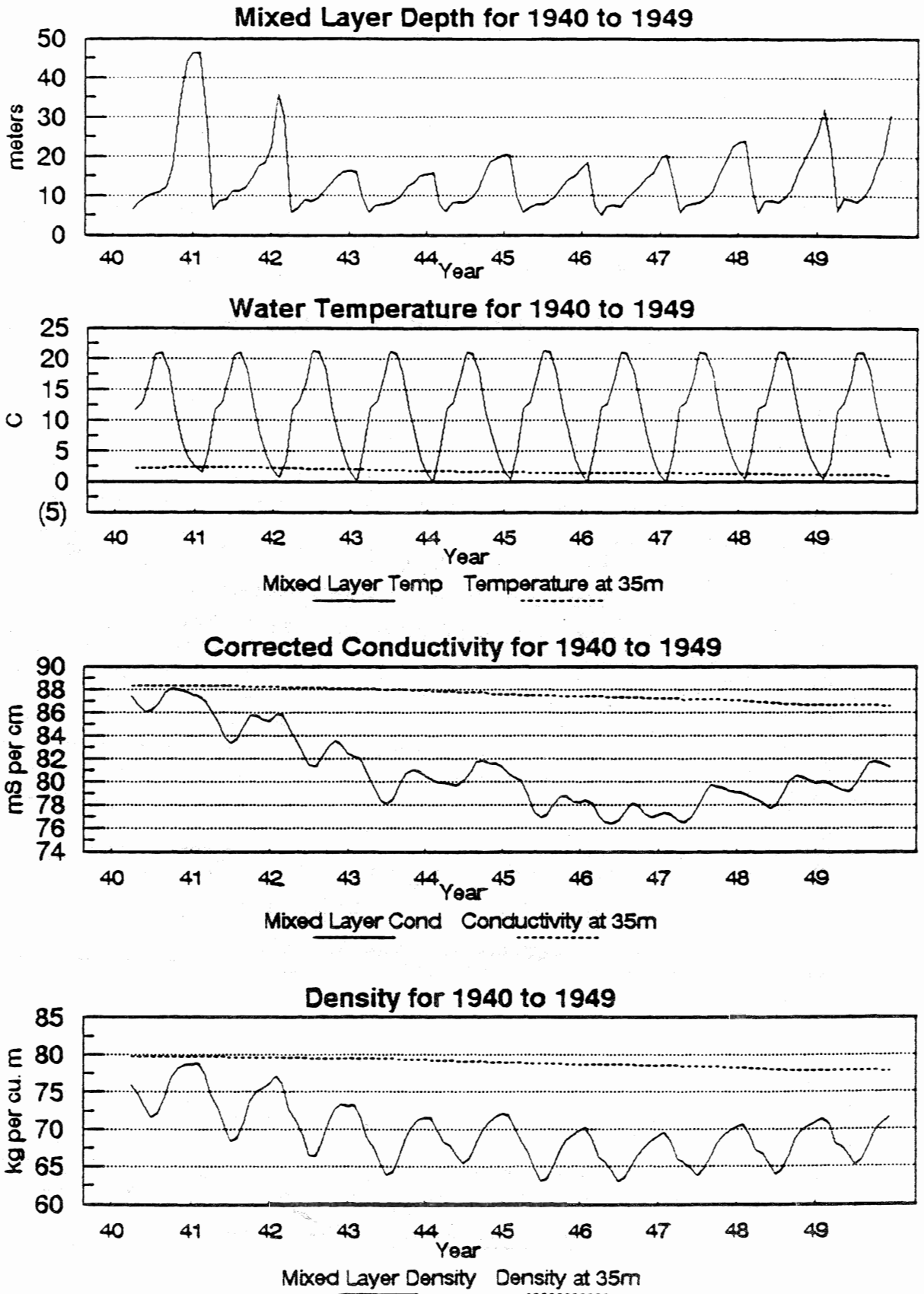
**Yearly Ungauged Stream Discharge and GroundWater
Estimates from DYRESM and LAAMP
1941 to 1989 (6383 ft Scenario)**

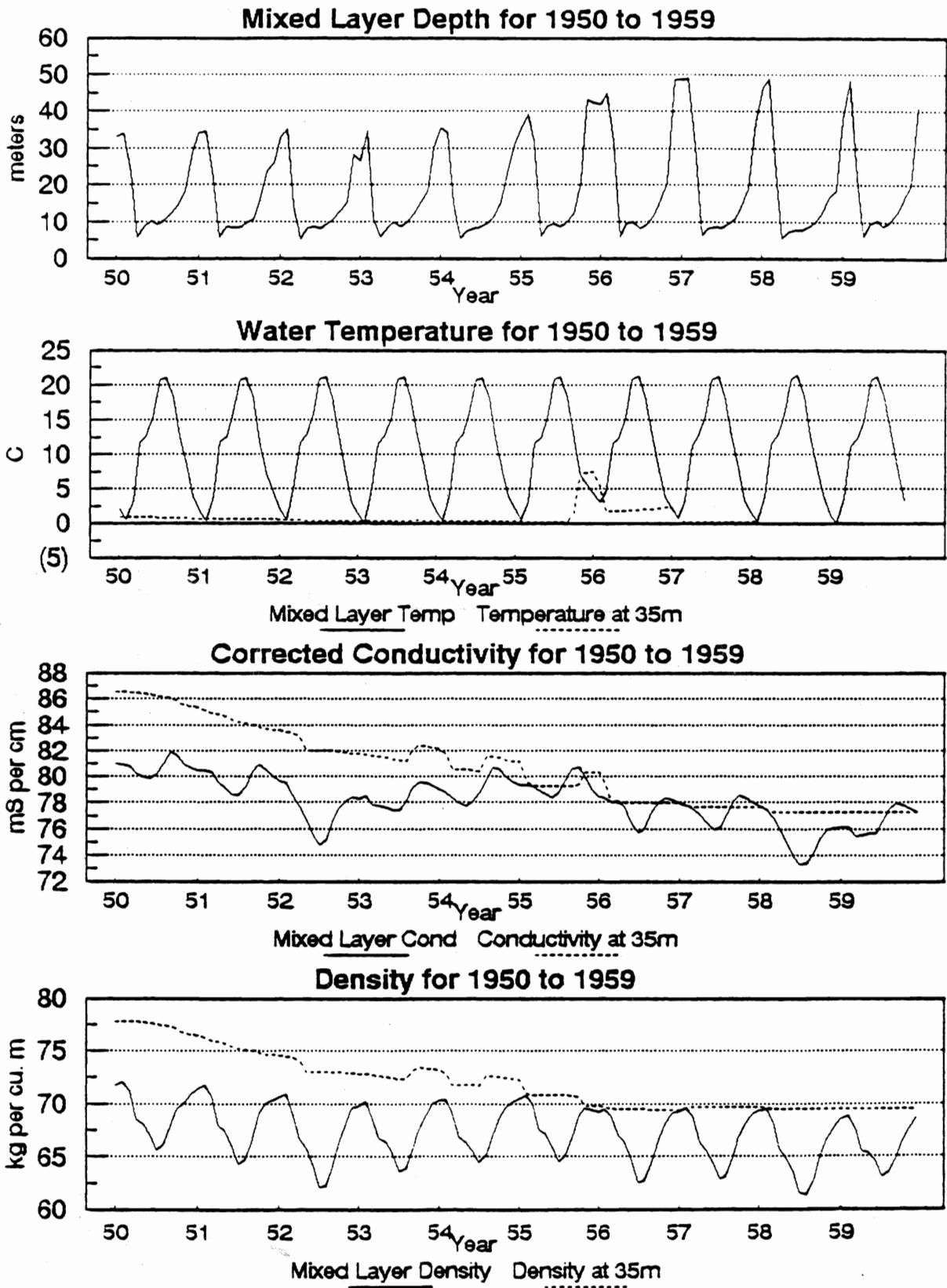


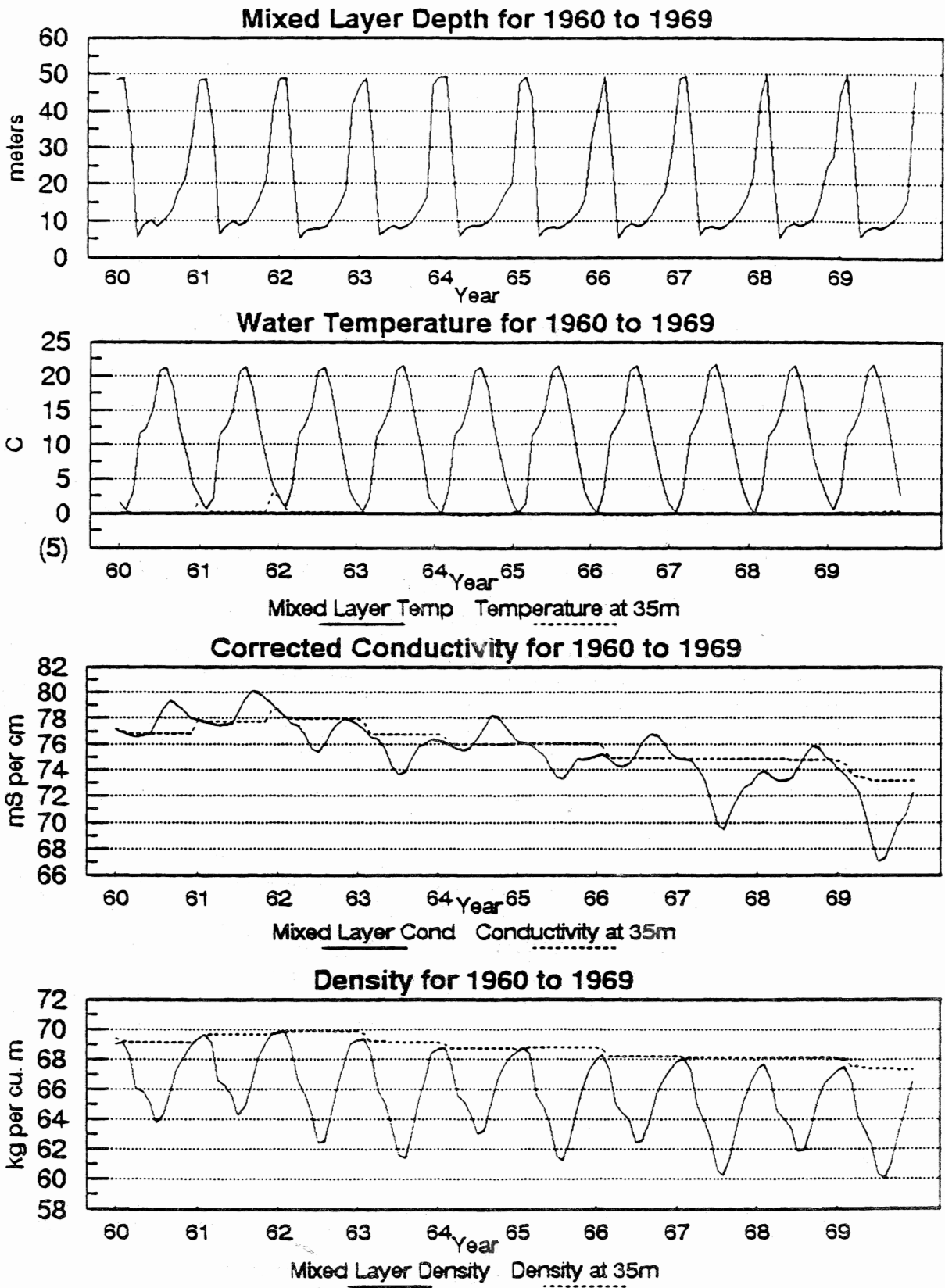
Lake Elevation (6390 Ft Alternative)

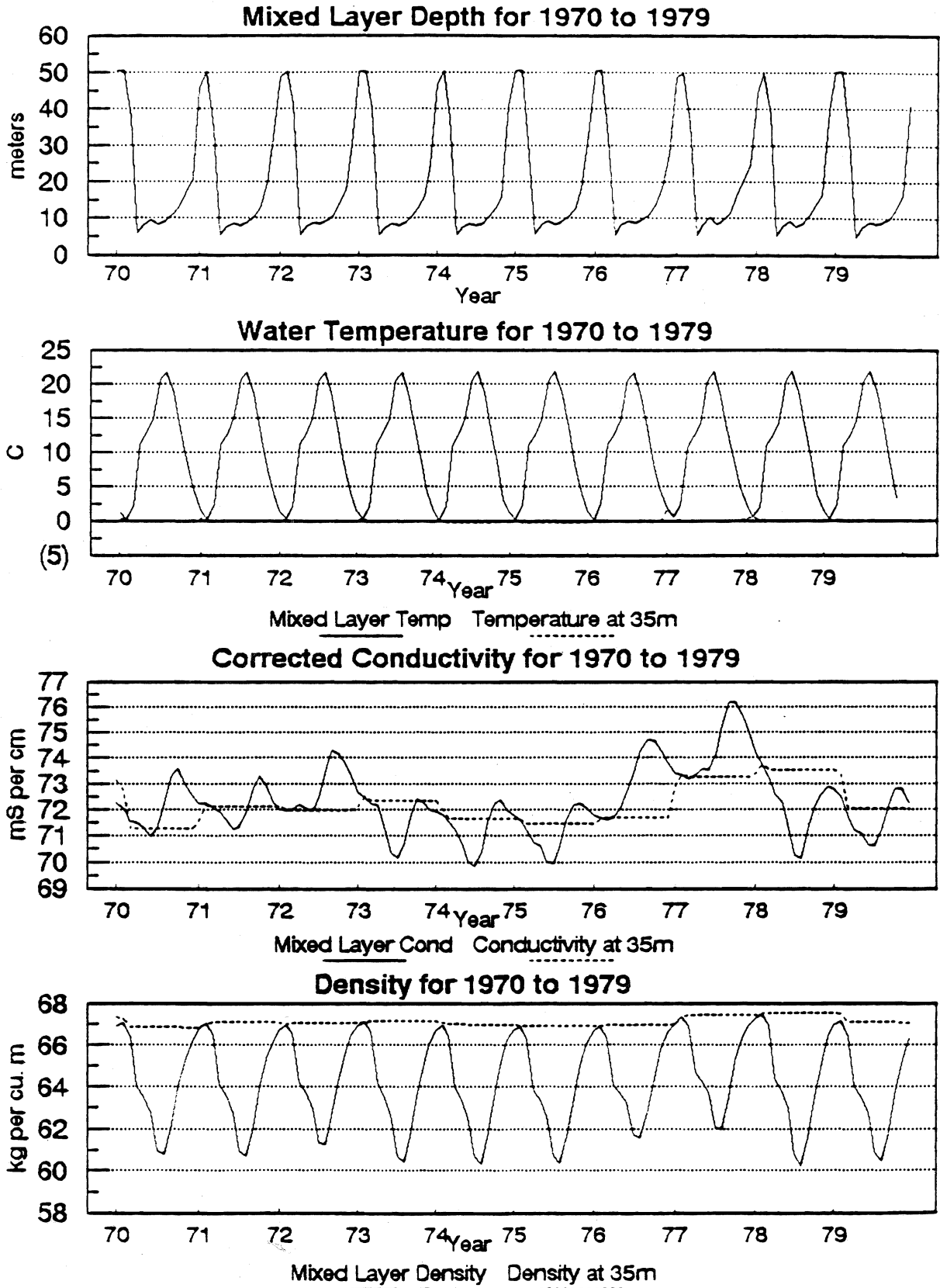


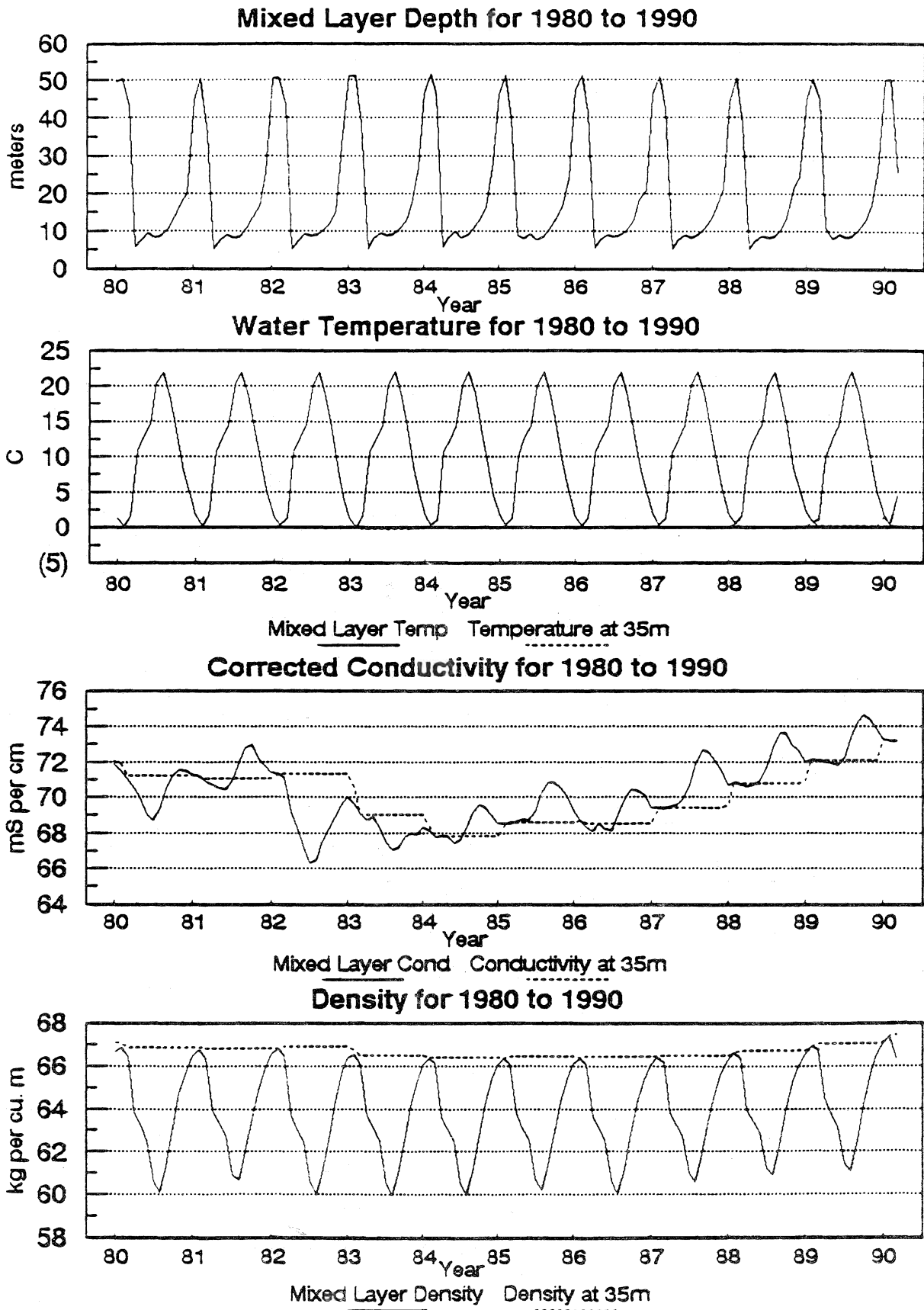




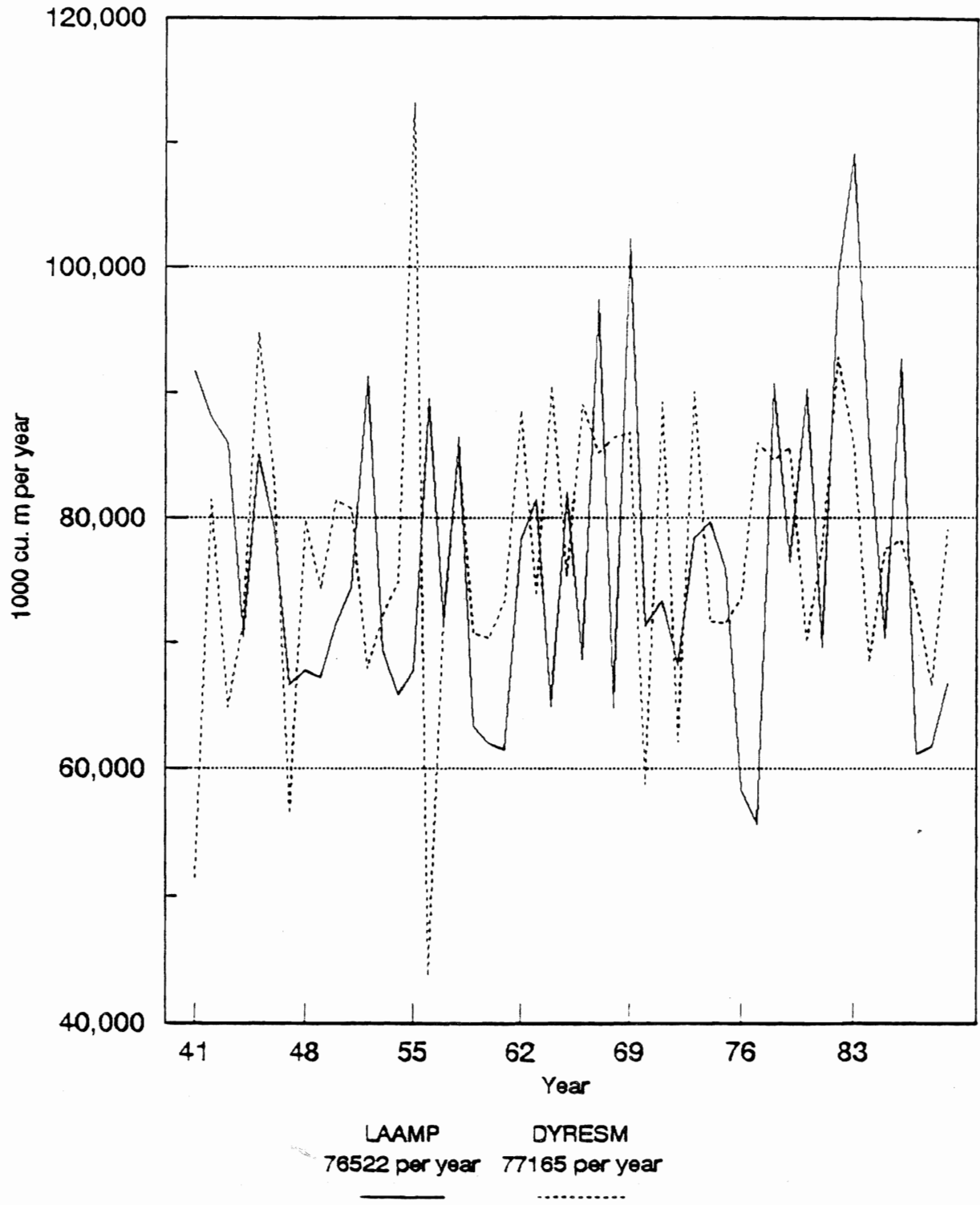




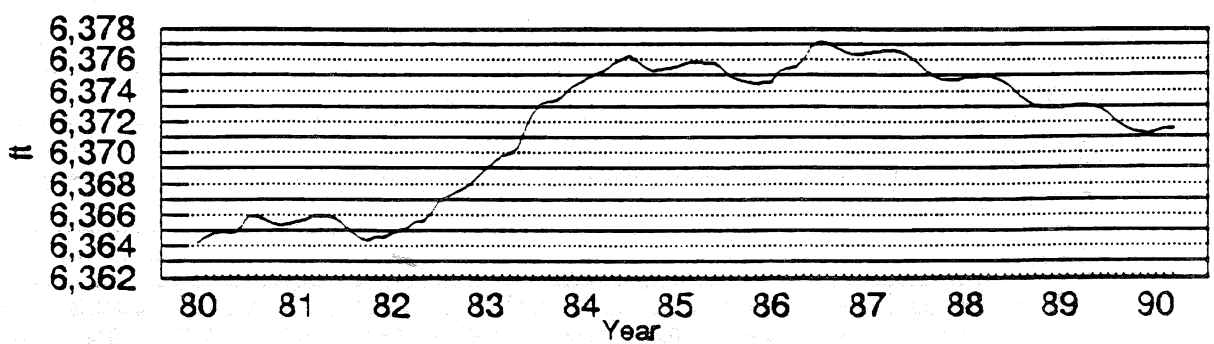
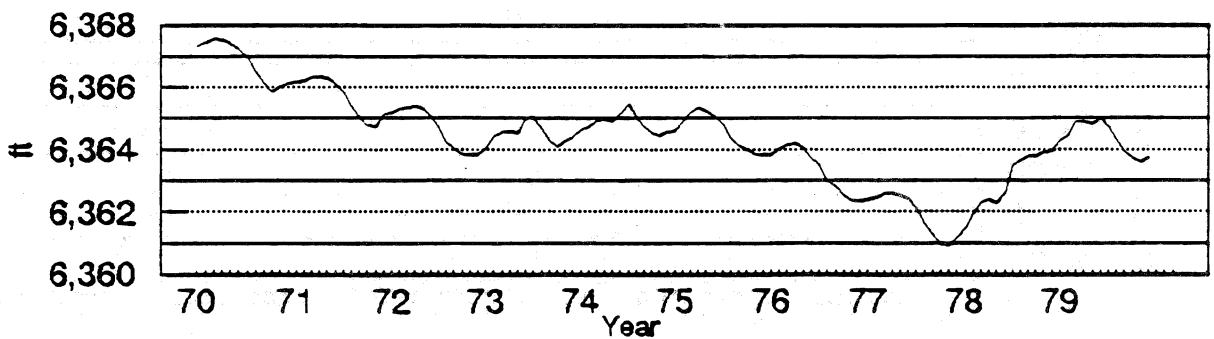
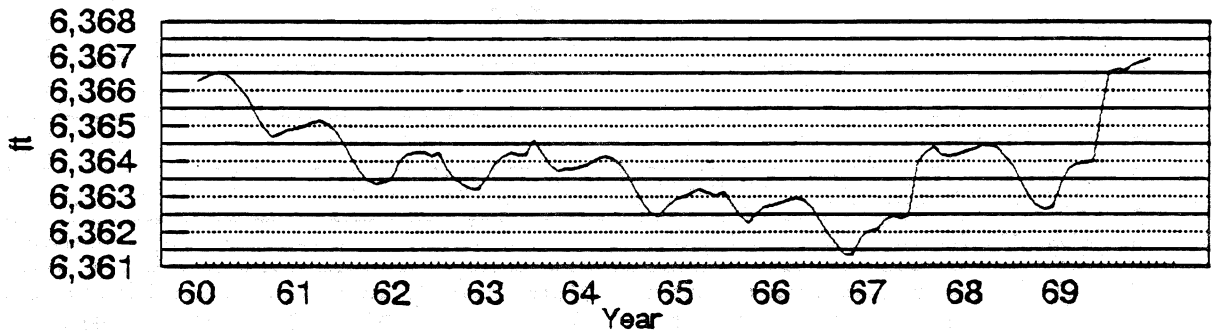
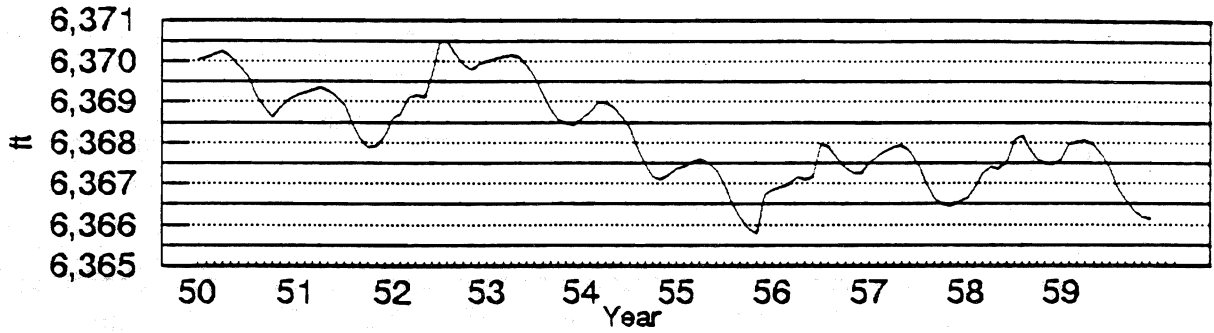
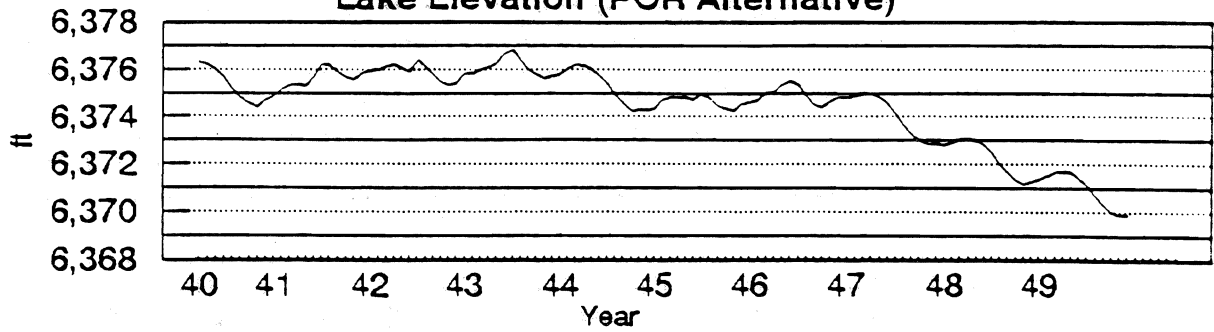


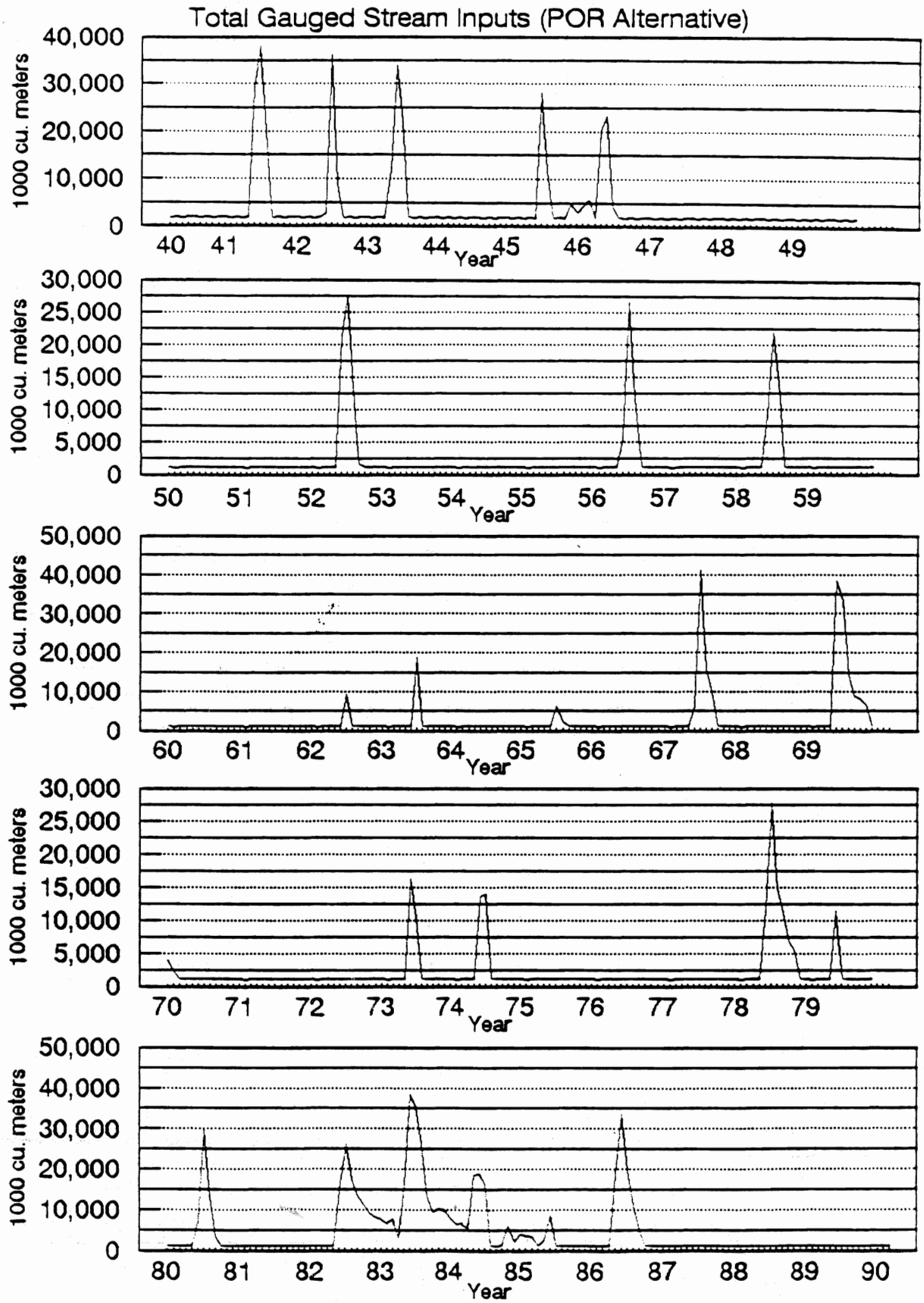


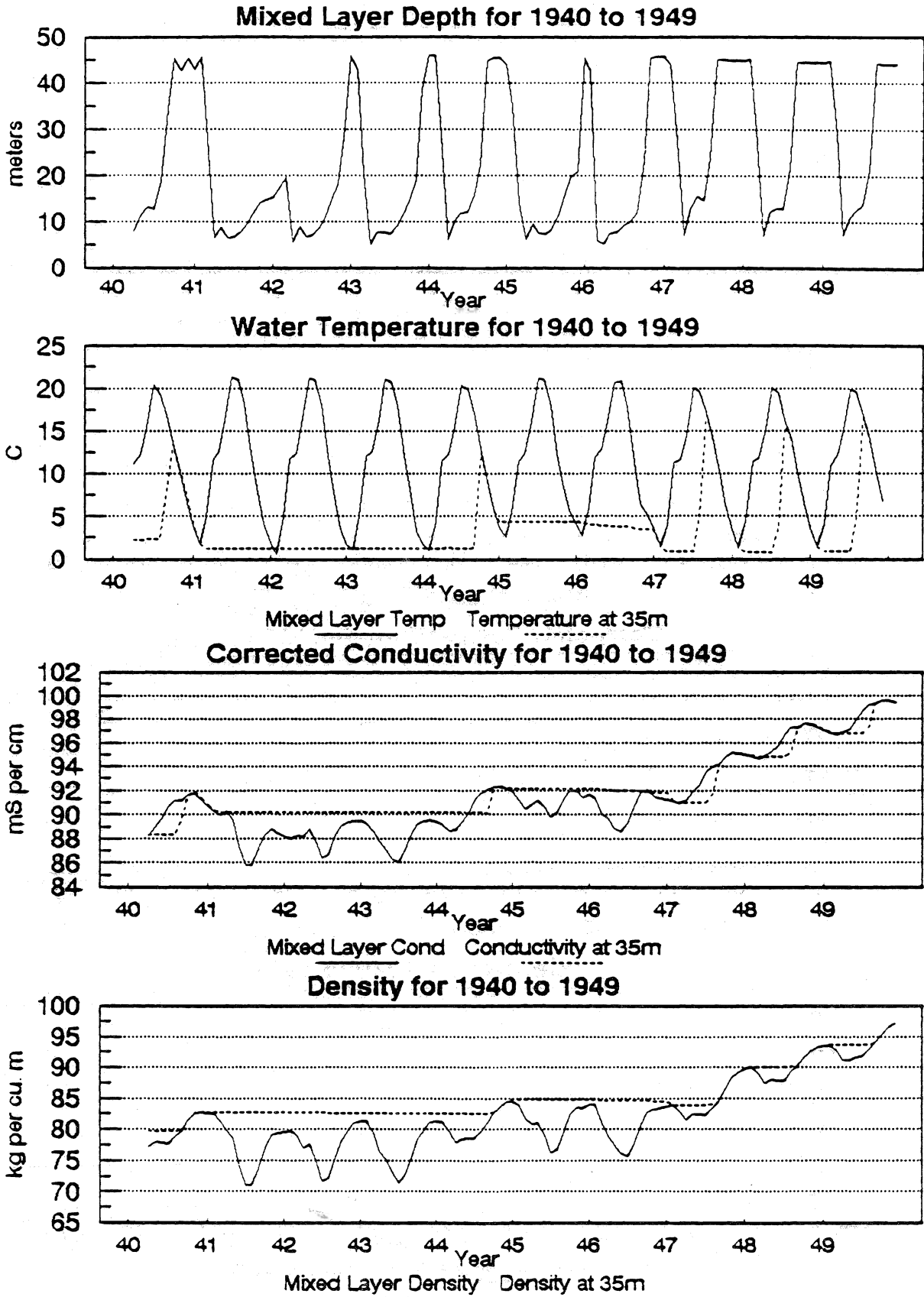
**Yearly Ungauged Stream Discharge and GroundWater
Estimates from DYRESM and LAAMP
1941 to 1989 (6390 ft Scenario)**

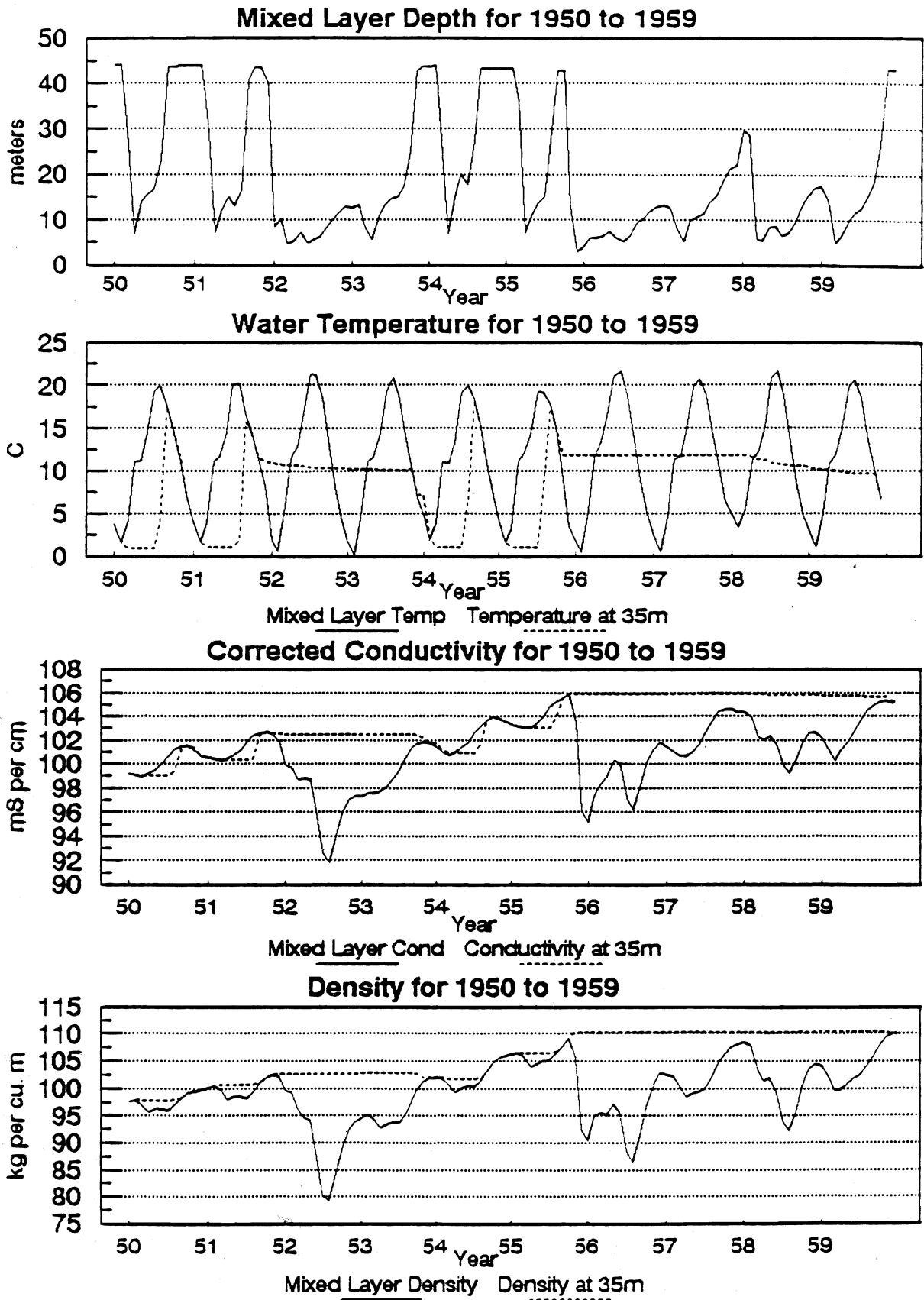


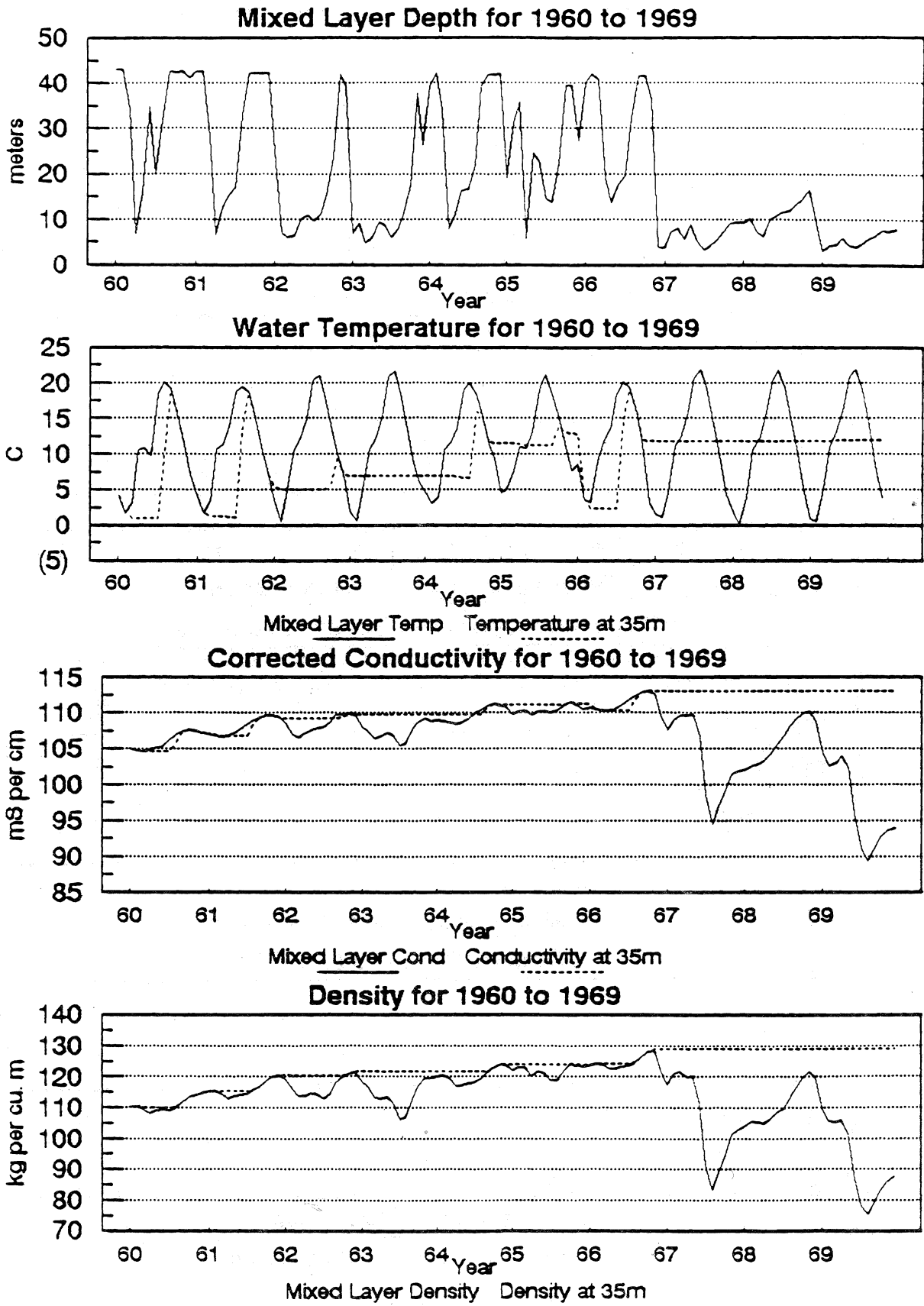
Lake Elevation (POR Alternative)

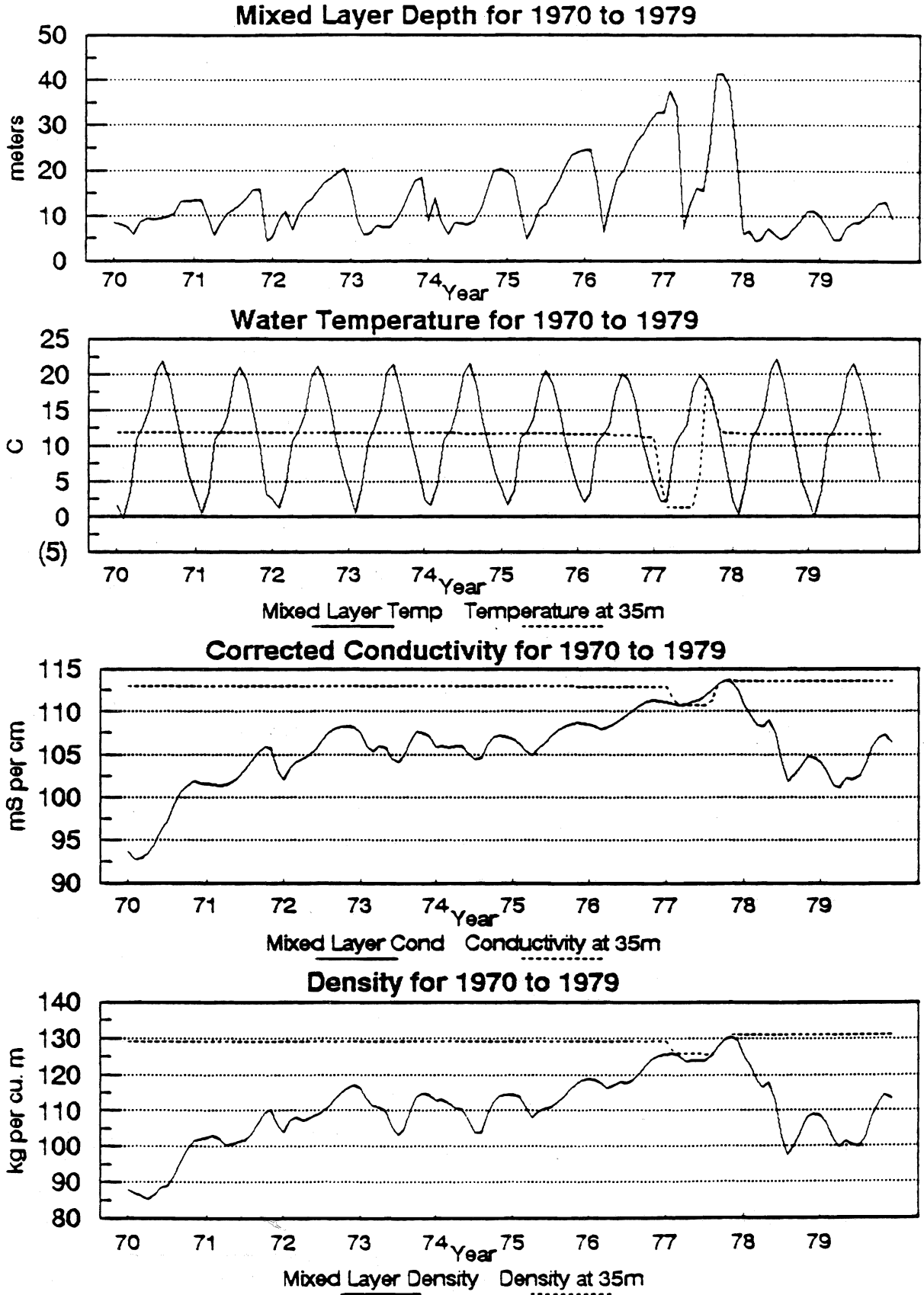


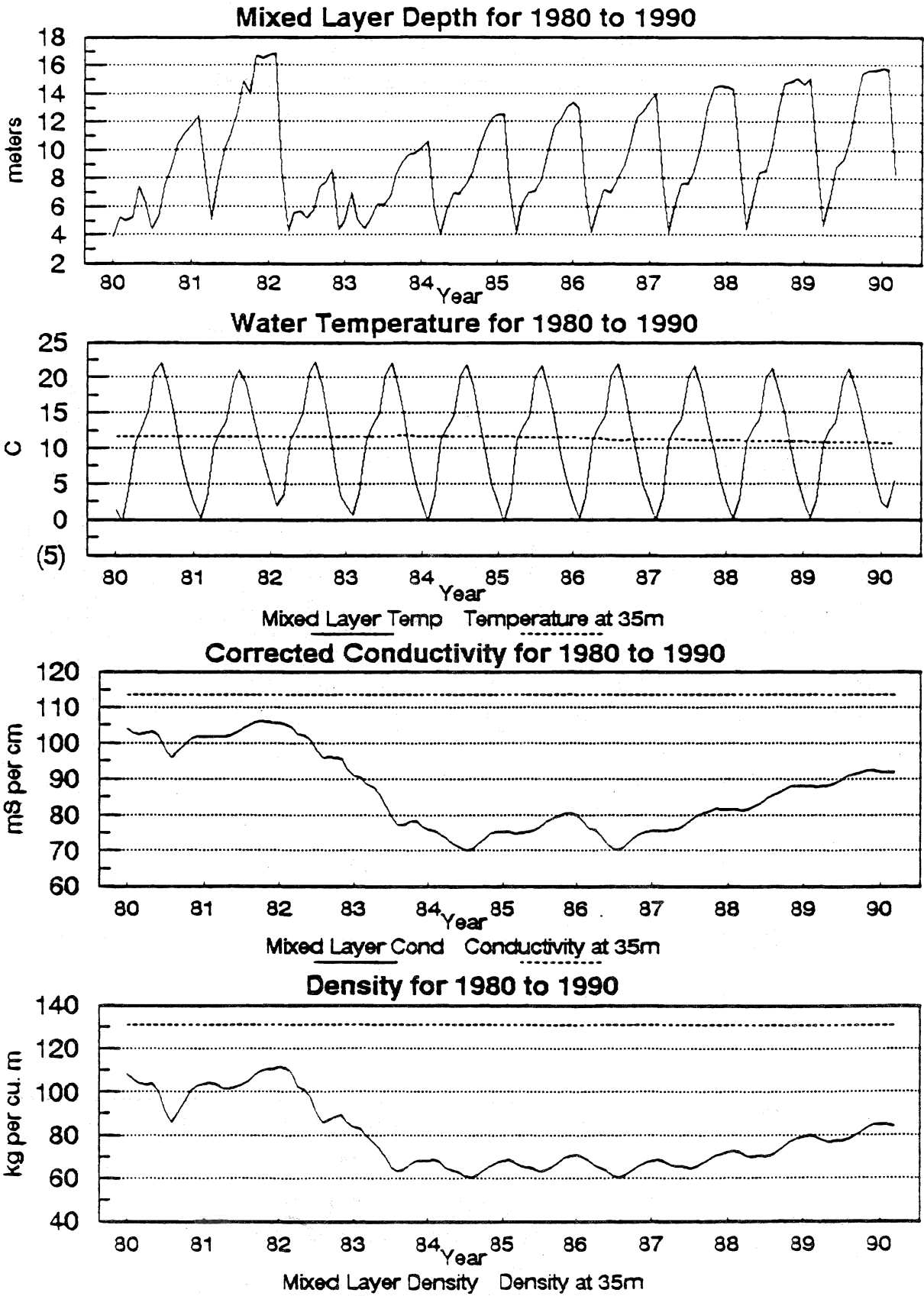




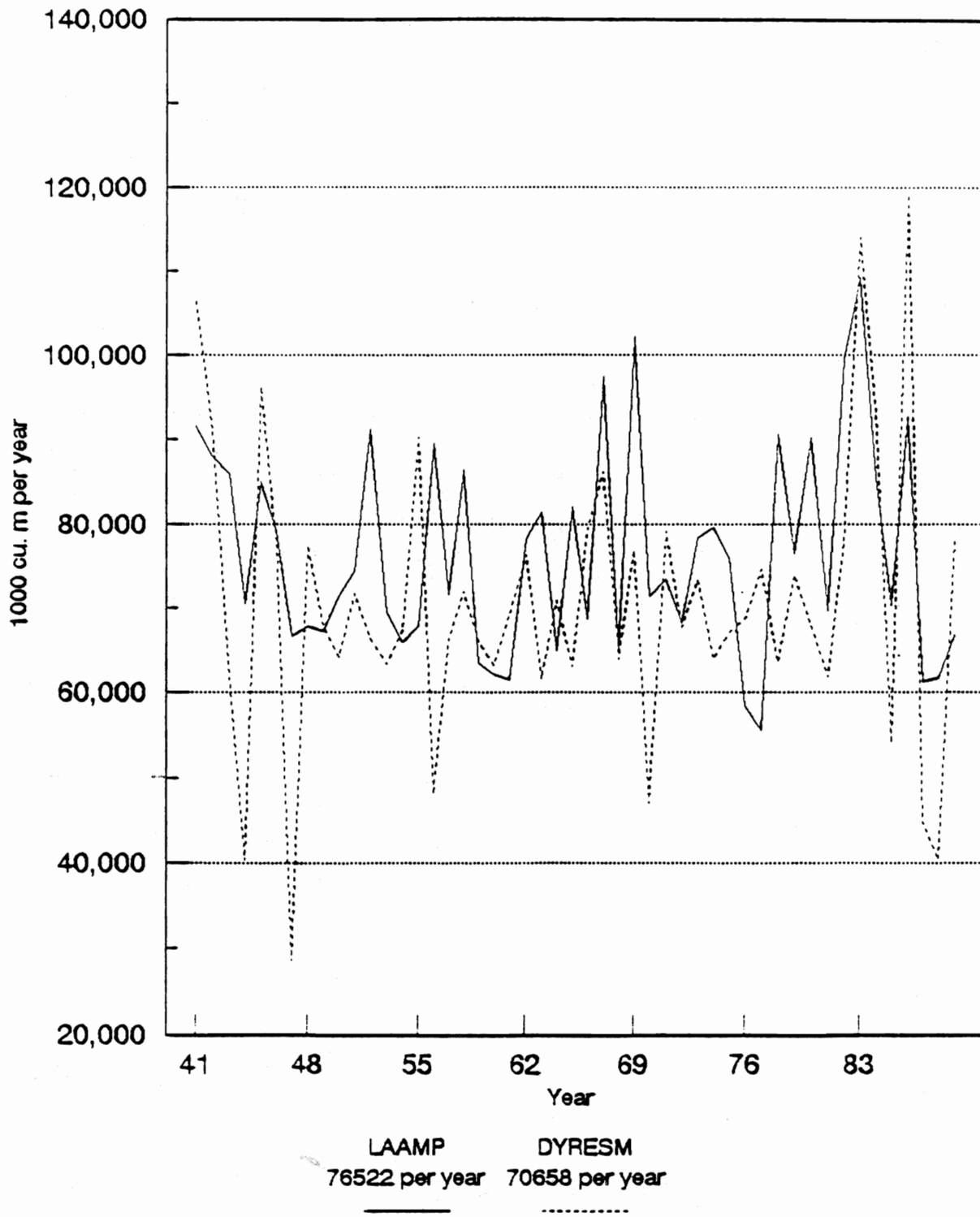








**Yearly Ungauged Stream Discharge and GroundWater
Estimates from DYRESM and LAAMP
1941 to 1989 (POR Scenario)**



Occurrence and Duration of Meromixis for Mono Lake EIR Alternatives

